

# Chapter I

## Introduction

### 1.1 Research Background

Aircraft landing on carriers requires precise control. Historically, this critical phase of flight landing caused the greatest number of accidents (Eldridge, 1961). Thus, the final approach of an aircraft before the wheels contact the surface of the carrier's deck requires superior handling quality with the pilot overcoming the challenges of visibility, engaging an arrester hook, with short landing, and the uncontrolled oscillatory motion of the carrier due to sea state disturbance (Durand and Wasicko, 1965).

Aircraft dynamics and control theories have evolved significantly during the last century. Since (Bryan,1911) laid the foundation for a 6 degrees of freedom model which governs aircraft motion in space and (Lanchester, 1908) developed the mathematical model for the dynamic characteristics of aircraft. Almost all studies thereafter used the same basic principles but with different applications due to the advent of digital computers and advanced control theories (Cook, 2007).

The diverse nature of aircraft dynamics and the attendant interaction between the different axes of motion have introduced higher levels of complexities in dealing with this subject, as a single concept or as a complete theory. Instead, the flight dynamics throughout different axes and within various flight envelopes are subdivided into smaller segments to be analyzed and improved in an attempt to join the pieces of this procedure and realize the best characteristic for flight dynamics under all flight conditions. This necessitates the extension of each analysis segment to be

investigated as point of whole aircraft envelope to ensure the interactions with the remaining dynamics are not adversely affected.

Hence, dynamic flight motion was basically treated under two main topics; Longitudinal and Lateral Dynamics. The symmetrical nature of most aircraft about their centerlines validate the assumption that moderate changes in the angle of attack, heave and pitch rates (Dynamic Control) will have a minor influence upon yaw and roll (Lateral Control). The commonly used theory of longitudinal motion and corresponding dynamic and static stability was developed by (Gates and Lyon, 1944). Further elaboration and detailed studies of the findings of Gates and Lyon could also be founded in (Duncan, 1959) and (Babister, 1961).

Lateral dynamics concerns yawing and rolling of the aircraft which, in major parts of flight envelope, is not critical in maintaining stability due to the lateral symmetry of the wings, tails, and vertical fin about the airplane center of gravity. Figure 1.1 depicts the 6 axis of airplane motion and the corresponding control surfaces. The locations of the control surfaces on an airplane are shown in figure 1.2.

Although longitudinal and lateral motion stabilities are inseparable, it is a common practice to analyze these separately for the aforementioned reasons. This is known as Decoupled motion dynamics.

This response motion resulted from control surface input or external disturbance that is constrained in the longitudinal plane of symmetry, referred to as Decoupled longitudinal motion. It is described solely in terms of axial force, normal force, and the pitching moment equation. Decoupled lateral-motion exclusively involves roll, yaw, and side slip (V.Cook, 2011).

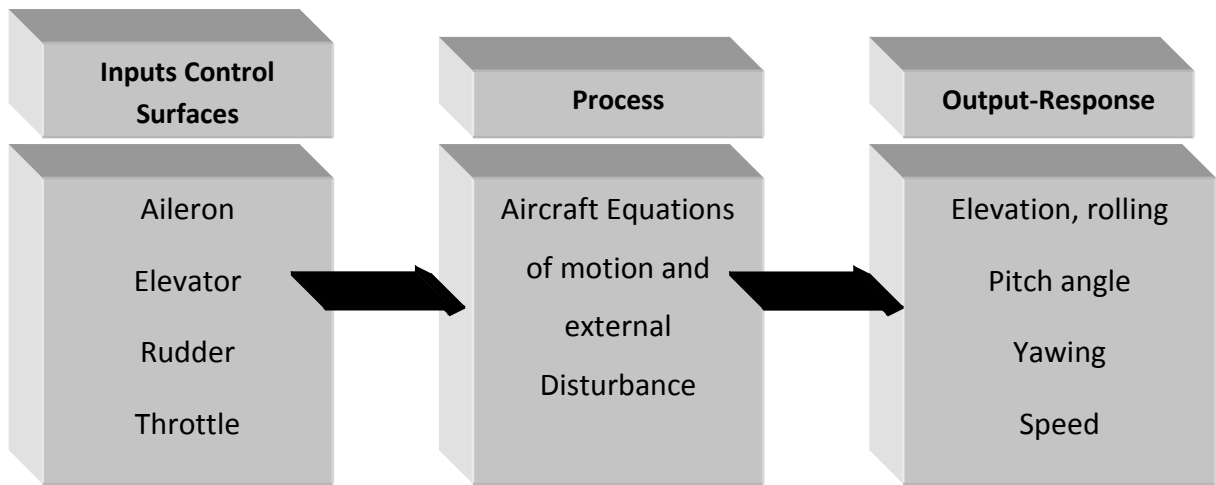


**Figure 1.1** Control-Response relationships

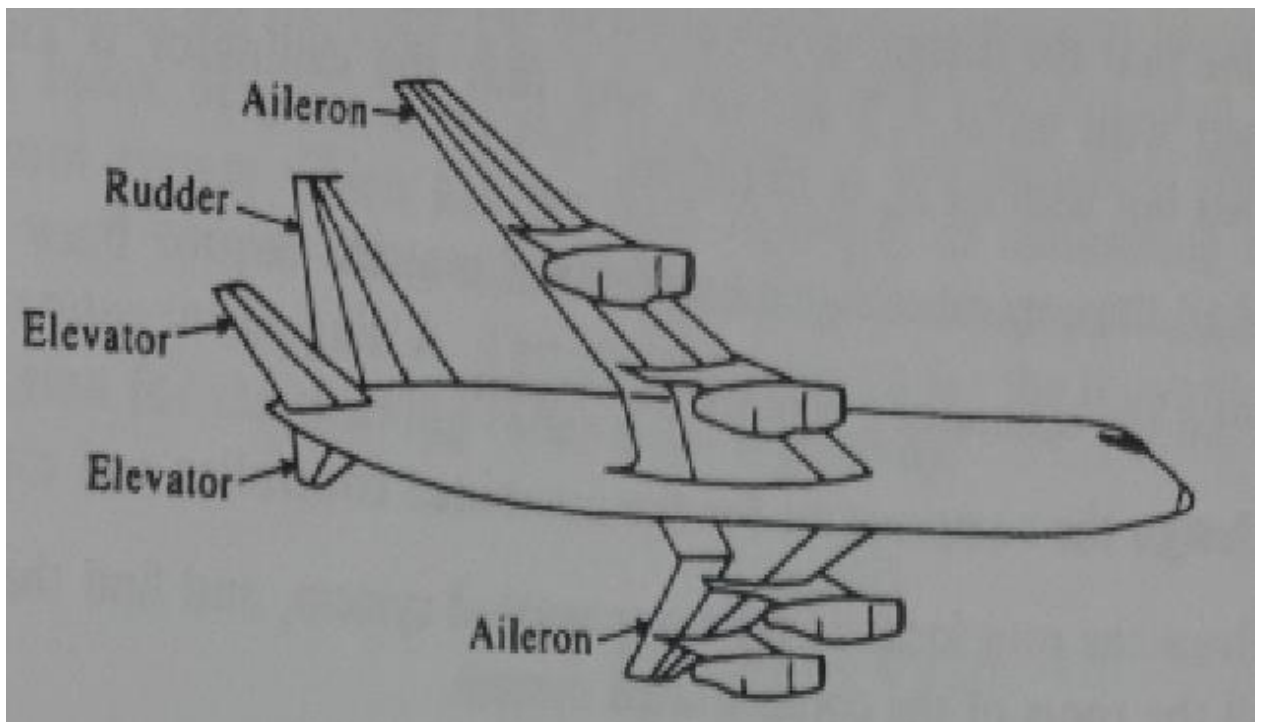


**Figure 1.2** Location of Aileron, rudder, elevator on the aircraft.

In figure 1.2, the control surfaces on both wings are used basically to control the heave rate of the airplane while aircraft speed is constant in the context of longitudinal dynamic control, whereas elevator movement in the horizontal tail mainly controls the pitch of the aircraft.

Knowing that these control surfaces are interactive, and the corresponding responses are highly dependent on both of them. This contribution will investigate these two input controls in the context of multivariable control and study two controlling methods to achieve the optimum controller design for the airplane during landing.

The landing of military aircraft on carriers adds further challenges to the pilot, where he or she needs to arrest the aircraft safely within a relatively short distance. This raises the importance of handling qualities which help the pilot to better handle the controls and consequent the aircraft response during this critical phase of landing on aircraft carriers.

To recapitulate, the multiple tasks imposed on the pilot at the landing stage add further pressure. For Example, in lateral control, (G. E. Cooper and R. P. Harper, 1969) summarized three main tasks to be performed by the pilot simultaneously as the aircraft approaches the ship: guiding the aircraft along the extended centreline of the flight deck, maintain the aircraft on the correct glidescope, and maintaining the correct speed. This necessitates minimizing, by design, the required inputs to be handled by the pilot when it comes to longitudinal control such as heave and pitch rate control which is the subject of this paper.

## **1.2 Research Problem Statement**

The control of pitch and heave rate will be investigated in this paper. The theme for this problem is presented by the model of (Whalley & Ebrahimi, 2000) in designing a controller with

one input-two-output model. Another control surface will be added to the aircraft, at the horizontal tail, in order to have better controllability on pitch rate with minimum decoupling between the two system outputs.

During critical flight modes, such as landing, the pilot controls the aileron on the wings and horizontal tail planes to ensure precise and safe landing on the carrier's deck. Responsiveness within reasonable time for pilot's input is also a major concern when designing the controller.

The coupling between system outputs is a common problem in multivariable system analysis. The alteration of one input could effect on all system outputs. Because this may adversely affect the whole system behavior, controller design should minimize the effect of decoupling.

External disturbances and air gusts may lead to catastrophic consequences if not properly perturbed by proper design for the controller. The aircraft structure and configuration has also a considerable role on disturbance recovery.

The limited available power from the aircraft and the desire to minimize the actuator movement, wear and heating motivate the effort to control the aircraft motion with minimum possible power. The movement of control surfaces needs a reliable source of power. However, the power consumption can be minimized by a creative structure design of the aircraft's planform and the control method employed. The achievement of this approach will be reflected not only on minimizing the consumed fuel, it will also elongate the life of components of the control system, reduce the noise, wear and maintenance requirements.

### **1.3 Research Aims and Objectives**

The least effort optimization approach presented by (Whalley and Ebrahimi, 2004) is deployed in this research to take the advantage of multivariable controller with minimum

consumption of energy. The proposed controller aims to fulfill the requirement of effective heave and pitch rates of the aircraft with minimum compromise of conflicting design requirements. The fast response time and acceptable dynamics are also targeted in designing the controller. Stability of the closed loop system must be achieved with maximum possible decoupling between system outputs. An attempt to fulfill the requirement of disturbance recovery will also validate the robustness of the system.

A design strategy to improve aircraft motion control is to be introduced by adding another input to the model suggested by (Whalley and Ebrahimi, 2000) taking into account the configuration of the aircraft and the existing dimensions. Then, the control strategy is considered to improve the aircraft motion control particularly under deck landing conditions.

### **1.3 Research Dissertation Organization**

Chapter one introduces the problem of aircraft landing in limited and on moving surfaces such as carriers and suggest the solution of handling quality from a structure design and control perspectives.

Chapter two provides a literature review of previous work in the field of aircraft dynamics and the control system design. The impact of major historical events such as World Wars I and II on the development of aircraft design will also be presented. It also introduces the two important related subjects of stability and handling quality.

Chapter three shows the parallel evolvement of aircraft dynamics and control theory. It also presents the advantages of adjoining these two fields of study. A comparison between classical and modern control theories is explained with advantages and limitations of each approach.

Chapter four presents the model of the aircraft dynamics and the control methodology applied to the F-14 Grumman aircraft. Two control strategies and full derivation are implemented: firstly, the least effort controller with inner and outer loop analysis regulator is shown in details. Secondly, the inverse Nyquist method with full derivation is presented. Finally, the chapter concluded with derivation for the distance required by aircraft to reach complete stop with assistance of arresting gear.

Chapter five implements the least effort strategy and inverse Nyquist on the system model. The simulation and results will be discussed, including the response for step inputs and the disturbance recovery characteristics. Energy dissipation using each control methodology will be simulated for sake of comparison.

Chapter six demonstrates the advantage of two-inputs, two-outputs compared to single-input, two-output system. The value of adding another input to improve the handling quality and decoupling between system outputs will be also addressed. Another comparison will be discussed between the two control methodologies simulated in chapter five, the pros and cons of each methodology will be highlighted.

Chapter seven concludes the research and discusses the advantages of the new control methodology and recommendations for future work and development.

## **Chapter II**

### **Aircraft Development Review**

#### **2.1 Introduction**

The Wright Flyer, in 1903, was the first sustainable, powered flight. The problem was to overcome the force of gravity using the engine's thrust and aerodynamic forces on the wings in a controllable manner. Based on the progressive studies of the aerodynamic forces and aerodynamic moments, a new methodology was used for analysis (Tewari, A., 2007).

Several attempts had been made before the Wright brothers demonstrated their first man carrying flight. The most famous attempts were made unsuccessfully by Otto Lilienthal (1848-1896), Hiram Maxim (1840-1916), and Dr Samuel Langley (1848-1896). Lilienthal experiment resulted in a catastrophic result which led to his death. Langley's uncontrolled flight flew successfully at quarter scale and fell apart at full scale. Maxim's airplane was broken even before leave the ground on its test track. At this point of airplane development history, airplane design was done empirically while scientists and mathematicians were forming the foundation of fundamental aeronautical theory. For example, Wright brothers stated, after building the first flying aircraft, that solutions to the stability and control had to be found. Aeronautical theory started to have an impact on practical aircraft design after World War I (Abzug and Larrabee, 2002).

In the period between the two World Wars, priority was given in Great Britain to satisfy the requirement of military aircraft handling quality. The (Mark Series) British

military aircraft were equipped with single and two axis control. For example, Mark I aircraft utilized a single axis Gyroscope which was used to measure the pitching and heading positions as feedback to control the rudders and the elevators by pneumatic servos. In applications involve automatic pilot in aerial map-making, single axis gyroscope were more efficient compared to three axis Gyroscope which developed by E. Sperry. The three axis gyroscope, however, prove superiority when high level of maneuverability is required (Mc Reur et el, 1973).

The lateral directional motion was investigated in 1926 by Garner using feedback control. His work leaned on earlier work of Baristwo and Glauert, and the method suggested by S.B Gates. Further elaboration was developed by including the time delay in the control response analysis of airframe. (Mc Reur et el, 1973).

The year 1933 cultivated earlier efforts to develop a reliable automatic pilot which was finally used to realize a flying of aircraft around the World in 7 days.

The final significant improvement in aircraft development before World War II was the utilization of magnetic compass by the German firm of Siemens in 1935. The magnetic compass was used to control the elevator and rudder by hydraulic servos and rate gyro feedback (Mc Reur et el, 1973).

The first Jet transport aircraft came to light in 1949 with the name, de Havilland Comet. Designers aimed to reach new limits in terms of supersonic speeds, exceeding Mach 3. In the early 1950s, special fuels, special material, high speed aerodynamics, aerothermodynamics were also thoroughly studied disciplines during the five-year test program which started in 1951. By the end of 1950s, the X-15 Rocket plane exceeded Mach

6 at 300,000 ft. Altitude and an adaptive control system was utilized instead of aerodynamic control to overcome the inefficiency of this procedure, at high altitude. In the early 1960s, the French Mirage and later F-4 Phantom made record breaking speed of Mach 2.3 and 2.4 respectively. The Boeing 707, Douglas DC8 passenger jets, and the Aerospatial-British Aerospace Concorde SST are all examples of civil aircraft designed during 1960s. The digital computer was starting to have a major impact on aircraft design and the techniques used to control them. Numerical analysis techniques and simulation of aircraft control started to have greater effect on the reliability and design cost (Stevens and Lewis, 2003).

## **2.2 Aircrafts Development in the 20<sup>th</sup> century**

Theoretical and practical approaches for aircraft design had a considerable disjunction in the first half of twentieth century. For example, Garner and Cowley of Royal Aircraft Establishment (RAE) extended the work of Bryan (1911), Bairstrow and Melvill (1913) on aircraft stability, but they had to leave a provision in their theoretical approach to compensate for the time lag in the control actuators. The reason for the gap between theory and practice was mainly due to difficulties in computing the large number of equations used to describe the motion of aircraft and the corresponding stability of the mathematical models (Bennet, 1993).

Trial and error, cut and try, and proportioning methods were the dominating approach for stabilizing and sizing control surfaces during the first 50 years of aviation. With absence of systematic approach for dynamic and control of the aircraft, study of aircraft dynamics and control lagged behind practical design. However, mathematical theory and stability

techniques were developed at that time but they were not properly utilized in the analysis of aerodynamic motion. The twin pillar for aircraft design procedures, Simulation and analysis, were developed during world war II with the application of servomechanisms and digital computer methods. This was stimulated by the need for extend flight envelopes, VTOL airplanes, helicopters, hydrofoil boats, winged missiles, and many other applications which affected the techniques of the design of automatic flight control system design (McRuer et al., 1973).

### **2.2.1 Aircraft Dynamics**

Professor George Harley Bryan laid the foundation for airplane motion mathematical modeling, by assuming a 6-degrees of freedom rigid body motion. About a decade earlier, the longitudinal equations of motion for aircraft were developed by Bryan with collaboration with W.E Williams. These contributions by Bryan leaned on Sir Isac Newton's (1642-1727) and Leohnard Euler's (1707-1783) theories. Bryan's equation of motion introduced in 1911 are still used in the design and simulation of today's aircraft (Abzug and Larrabee, 2002).

There were momenteous achievements during the first decade of twentieth century in aerodynamic design. With many improved flight demonstrations by Wilbur Wright in France and Orville Wright in United States respectively in 1908, airplane builders such as Curtiss, Bleriot, the Voising, Bachereau, Farman, Lavavasseur, Esnault Pleterie, and others even flew faster than Wright could do. However, all those demonstrations were done without a profound understanding of aerodynamic theory (Abzug and Larrabee, 2002).

Bryan and Williams, in 1903, developed the first powered flight using conventional mathematical models. The equation of motion were linearized around trim conditions which established further studies of dynamic stability and response to the control inputs. Later (Bryan, 1911) presented the theory of longitudinal and lateral motions. He utilized Euler's six equations of motion for rigid bodies for small perturbation around steady state conditions. With those assumptions, the equations of motion were shown to be separable into two groups. One group is the motion around the plane of symmetry; the other is out of the plane of symmetry. The complete Solution for those equations was due to (Melvill, 1934) who solved the equations of motion overcoming all the challenges and difficulties experienced at that time.

From the fact that the motion of an aircraft is modeled for small perturbation about the equilibrium trim state, the response variables and transfer function are linear. Hence, the response to control is assumed linear about "small perturbation". Practically, the errors incurred with such assumption are acceptably small with tendency of airplane to exhibit linear aerodynamic characteristics within its flight envelope. For extended flight envelopes, non-linearity in aerodynamics arose and it is not a common practice to model the equation of motion for small disturbance under these circumstances. With advent of powerful computational tools nowadays, solutions for the equations of motion can be easily achieved. The superior ability of computers in handling numerical, matrix calculations drew attention toward developing methods for solving linear dynamic system problems, in modern applied mathematics (Cook, M. V., 2007).

The wire braced biplane with tail surface aft of the the airplane was established during World War I, in 1917, as a result of trial and error approach. The main limitation of that design was the torsionally rigid structure adversely affect the airplane twisting leading to instability at higher speeds. Roll motion could be applied by aileron deflection, pitch angle could be modified using the elevator deflection, and the yaw action was controlled by the movement of the rudder. The controls were affected by aerodynamic hinge moments (Abzug and Larrabee, 2002).

The static and aerodynamic coefficients of aircraft can be identified using wind tunnel test. To measure static coefficient (coefficients appear in the equation of motion measures the coupling between lateral and longitudinal motions), a mounted scale model is used with attached strain gauges at different location on its surface. Aerodynamic coefficient models are subjected to oscillatory motions, hence, derivatives of acceleration and damping are measured as shown by (Queijo, 1968). However, empirical methods are used to impose certain frequency limits on the steady flight conditions and quasi-steady assumption as suggested by (Duncan, 1952).

Test-flights are also used for measuring aerodynamic coefficients. (Maine and Iliffe, 1980) suggested that coefficients are measured by simulating the disturbances from steady state conditions by the movement of the control surfaces. This method relates coefficients with altitude and Mach number for a certain flight configuration. Another common method was developed to measure aerodynamic coefficients is CFD. This is a computer program technique with the theory of stability and control which are built into its code (Hoh et al.,

1982). This method used the aircraft geometrical configuration as input data (Stevens and Lewis, 2003)

In 1922, NACA (National advisory committee for Aeronautics, the predecessor of NASA) built a wind tunnel in Virginia for subsonic flight model testing. It was, in simple approach when a pressurized tank (up to 20 atm) called the variable density tunnel (VDT) which was used during 1920s and 1930s to provide data related to NACA airfoil sections, at different Reynolds numbers with free flight conditions (Anderson, J. D., 2001).

In the next half of last century, mathematical framework required a convenient axis, hence, (Hopkins, 1972) developed a notation system axis describing the motion of an aircraft. Further development and evolution for this notation scheme can be found in (Etkins, 1972) and (Mc Reur et al, 1973).

### **2.2.2 Aircraft Control**

The basis of aircraft motion control depend on the flap-type control surfaces employed. A portion of the wing or tail surface is hinged to generate the control forces and moments on the airframe corresponding in airplane motion. At supersonic speeds, the effect of control surfaces reduce and different control strategies are used. For example, the F-14 aircraft uses the swept-wing to reduce drag effects at high speeds. Figure 2.1

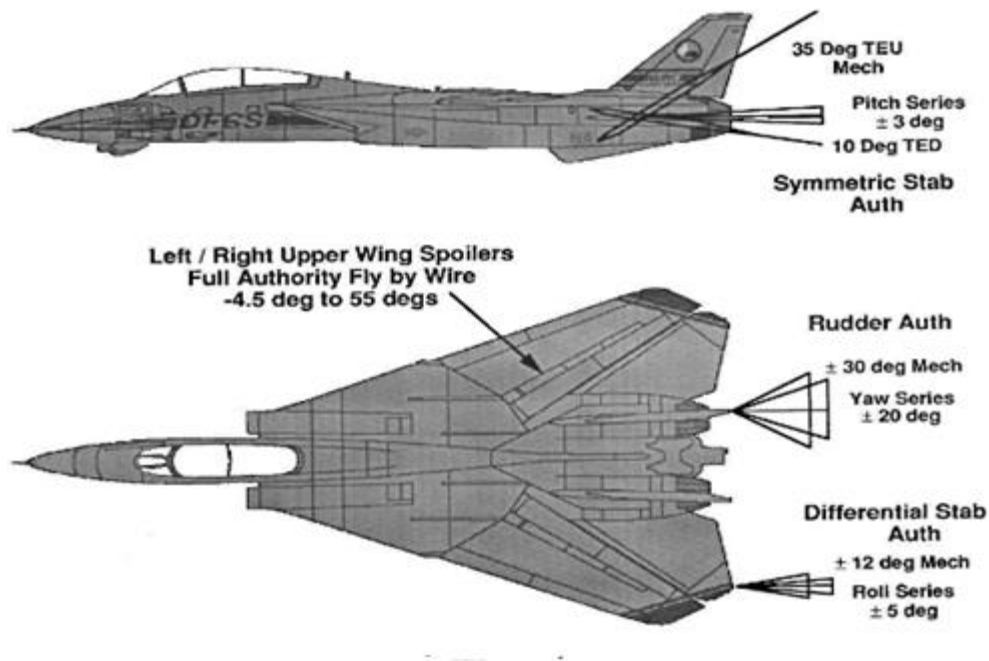


**Figure 2.1** F-14 Aircraft actuator surfaces

(Balas et. el., 1998)

The first flap-type lateral control flight was built by Glenn Curtiss in 1908 in what is considered an improvement on Wright Brother’s wing warping. The Curtiss design was simply connecting the input control to internal struts attached to both moving wings. Flap-Type control surfaces were first called as “aileron”, while The Germans used the term “querrudern”. The term “aileron” has persisted in the English language, although the first aileron control was built in the first decade of twentieth century by French Farman biplane. Flap-type aerodynamic theory was did not exist untill 1927 unilt the design by Herman Glauert. The small movable parts at the rear of the wings, elevators, and rudders are known as control surfaces. The aerodynamic pressure generated by these tabs by a moving moment arm about the control surface hinge line. Control surfaces are deflected in the opposite

direction to the deflection of the tab with main airframe surface as a reference (Abzug and Larrabee, 2002).

Bryan's book was lacking information about moments and force control, and the treatment of airplane as a control object. Although his famous perturbation equations incorporate stability, they did not include control derivatives. Also gust effects or external disturbances were not addressed. However, Bryan recognized those uncovered topics and recommended further studies which were considered for years of research thereafter (Abzug, and Larrabee, 2002).

Different types of flap geometries are used as shown in figure 2.2. Different geometries have advantages and, naturally, drawbacks depending on the application, the airplane configuration, and the state of flight. Further explanation on geometry selection can be found in (Kroo, I., 2001) and (Raymer, D. P., 1992).

The structure of the airplane is subjected to aerodynamic loads, moments and forces, due to either external gusts or the movement of the flaps, or control surfaces. The movement of each control surface, usually, resulted in a significant movement of the aircraft about one of the 6-axes of motion, and minor effect on other axes of movement. This is known as the coupling effect and can be quantified by finding the aerodynamic derivatives introduced by (Bryan, 1911). These aerodynamic derivatives can be found theoretically or experimentally (flight tests and wind tunnels experiments). The control surfaces and corresponding major movements is shown in figure 2.3.

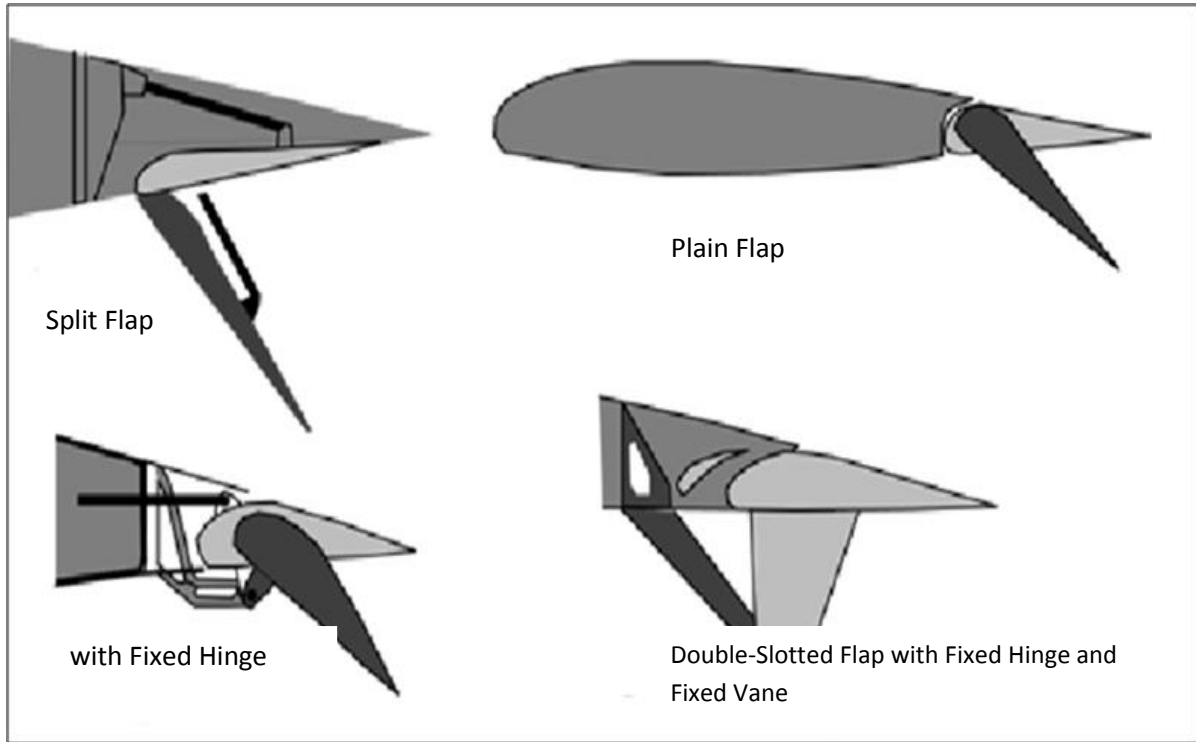


**Figure 2.2** Flap System Geometries

(Kroo, I., 2001)

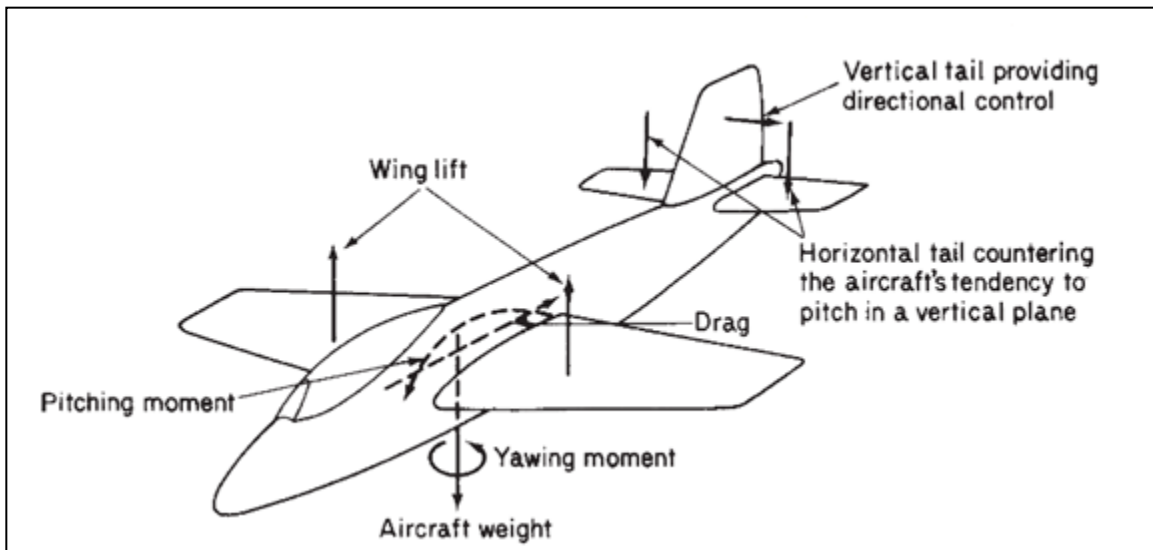


**Figure 2.3** Principal aerodynamic forces on airplane

(Kroo, I., 2001)

Several designs were developed to attached handles, pedals, and wheels to steer, man carrying, flying objects. One design was provided by Cayley who used a cruciform blade to change the vertical and horizontal direction of a glider, as shown in figure 2.4

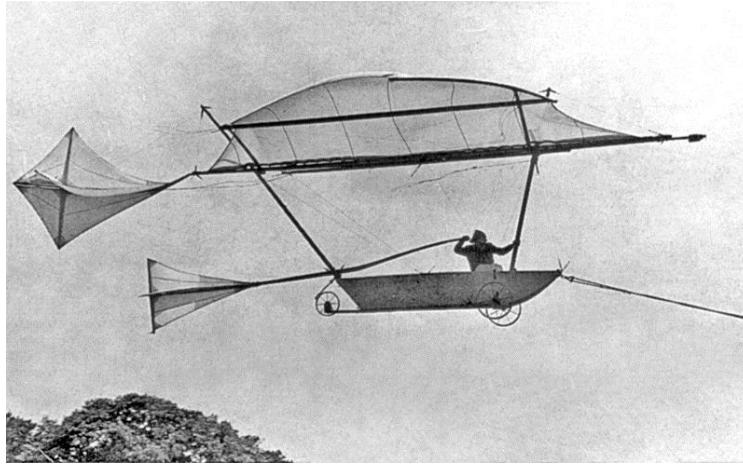


**Figure 2.4** Design of Cayle flying object

For small perturbation, the aircraft dynamic system analysis and solving the equation of motion is a prerequisite for designing and analyzing flight control system. Hence, the tools for multivariable system theory are used to solve the equations of motion (Cook, 2007).

Various dynamic systems in the field of aerodynamics using state space description can be found in Friedland (1987) and Shinnars (1989).

From the fact that the motion of an airplane is modeled about small perturbation about the equilibrium trim state, the response variables and transfer function are approximately linear. Hence, the response to control is assumed is considered linearized about “small perturbation”. Practically, the errors incurred with such assumption are acceptably small with tendency of the airplane to exhibit linear, aerodynamic characteristics

within its flight envelope. For extended flight envelopes, non-linearity in the aerodynamics arise and it is not common practice to model the equation of motion-response combinations about small disturbances (Cook, M. V., 2007).

The German inventor Anton Flettner was the first who introduced the tab concept in 1922 and applied them on steamboat rudders. In some reference, the term “Flettner’s” is still used interchangeably with tabs. In aeronautic applications, Flettner described a spring type tab device. W.G. Perrin extended Glauret’s aerodynamic flap-type controls theory to the tab case during 1928 (Abzug and Larrabee, E. E., 2002).

For large parameters variations, the analysis of mechanical systems and structures were investigated by (Whalley and Ebrahimi, 1997).where the variation in performance accompanied with operational conditions was studied. The paper shows that for aircraft applications there are significant changes of tailplane and rudder rigidity at different velocities. This becomes critical at lower speeds.

Multivariable control was also used in (Whalley et. el., 1999) to analyze the whole mechanical drive system for weapon platforms to control the armature regulator changes and load inertia position by two inputs which are motor torque variation and retarding unit torque changes.

For small perturbation, the aircraft dynamic system analysis and solving the equation of motion is prerequisite for designing and analyzing flight control systems. Hence, the tools for multivariable system theory are available to solve the equations of motion (Cook, 2007).

### **2.2.3 Automatic feedback control of aircraft**

Aircraft design progress had a great impetus during World War I between 1914 and 1918. Although a pilot was able to perform control and stabilizing functions on aircraft, a sustained development of automatic control was not available. Leaning on Bryan's theory of small perturbation about steady state conditions, in 1920's, stability derivatives, or coefficients, were measured and calculated; and Bryan's theory was further confirmed through flight-tests. There was still a gap between theory and practice mainly due to the difficulty of finding the roots of equations at that time. Using a reference sensor, Gyroscope, and pneumatic servomechanisms to position the control surfaces, had fueled the development of autopilots. A Sperry autopilot assisted in the first flight around the world in less than eight days, in 1933 (Stevens and Lewis, 2003).

After World War I, radio-controlled aircraft and autopilots were of special interest, particularly with the military authorities. In the USA, the driving authority for that interest was: the Naval Research Laboratory, while in Britain, the Royal Aircraft Establishment (RAE) carried out secret research programs related to autopilot and radio-controlled aircraft. However, some patents, such as Meredith and Cook in 1926 and 1927, were allowed to register after the RAE removed all data which might be used by others to develop pilotless aircraft. In Germany, Edward Fischel successfully directed a research program by Siemens to develop an electro-hydraulic system that provides a stabilizing role in pitch and roll (Bennett, 2008).

During 1940s, control engineering emerged as a new discipline. Mathematical analytical methods were developed and practiced which for positioning heavy masses

precisely such as guns' launchers and heavy ships were highly critical in war time. However, this was has its origin in 1920 following Minorsky's work on automatic steering for ships and the positioning of guns (Nagrath, I.J. and Gopal, M., 2007).

#### **2.2.4 Stability of aircraft**

Great strides in the design of aircraft were made during the World War I. It was found that acceptable stability for pilots could be achieved by suitable sizing and shaping of aircraft's aerodynamic surfaces. However, many aircraft in use exhibit unstable characteristics which could be eliminated by the pilot by using feedback control. In warplanes, automatic pilots and stabilizers were found to be unsuccessful (McRuer et al., 1973)

Many flight conditions exhibit inherent stability at certain attitude and dynamics which, naturally, imply that there was no need for control effort, to sustain stable flight characteristics. However, augmentation of aircraft control systems becomes common practice, as flights with no requirement for control or guidance are seldom used nowadays (Tewari, 2011).

The first Serious attempt to analytically investigate the dynamic stability of aircraft were presented by (Lanchester, 1908). He made his studies on glider models and analyzed the motion of a symmetrical plane in the form of equation of motion. He first used the term "Phugoids" to describe the flight paths, which still used to this day.

The inherent stability concept as suggested by Bryan quoting as follows:

“ apart from the fact that movable parts are liable to get out of order, it must be remembered that they increase the number of degree of freedom of the machine, this further adding to the number of conditions which have to be satisfied for stability- a number quite large enough already. I anticipate that the successful airplane of the future will possess inherent not ‘automatic’ stability, movable parts being used only for purpose of steering.”  
(Bryan, 1911)

Several attempts were made to build aircraft which were inherently stable. The first inherently stable flight attempt was made by O. Lilienthal which, unfortunately, killed him. He sat up the mass as a reference for the achieved stability instead of the ground, and the control power to his flight was insufficient to overcome gust disturbances. The concept of inherent stability was rejected by Wright brothers who stated “we therefore resolved to try a fundamentally different principle. We would arrange the machine so that it would not tend to right itself.” Pilot intervention was required to fly their airplane, therefore, control surfaces were provided to enable him to do so. However, sensation of the aircraft motion was required by the pilot with visual contact with the ground. This, in dark and foggy conditions, was a challenging task for the pilot (Bennet, 1993).

Unfortunately, aircraft dynamics do not possess inherent stability. Correction and augmentation should be applied to modify the stability characteristics of the airplane. This was realized by adding feedback mechanism. The first automatic feedback control utilized for aircraft was developed in 1914. It was aimed at meeting the handling quality requirements in full flight. Although it was largely empirical at that time, they have made significant progress in the period until end of World War II (McRuer et al., 1973).

In 1914, Sperry demonstrated the first autopilot airplane in Paris. He used a gyroscope as a stabilized reference platform; with a train of mechanical, electrical and pneumatic components used to detect precisely the aircraft position relative to a reference and apply correction signals to the aircraft's control surfaces. Longitudinal motion, represented by pitch, and lateral motion, represented by roll, were controlled by a stabilizer with two minor feedback loops taken from the deflection control surfaces. Sperry's system also showed some level of adaptability; the anemometer signal used to adjust the fulcrum lever to adapt the gain value to match the airplane's speed requirements (Bennett, 2008).

From practical stand point, providing sufficient information about stability is realized by stability computation, about small disturbances from the steady state, in other words, the linear eigenvalue problem which is part of the system study is used (Raymer, D. P., 1992).

The longitudinal static stability theory was analyzed by (Gates and Lyonn, 1944); Static and dynamic longitudinal stability which was analyzed and investigated.

Bryan's stability derivatives were calculated, based on the assumption that the forces on the airfoil are perpendicular to the airfoil chord. However, the limitations of this assumption were pointed out by W. Hewitt Phillips who showed that this assumption, surprisingly, is more accurate for supersonic aircraft rather than subsonic aircraft (Abzug and Larrabee, 2002).

Since the first successful flight until the 1940s, the Routh-Hurwitz testing criterion for instability for airplane motion was occasionally used. G.H Bryan and W.E Williams analyzed the longitudinal stability of an airplane. They wrote:

“in order that the steady motion may be stable, the roots of the bi quadratic [  $A\lambda^4 + B\lambda^3 + C\lambda^2 + D\lambda + E = 0$ ] must either be real negative, or complex with their real parts negative and Routh finds that this will be the first case if the six quantities  $A, B, C, D, C$  and  $BCD - AD^2 - EB^2$  are all of the same sign” (Bryan,1911)

In most cases, input disturbances applied to the linear equations of motion of an aircraft are not really small, so some degradation of the stability definition must be expected. Nevertheless, as is often the case, this will not lead to difficulties due to fact that the model of an aircraft degrades slowly with increasing disturbance amplitude. Therefore, linear system stability theory is still valid, for general aircraft applications (Cook, M. V., 2007).

Static and dynamic stability are inseparable and must be investigated as an entity in real applications. For safety purpose, aircraft must poses acceptable level of static and dynamic stability. Moreover, the degree of stability is crucial in identifying and quantifying the efficacy of the controls of the aircraft.

Assessing the stability and control characteristics of an airplane may give rise to failure in meeting the flying and handling qualities requirement. These deficiencies usually result from extending the flight envelope with the nonlinearities arises at extreme operating conditions. Because it is not practical to modify aerodynamic design once the design is finalized, remedial action is usually presented as an artificially augmenting, or modifying, airframe’s stability characteristics, by applying a negative feedback. This will raise the role of available powerful control engineering tools, in analyzing aircraft motion and stability in what is known as the “system approach” (Cook, M. V., 2007).

### **2.2.5 Handling quality**

In flight dynamics, flying qualities and performance are the main fields of study. However, aircraft design and control are of a prime importance when the flight attitude is needed to be measured and controlled (Boiffier, 1998).

The set of requirements and performance characteristics identification are prerequisites for designing a control system for aircraft applications. However, in pilot controlled aircraft it is quite a difficult task, sometimes impossible, to quantify those requirements due to the reason that acceptable performance parameters are highly dependent on the aircraft type, phase, task, and pilot opinion. This latter factor involves many tangible and intangible parameters which differ from one pilot's opinion to another. For example, for commercial transport airplanes the concern and priorities of the pilot is completely different when compared to a pilot who is maneuvering with a fighter.

Modern aircraft design concerned with handling quality rather than stability and control theory although latter is main constituent of the concept of handling quality. Handling quality, or interchangeably called "pilotability" is defined by (Boiffier, 1998) as the "translation of the pilot's ability to accomplish his mission with aircraft".

Because of the aforementioned reasons, handling qualities are influenced by parameters that exceed the control system and aerodynamic property considerations. Visibility of the pilot inside the cockpit, the accessibility to aircraft consoles, and the ergonomics inside the cockpit are among the main factors which affect handling and flying qualities. Therefore, (Cooper and Harper, 1969) introduced a scale which defines a rating for

pilot opinion about aircraft handling quality uses a systematic method. Another contribution in this field was by (Chalk et al., 1969; Moorhouse and Woodcock, 1982) laid the background information about military aircraft handling quality specifications, as considered in MIL-F-8785B and MIL-F-8785C standards.

A summary of requirements for the flying qualities of military aircraft were established by the British Defence Standard DEF\_STAN00-970 “liberal reference” while in USA the American standard for military aircraft is MIL-F-8785C. The first attempt to standardize the requirement of suitable flying qualities in highly augmented airplanes, were presented by Hoh et al (1982) and (Cook, M. V., 2007).

In flight dynamics, flying qualities and performance are the main fields of study. However, aircraft design and control have prime importance when the flight attitude is biased towards the aircraft definition (Tischler, 1987).

## Chapter III

### Control Theory Review

#### 3.1 Introduction

Prior to 1940s, designers and engineers were practically far ahead of the theoretical advancement in the field of control engineering. Automatic control was indeed an art rather than science in most cases (Nagrath and Gopal, 2007).

Looking at control system design as integrated whole is not a new approach, a quote from Zielger and Nichols paper in 1943:

““ In the application of automatic controllers, it is important to realize that controller and process form a unit; credit or discrete for results obtained are attributable to one as much as the other. A poor controller is often able to perform acceptably on a process which is easily controlled. The finest controller made, when applied to a miserably designed process, may not deliver the desired performance. True, on badly designed processes, advanced controllers are able to eke out better results than older models, but on these processes, there is a definite end point which can be approached by instrumentation and it falls short of perfection”” (Skogestad and Postlethwaite, 2005).

#### 3.2 Early History of Control theory Development

The mathematical tools required to describe control systems were developed in the eighteenth century. Although differential equations concept was developed by Isaac Newton (1642-1727) and Gottfried Leibniz (1646-1716) in the late seventeenth century, it was not utilized in the context of modeling for dynamic systems until Joseph Lagrange (1736-1813)

described mathematically the Watt fly ball governor. Further development for Lagrange's work was presented by Sir Hamilton (1805-1865) during the nineteenth century (Chalk, C.R. 1958).

Inspired by these events, the speed control unit for a telescope was built by George Airy (1801-1892) in the nineteenth century. The purpose of Airy's speed control unit is to compensate for the changing position of the telescope due to the earth's rotation. James Maxwell (1831-1879), then, analyzed systematically the stability of a governor that is similar the one used by Watt's steam engine. Maxwell linearized the equation of motion around the governors' operating point, presented the concept of the characteristic equation, and showed that roots of characteristic equations must have negative real components, as a condition for stability. This was considered as the foundation work for control theory (John and Lumkes, 2002).

Applications such as windmill, water wheel and steam engines, were known as prime movers in the 19<sup>th</sup> century. The same concept and terminology was extended to include a weight-driven apparatus for water and steam turbines. Engine governors were widely used in various applications at the end of 19<sup>th</sup> century. The challenge of regulating prime movers was met by scientists, and instability issues were resolved in spite of not yet having methods of measuring small fluctuations in speed. Instead of working on the dynamics of the governors, the focus was mainly on mechanical aspects such as; size reduction, friction reduction to adjust the speed, and improved relay mechanisms. However, investigations of dynamic behavior and the formulation of criteria for determining stability were stimulated by the use of governors, such as Airy's work on regulation of the motion of telescopes (Bennett, 2008).

### 3.3 Development of Classical Control Theory

The term “feedback” appears in 1920, although it was called “closed cycle” by scientists in the United States and “reset” by English scientists. It was adopted by the Bell Telephone laboratory by communications engineers. Although it has its roots in analyzing economical and political systems, the theory of feedback systems and its mathematical formulation were mainly developed by engineering (Bennett, 2008).

The twentieth century heralded further applications and advancements in control system design. The impetus for these developments and growth as suggested by (John and Lumkes, 2002) was: the introduction of the Telephone, World War II, and microprocessors. The three mode controller was analyzed by the Russian Nicholas Minorsky (1885-1970) in 1922 during his study for automatic ship steering system. Minorsky’s three mode led to what is known today as: the PID controllers. The Feedback amplifier was invented by Harold Black (1898-1983) near the same time, driven by the development of the telephone. He demonstrated the important role of amplifier and negative feedback in amplifying the voice signal particularly for long distance communications. The period thereafter marked a significant interest in the study of automatic control theory. Harold Hazen’s(1901-1980) introduced the theory of servomechanism. Relying on Black’s amplifier, Harry Nyquist(1889-1976) and Hendrik Bode (1905-1982) worked on system stability. In 1932, Nyquist, also working on telephones at the Bell laboratories developing his famous stability criterion by using polar plots for complex function. Few years later, in 1938, Bode introduced the concept of gain and phase stability margins using frequency response plots. The work of

Bode and Nyquist had major impact stability and stability margins for systems designed in the frequency domain.

During World War II, mathematicians and engineers jointly established the concept of control engineering. The critical demand of controlling large loads precisely and with high speeds in applications such as weapons and rocket launchers, led to the concept of servomechanism and the coherent subject of control systems engineering (Bennett, 2008). In addition, the need for improved, volume manufacturing and rapid production processes, led to the use of automatic control. Examples of these processes are the treatment of chemicals and metal which became more efficient where processed by the use of automatic control (Nagrath and Gopal, 2007). This was the foundation for a systematic approach to the design of control systems.

### **3.3.1 PID Controller**

Ziegler-Nichols is an empirical method used to set up the parameters of PID controllers. This method leans on stability analysis where critical gains (gains at which the system is marginally stable) are identified and consequently, with empirical equations, the parameters for proportional, integral, and derivative components are presented (Zeigler and Nichols, 1942).

### **3.3.2 The root locus method**

Soon after the war, in 1948, a new graphical technique by W. Evans (1920-1999) “Graphical Analysis of Control Systems” that used a technique of tracing the migration of the roots of the characteristic equation was published. This technique, namely the root locus technique, had major contributions in massive number of applications. Along with frequency

response techniques, root locus is considered a key element of what is known as classical control theory (Evans, 1950).

Root locus is a powerful design method based on an open loop transfer function. It provides the position of closed loop poles with variation in, most commonly, the loop gain variable. With root locus diagrams, variation of the loop gain is plotted until the best closed loop performance is identified. Closed loop zeroes are a subset of the open loop zeros plus the feedback element  $H(s)$  poles. Thus root locus plots can be used to find all possible closed loop transfer functions, and corresponding performance, with the variation of one variable (Dutton et. al. , 1997).

### **3.4 Modern control History**

With the advent of digital computers, optimal control theory and the state variable approach introduced; modern control theory. This term dominated control theory during 1960s. During 1960s and 1970s massive amounts of work on modern optimal control theory was performed and applied. A new technique emerged in 1980s, known as  $H_\infty$  control theory that combines classical and modern control theory approaches to provide a complete answer. Credit was given to Zames for introducing this method in his paper in IEEE (Zames, 1981). Zames  $H_\infty$  dominated the control system development in 1980s and 1990s (Shinners, 1998).

The first known usage for digital computers in automatic controllers was in the 1950s when the aerospace company TRW developed a MIMO digital control system. While the cost of analogue systems increase with the increase of controller complexity, the initial cost for digital computer which is able to handle arrangement of Multiple-input Multiple-Output systems can be justified. This is why many digital controllers were in use in a variety of

applications in industries in early in 1960s. In the same decade, many new theories were presented in what was considered as the eruption of modern control theory. Several papers were published by R. Kalman detailing the application of Lyapunov's work. Also Kalman developed Kalman discrete and continuous filter in the field of optimal control and optimal filtering. To allow digital controller design in the frequency domain, classical theory was also revisited from new perspective (John and Lumkes, 2002).

### 3.4.1 State Space Method

State space technique was introduced by (Kalman, 1960) in which he defined the system based on time dependent parameters called state space. The state of the system as defined by (Dorf and Bishob, 2012) is:

*“a set of variables whose values, together with the input signals and the equations describing the dynamics, will provide the future state and output of the system”.*

He also describe the function of state variables as:

*“ The state variables describe the present configuration of a system and can be used to determine the future response, given the excitation inputs and the equations describing the dynamics.”*

However, state space variables are not necessarily measurable nor controllable which make it different from the system output which must be measured and controlled.

State space presentation is basically represented by two equations: first equation is first order differential equation relate the input to the system to the minimum set of time domain variables, or state space:

$$\dot{x}(t) = \mathbf{A}x(t) + \mathbf{B}u(t) \tag{3.1}$$

The second equation represents the output of the system based on the input and the state of the system described in the above equation:

$$y(t) = \mathbf{C}x(t) + \mathbf{D}u(t) \quad 3.2$$

Where **A, B, C, and D** represents matrices which best describe multivariable control system. After some manipulation and linearization, the transfer function for strictly proper ( $D = 0$ ) system become in frequency domain form:

$$Y(s) = [sI - \mathbf{A}]^{-1}\mathbf{B}U(s) \quad 3.3$$

Or in transfer function format as:

$$G(s) = [sI - \mathbf{A}]^{-1}\mathbf{B} \quad 3.4$$

Multivariable theory has proved to be superior for applications with independent inputs due to its powerful computational capabilities. By way of, unlike scalar Laplace transfer function methods, accurate system modelling is crucial to obtain acceptable results, which is challenging for many applications.

### 3.4.2 Optimal Control

In the late 1940's, (Wiener, 1949) presented the idea of optimum design based on optimization of a performance criterion. A year later, (McDonald, 1950) extended the concept of optimization to control systems setting a goal of minimizing transient time of a relay type feedback control system subject to a step input. Minimizing fuel consumption of internal combustion engine using the concept of minimizing (or optimizing), was theoretically presented by (Darper and Li, 1957).

The plant's performance parameters are incorporated into mathematical form, which is called performance index, and the process of controller design follows by selecting a controller that minimize the performance index. For example, key performance indicators such as rise time and settling time of the system output are incorporated in a mathematical expression, which in turn, is minimized by selecting suitable controller.

Optimal control methods heavily lean on state variable systems with feedback. By placing the closed loop poles, optimal control, fulfills the desired behavior. Although optimal control method does not have a definite answer, it aims to provide the "optimum" solution for combination of contradicting specifications requirements (Dutton, 1997).

The optimal control theory, as summarized mathematically by (Naidu, 2003) leaning on (Wiener, 1949) works on mean-square filtering which was used for controlling weapon fire during World War II:

$$J = E(e^2(t))$$

The performance factor  $J$  represents the square of errors  $e^2(t)$  for random inputs  $E(x)$ . Minimizing  $J$  was the aim of Wiener to design a filter with optimum parameters. This method is known as mean square error criterion.

The following integral quadratic is a general form of mean square error criterion:

$$J = \int_0^{\infty} e'(t)Qe(t)dt$$

While  $Q$  represents a positive definite matrix (Naidu, 2003).

## **Calculus of Variation**

The theory of finding maximum and minimum of a function can be traced back since 500 B.C. when Greek mathematicians used it to find peripheral of certain geometric shapes. However, Johannes Bernoulli (1667-1748) addressed the problem of finding the shortest path between two points in 1699 based on the problem presented in 1638 by Galileo (1564-1642). Inspired by Bernoulli and Leonard Euler (1707-1783), Joseph-Louis Lagrange solved the extremum problems using the method of first variation. Euler-Lagrange method became one of the most powerful tools as multiplier method in optimization, in that method, Lagrange treated end point problems introducing the multiplier method. Andrien Legendre (1752-1833) introduced the sufficiency condition for finding extremum of a functional by the calculus of variation (Naidu, 2003).

Calculus of variation has a fascinating history. Starting from Carl Gustav Jacobi (1804-1851) who introduced a sufficient condition for extremum rigorously in a method which was known as the Legendre-Jacobi condition, through Sir William Rowan Hamilton (1788-1856) who represented the motion of a particle in space with external forces exerted on it with a single function satisfies two first-order partial differential equation. Jacobi again who further improved Hamilton's work and demonstrated the efficiency of only one partial differential equation to represent the motion of Hamilton's particle in space, that equation, which had a massive influence on the calculus of variations, mechanics, optimal control and dynamic programming, was known as Hamilton-Jacobi.

Karl Weierstrass (1815-1897) addressed the distinction between weak and strong extremum introducing Weierstrass condition. Incorporating the constraints within differential

equations and providing a condition based on second variation was introduced and presented by Rudolph Clebsch (1833-1872) (Naidu, 2003).

In 1900, it has been shown by David Hilbert (1862-1943) the second variation as a quadratic functional with eigenvalues and eigen functions. With various thorough studies and theories in calculus of variation during first half of twentieth century, a new technique of dynamic programming was introduced by (Bellman, 1957) to solve discrete time optimal control problems. Later in the United States, in 1960, to design optimal feedback control, (Kalman, 1960) has presented linear quadratic regulator (LQR) and Linear quadratic Gaussian (LQG) theory. Kalman used matrix Reccati equation in his filtering techniques, which was published by Riccati in 1724.

Kalman also found that when optimal control method is applied to systems which are not completely controllable, naturally, the controller will not be able to move the uncontrolled poles. State Controllability is defined for the constants (A,B) in the dynamical system  $\dot{x} = Ax + Bu$  as state controllable if, for initial state  $x(0) = x_0$ , there is an input  $u(t)$  where that  $x(t_1) = x_1$  at any time  $t > 0$ . Otherwise, system is uncontrollable. A method for controllability test was developed by (Chen and Dosoer , 1966) and summarized in (Zhou et al., 1996, p.52).

Measuring and Observing state parameters within the system, led to the common term: State Observability. The system is state observable in the state space equations  $\dot{x} = Ax + Bu$ ,  $y = Cx + Du$  when, for initial state  $x(0) = x_0$  can be identified from the previous values of the input  $u(t)$  and the output  $y(t)$  within certain time period. Testing method for observability was developed by (Chen and Dosoer , 1966) and summarized in (Zhou et al., 1996, p.52).

### 3.5 Robustness

For many applications, there are degrees of uncertainties in terms of parameters and/or system models. The robust control analysis, which utilizes a standard control procedure, ensures that the output performance remains acceptable even if the plant differs from nominal.

In situations where there is plant uncertainty, external disturbance, and parameter variation, robust control design is utilized to achieve control goals that are robust (insensitive) to all those uncertainties. Stability and accuracy of the system should be, to some extent, are fulfilled (Shinners, 1998).

Building on Wiener work of optimal control filtering in 1940s, the subject of optimal control reach maturity during 1960s with what is called now quadratic Gaussian or LQG control. although LQG were successfully applied in the Aerospace engineering field, control engineers found difficulties in applying it to industrial problems; the questionable robustness of LQG method fails to reach the acceptable level in the presence of uncertain plant models and unstructured disturbances. This led to the emergence of new innovative optimal control method introduced by Zames which is known as  $H_\infty$  optimization method in an effort to improve robustness (Skogestad and Postlethwaite, 2005).

Hence, there was a considerable shift in 1980s toward  $H_\infty$  optimization for robust control which was motivated by the limitations of LQG control. Inspired by the work of (Helton, 1976), (Zames, 1981) laid the foundation for robust control using  $H_\infty$  demonstrating the shortcoming of LQG (Dutton, 1997).

The extension of classical methods was made formal during 1980s. by considering  $H_\infty$  norm of the weighted sensitivity function, this method was heavily based on shaping closed-loop transfer functions (Skogestad and Postlethwaite, 2005).

The IEEE transactions on Automatic control published in 1981 the issue of linear multivariable control systems, it explained the analysis and design of multivariable feedback systems using singular values. An influential paper published by (Doyle and Stein,1981) where it explained how to achieve the benefit of feedback control with the presence of uncertainty using singular values, also it showed the generalization of the classical loop shaping concept of feedback to multivariable systems.

The conflicting design objectives necessitate trading offs in building controller for feedback system, however, the conflicting design requirements usually occur at different frequencies. For example, large loop gains usually used to mitigate external disturbances which is desired, on the other hand, small gains are used at low frequencies to avoid noise generated by measuring instruments. Other design requirements, such as system dynamics parameters are sometimes compromised for sake of fulfill the minimum requirement of other parameters. Steady state error, over shoot, and settling time are among the most important dynamic parameters.

### **3.6 Stability**

As a consequence of Maxwell's study on governors, Routh developed his famous stability criterion. The importance of Routh contribution was not well-recognized until 1940 when new inventions were already realized, such as the airplane and electrical machinery. First paper dealing with the dynamic analysis was published in the year 1940.

Ahead of his time, Aleksandr Lyapunov (1857-1918) found a method sufficient to determine stability for ordinary differential equations in 1899. The innovative works related to controlling dynamic systems, particularly non-linear, systems' stability, probability and potential theory was not realized till twentieth century with the advent of digital computers (John and Lumkes, 2002).

### **3.7 Comparison between Classical and Modern control Theory**

The use of Laplace transfer function in the complex frequency domain and root locus technique in frequency domain plots are classified as a classical control techniques. State space presentation is a technique which is considered to include modern control techniques; it is a time based approach which can be utilized for linear, time-invariant Single input single output system and efficiently extended to nonlinear time-variant single input single output systems (John and Lumkes, 2002).

Classical control theory has its roots in feedback amplifier which were built for telephones based on frequency domain analysis for complex variables. Plots such as Nyquist, Bode, and Nichols are among the common tools in frequency domain analysis. Classical control theory approach has many advantages: besides it is easy to understand and easy to perform the design analysis graphically in order to fulfill performance requirements, physical systems can be described easily using block diagram and transfer functions to show the input-output relationships which, in turn, leads to a straightforward techniques for the design of controllers such as, frequency plots and root locus plot. However, these advantages have an attendant cost; the classical transfer function techniques are limited to linear time-invariant

single input single output systems. It becomes rapidly complex for systems with increasing non linearity, time variation, and multivariable systems and turn to be more like a trial and error method for such situations. (John and Lumkes, 2002) The reason for sensitivity of state space approach compared to transfer function approach is that: transfer function approach has an iterative nature; the graphical method of transfer function allows the inspection of the changing parameters directly on the output and tuning to reach robustness. On the other hand, state space methods mainly rely on mathematical algorithms which are mainly based on the accuracy of the model. With poor models, state space methods may not be the best choice (Dutton et. el., 1997).

State space method still is considered, in general, the best method for multivariable systems particularly because the design method does not change with increasing number of inputs or/and outputs. Practically, in aircraft and space vehicle control, state space methods proved successful and reliable. It is still used for such applications where the system models for aircraft and aerospace problems are relatively accurate (Dutton et. el., 1997).

Modern control theory advantages become more evident increasing demand in designing controllers for more complex systems that exhibit non linearity, time variation, and multiple input multiple outputs nature. With the advent of digital computers, it is easy to perform controller analysis for multivariable systems without increases in computational complexity; using matrix algebra manipulation and techniques is simple practice with digital computers compared to cumbersome approach using hand computation. Naturally, the price at which this occurs is reflected in accompanying limitations. Physical system under study become less visible during computation and the technique becomes more “math” rather than “design” when it is compared to transfer function approaches. State space method also has

questionable robustness in large scale applications with some degree of system variable uncertainties (John and Lumkes, 2002).

There are three most-common-types of compensators used to fulfill control system performance requirements: First is proportional action “P-Action” is used when well-behaved transient and higher speed closed-loop response is desired compared to open-loop response. It uses a signal that is proportional to the error signal. Second is the Integral action “I-Action”, or lag compensator, which is mainly used to decrease steady state error. The actuation signal of I-action is proportional to integral of error signal that resulted from the feedback loop. Finally the derivative action “D-Action” or “Lead compensator” has no effect on steady state error, it tend to increase the response speed of the system. Its actuation signal is proportional to rate of change of the error signal. Most commonly the three compensators are used together in what is known as PID, or three-term, controller (Dutton et. el., 1997).

The modern state variable time domain approach and the classical frequency domain approach complement each other and sometimes can work together simultaneously (Shinners, 1998).

The advantages of Laplace transfer function and matrix methods can be combined using the multivariable frequency-domain methods. The usage of computers makes the tediousness of calculating multivariable systems controller parameters in the frequency domain possible, and in many cases, practical.

### 3.8 Inverse Nyquist Array (INA)

In effort to combine the benefits of elegant matrix methods for multivariable systems with the advantages of the graphical design approach of frequency domain without incurring the apparent limitations, theorists in UK developed the generalized frequency domain techniques to multivariable systems; Such as Bode and Nyquist.

Two major contribution in this field was introduced by (Rosenbrock, 1969) and (MacFarlane and Kouvaritakis, 1977) who developed the Inverse Nyquist array (INA) and characteristic Locus (CL) methods respectively. The amount of computations involved in these methods had remained a great challenge compared to single input single output systems until a reasonable harness for computers-graphic powerful capability was realized to handle these computations quickly and precisely. Other, less famous, methods to design and analyze multivariable systems were also developed. For example, the sequential return difference method which was introduced by (Mayne, 1979), the principal gain and phase methods was developed by (Postlethwaite et al., 1981). Those methods contributed in designing control systems for several practical applications but were not as common as INA and CL methods among control designers.

The basic methodology for INA aims to realize the decoupling of multivariable system by satisfying diagonal dominance condition of transfer function matrix at all frequencies lay within the boundaries of system's operation. Thereafter, multiple single input single output transfer functions can be treated easily and separately with common procedures. In order to achieve diagonal dominance, single input single output compensators usually work satisfactorily.

The Matrix can be described as diagonally dominant if each element on the leading diagonal has a value greater than the sum of elements in the same row or the same column. Row dominance is tested with direct Nyquist array, while column dominance is tested using Inverse Nyquist array (INA). It is important that diagonal dominance is tested along all possible frequencies.

Mathematically, diagonal dominance can be defined as following:

$|q_{ii}(s)| > r_i(s)$  for  $1 \leq i \leq n$  and for all values of  $s$ .

$$r_i(s) = \sum_{j=1, j \neq i}^n |q_{ij}(s)| \text{ for row dominance}$$

$$r_i(s) = \sum_{j=1, j \neq i}^n |q_{ji}(s)| \text{ for column dominance.}$$

The INA method considers the feedback gains  $F = \text{diag} \{f_1, f_2, f_3, \dots, f_n\}$  as shown in figure 2.5. With  $Q(s) = G(s)K(s)$ , the closed loop transfer function becomes:

$$H(s) = [I + Q(s)F]^{-1}Q(s)$$

In order to ensure the existence of  $Q(s)^{-1}$ , an appropriate choice of  $K(s)$  must be selected. Hence, the closed loop transfer function equation can be inverted to:

$$H^{-1}(s) = Q^{-1}(s)[I + Q(s)F] = Q^{-1}(s) + F$$

which, in turn, can be traced more easily.

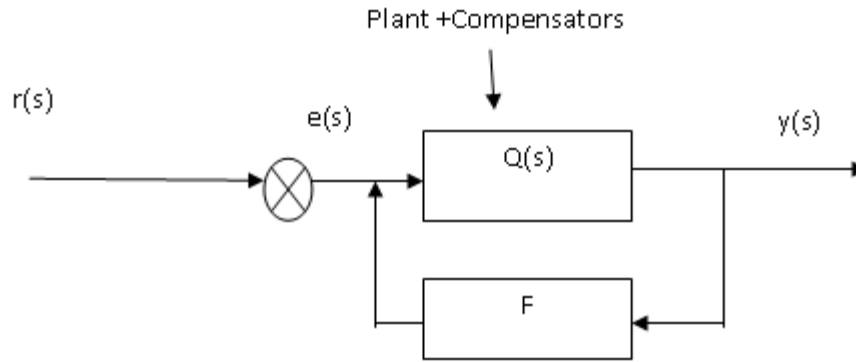


**Figure 3.1** Closed loop diagram for multivariable system

Afterward, as the Nyquist D-contour is traverse clockwise, the element of the inverse forward path  $q_{ij}^{-1}(s)$  traces a contour resembles the inverse Nyquist plot. Then, plotting all elements of  $Q^{-1}(s)$  will end up with a complete Inverse Nyquist array plot for the whole system. It is worth noting that only diagonal elements are considered in stability analysis due the pre condition of diagonally dominance, thus, a compensator must be applied to fulfill the requirements of diagonally dominance before proceeding with any stability analysis. Analysis of the encirclements follows after diagonal dominance is realized.

The generalization of the Nyquist stability criterion for single input single output systems to multivariable systems using the number of encirclements were performed with removing the interaction between feedback elements.

### 3.8.1 Greshgorin's Theorem

A technique introduced by (Gershgorin, 1931) to eliminate the interaction within the system in the INA method was developed. Extending the concept of investigating the open loop plot to study the behavior of closed loop system which is used in Single input single output methods by Nyquist, the same concept in the context of INA for multivariable systems

means that the  $i_{th}$  loop ( $1 \leq i \leq n$ ) attitude for the closed loop must obtained from the open loop plot for the  $i_{th}$  loop with all other loops closed.

Due to the fact that transfer function matrix are not perfectly diagonal, only diagonally dominant, the interaction between loops inhibits from reaching a precise form of every single open loop plot with all other loops closed, and the resulting plot will differ when compared to the INA plot with all loops are open. Hence, the Greshgorin's theorem proved that the plot for the  $i_{th}$  open loop, with other loops closed, always located within a certain band. This band is formed by the union of superimposed circles on the inverse Nyquist plot of the all diagonal elements of  $Q^{-1}(s)$ . This will narrow the location of  $i_{th}$  open loop to a well-known band regardless of the other closed loops gains values.

To graphically obtain Greshgorin's band, the inverse Nyquiste-like plot is shown in figure 3.2 for the diagonal elements of  $Q^{-1}(s)$ , namely  $q_{ii}^{-1}$ . The radius of imposed circles equal  $r_i^{-1}(s)$  are represented in equation below and calculated at different frequencies

$$|q_{ii}^{-1}(s)| > r_i^{-1}(s) \text{ for } 1 \leq i \leq n \text{ and for all values of } s.$$

$$r_i^{-1}(s) = \sum_{j=1, j \neq i}^n |q_{ij}^{-1}(s)|$$

Greshgoring band lay within the union of the imposed circles which are centered on the plot of inverse Nyquist –like plot of  $|q_{ii}^{-1}(s)|$ . The actual plot with all loops closed, but  $i_{th}$  loop, lay anywhere inside Gresgorin bands formed by the union of the circles (Dutton, 1997).

### 3.8.2 Achieving diagonal dominance

A proper compensator  $K^{-1}(s)$  should be selected to achieve diagonally dominance of the inverse forward path:

$$Q^{-1}(s) = [G(s)K(s)]^{-1} = K^{-1}(s)G^{-1}(s)$$

Usually a series of cascade compensators may be used, as used in CL method. After achieving diagonally dominance, single loop pre-compensators are simply selected.

Several methods were suggested to systematically approach diagonal dominance. For example, (Hawkins, 1972) developed Pseudo-diagonalisation method, (Mees, 1981) developed scaling matrix, and the technique of spectral factorization introduced by (Whalley, 1978).

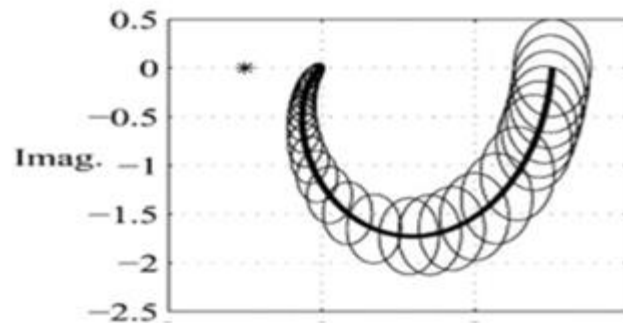


**Figure 3.2** Gershgorin Bands

### 3.8.3 Inverse Nyquist Plot

In principle, the inverse polar plot may be used to achieve the same objectives as direct polar plots. The Nyquist stability criterion, gain margin, phase margin, steady-state

error checks and the various closed-loop frequency response measures all have their counterpart in the inverse plane.

Ostrowski bands further shrink Greshgorin bands to locate, more precisely, the location of the inverse Nyquist-like plot. The shrinking factor, as calculated by (Maciejowski, 1989), would give a better idea about the phase and gain margin of the system as far as more accurate values are concerned.

The main disadvantage of INA method is the uncertainties of the location of the poles as they occur within certain bands and not in specified locations. This may have adverse effects on the robustness of the control system.

### **3.9 Least Effort Methodology**

The least effort regulator design technique was introduced by (R Whalley, and M Ebrahimi, 1999) by minimizing performance index  $J$ . Inner loop analysis, which will be used in this contribution, will be analyzed to improve the dynamic behavior of the system output. Thereafter, the outer loop in final design is built to fulfill robustness requirement by acceptable level of disturbance perturbation and decoupling of the outputs steady state.

### **3.10 Joining of control technology and aircraft dynamic analysis**

The use of newly available computers in developing new methods for analyzing control systems, or feedback control, gave birth to a new engineering discipline “Systems Engineering” in late 1950’s. The multi-disciplinary nature of systems engineering allow the study for systems as a whole and simulate, using computers, system performance within system’s operating boundaries.

In 1970s, digital computers had crucial role in computational fluid dynamic, it also provided better view by analyzing and computing flutter or structural divergence, simulating dynamic systems, and onboard digital computers used in real-time guidance and control systems. Simulation techniques achieved attendant time and cost-saving by analyzing and improving dynamic behavior of aircraft, realistic pilot training and onboard automatic flight control even before the model of aircraft is built and hundreds of flight-tests are performed. A decade later, additional control surfaces were tested on airplanes that provide better dynamic performance such as direct lift and direct side force control. Examples at that time were the AFTI F-16 and the Grumman forward-swept wing X-29A aircraft. Those additional control surfaces raise the interest in multivariable and modern control theory to be applied to match the increasing complication accompanied with the additional inputs to the control system (Stevens and Lewis, 2003).

Stability agumenter was the first outcome of this marriage between the two disciplines, it is a feedback control used to modify inherent aerodynamic stability characterisitic of the airplane. Augmentation is fulfilled by imposing moments and forces on the stability derivatives through control surfaces and acuators. These forces would have a key role in modifying stability characteristic of the airframe during motion.

Transfer function techniques, in the context of frequency response, are used in the design of aircraft and aircraft's control system since early stages of aircraft control history, however, their use spread quickly as part of designing actual aircraft contorl system.

The famous method of root locus invented by Evans was inspired by solving the problem of aircraft control. Other tools for system engineering mainly included, but not

limited to, Laplace transformation, frequency response techniques, the stability criterion of Nyquist, root locus method, and analogue computers are all used in aircraft control system design and analysis in 1950s onward (McRuer et. el., 1973).

The system approach becomes necessary when scientists realized the importance of examining the problem of control as a whole. Positioning large masses precisely and quickly, such as gun, launchers, and radars were the main impetus for the system approach. Also after Wold War II, scientists started to think in the long term instead of war demanded and piecemeal solutions and came to the conclusion that overall system approach might be more efficient (Bennet, 1993).

## Chapter IV

### Research Methodology

#### 4.1 Aircraft Mathematical Model

High performance aircraft exhibit oscillatory characteristics particularly with extended flight envelopes or near critical flight boundaries. The coupling occurs naturally in the feedback loops resulting from the applied aerodynamic forces, a single principal input usually have considerable effects on all the dynamics of the aircraft due to internal interactions. Regenerative feedback is applied to overcome the coupled feedback phenomenon; the undesired outputs are eliminated by measuring the errors and tuning the control surface in proportion to the errors or its derivatives (Whalley and Ebrahimi, 2000).

The equation of motion used to describe the aircraft dynamics is linearized about small perturbation around particular operating condition (Garnell and East, 1977). Thereafter, feedback control is applied to those equations.

In 1985, the bench mark problem of the F-14 model was revealed at the IEEE, Computer Aided Design Symposium, in Santa Barbara, California. The computer Aided Control system design was evaluated keeping the original manufacturer's design as the basis of the study (Frederick, 1987).

Leaning on the F-14 bench mark problem summarized by (Milne, 1989), (Whalley and Ebrahimi, 2000) presented a system model that describes the pitch and heave rate dynamics for the airplane as a result of control surface input on the F-14 wings. The single input, dual output block diagram is depicted in Figure 4.1

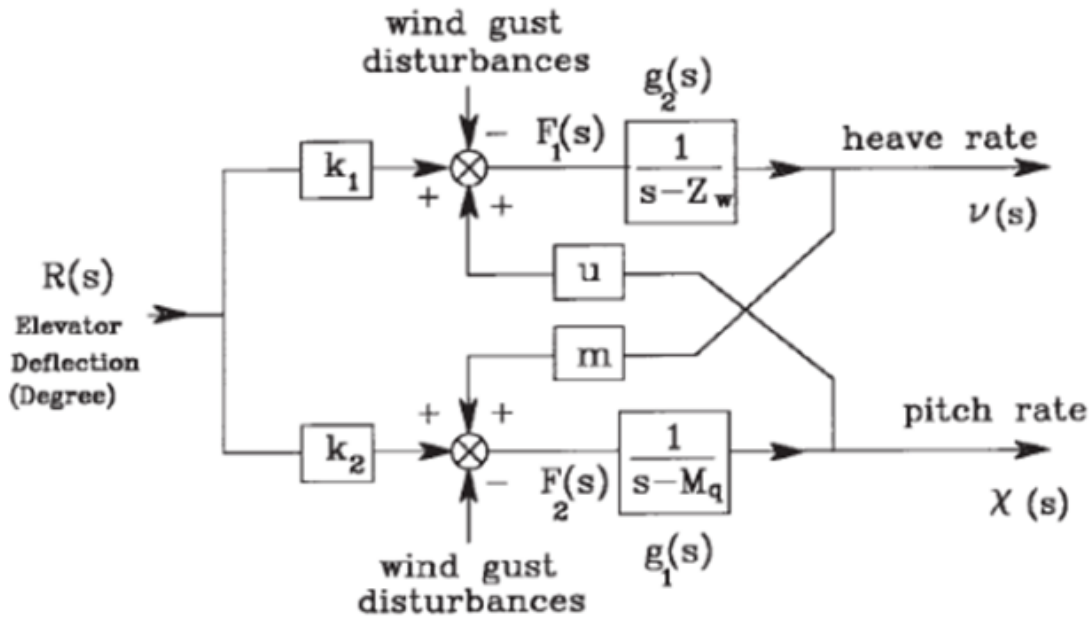


**Figure 4.1** Block diagram of the heave and pitch rate system for changes in elevator deflection.

(Whalley and Ebrahimi, 2000)

The chosen parameters for the block diagram, shown in figure 4.1 lead to the transfer function:

$$G(s) = \frac{\begin{bmatrix} 63.997(s+74.506) \\ -6.8847(s+0.6933) \end{bmatrix}}{\nabla} \quad 4.1$$

The determinant of the transfer function is:

$$\nabla = 1 + 1.2956s + 4.4867s^2 \quad 4.2$$

The elements in the transfer function matrix in equation 3.1 represent the heave rate and pitch rate response to elevator (input at the wing control surface) step inputs respectively, as shown in figure 4.2

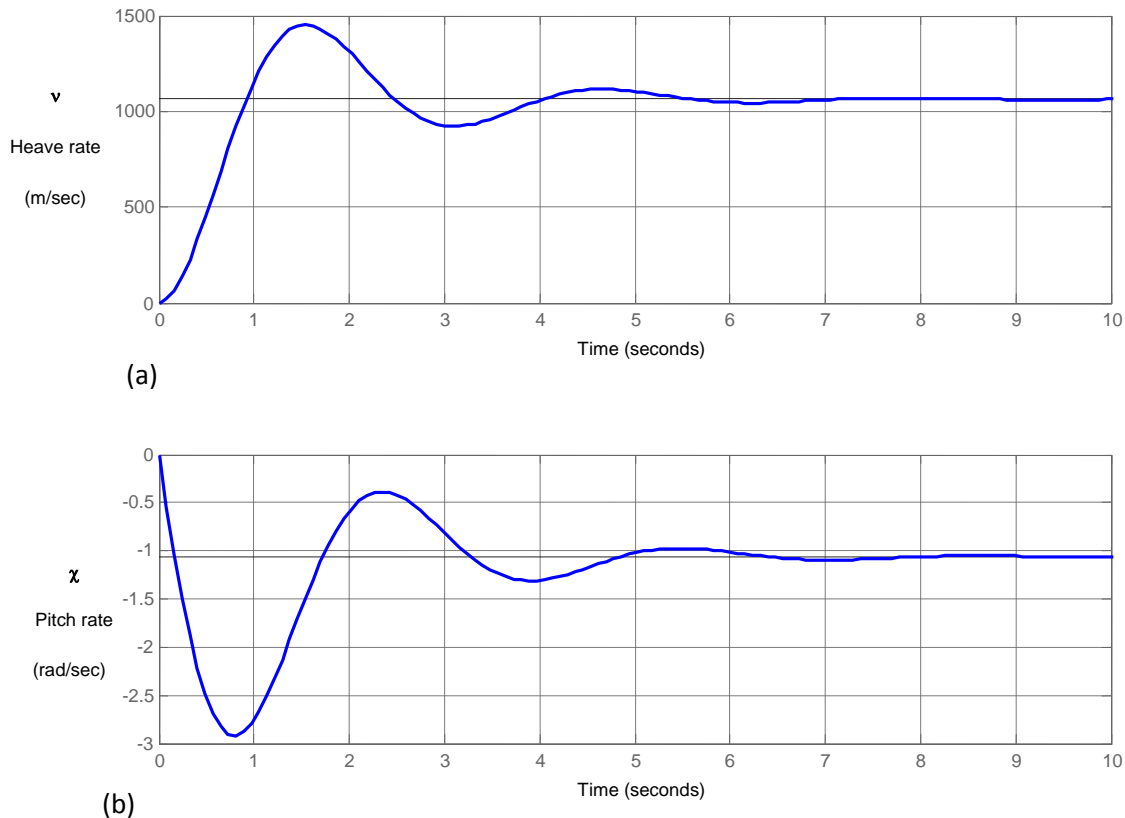


**Figure 4.2** Open-loop heave and pitch rate following a unit change in input (at wing) (Whalley and Ebrahimi, 2000)

In this contribution, another input is suggested represented by an additional control surface on the horizontal tail. The size of the control surface on the tail is smaller than the one on the wing which results in weaker effect on heave rate. However, as tail is located at a great distance from the center of gravity, consequently, the deflection of the elevator in the aircraft's tail would result in an increasing effect on the pitch rate.

From figure 4.3, which shows the dimensions of the F-14, the size proportion between the wing and the horizontal tail suggests identical proportions between control surfaces on wing and tail. However, many other parameters could be involved such as the angle of deflection of

the control surface

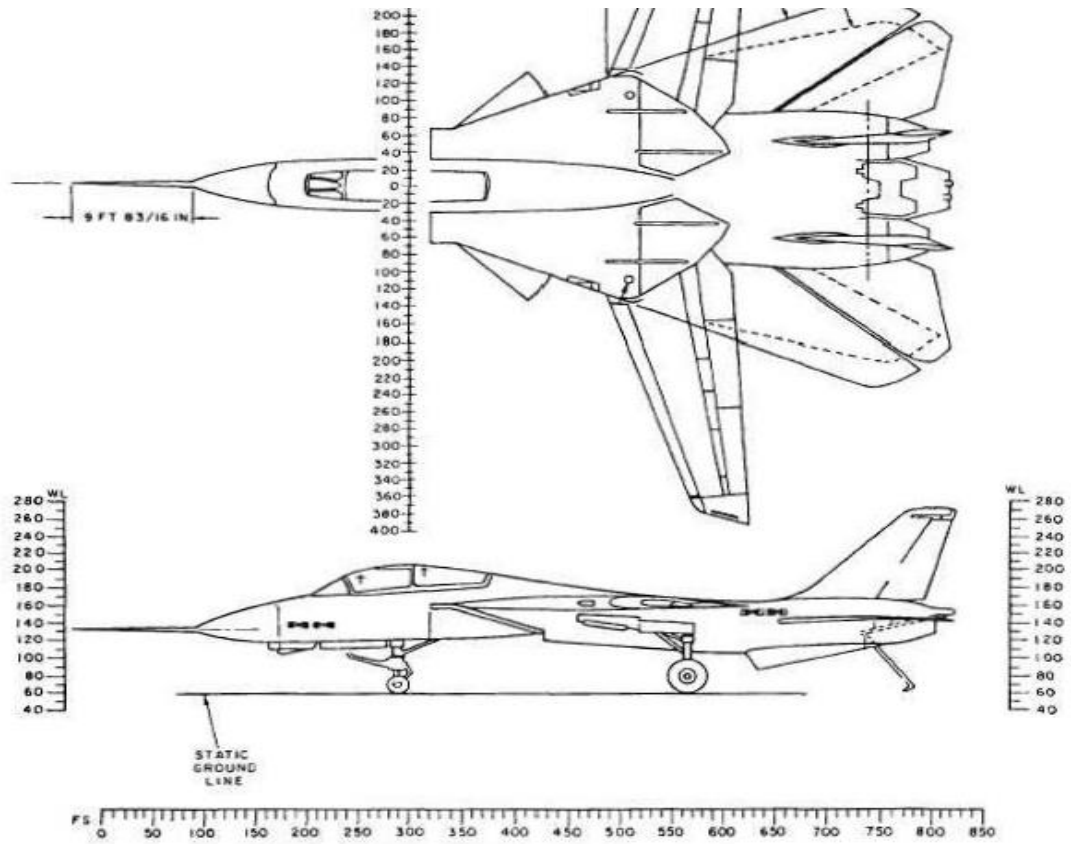


**Figure 4.3** F-14 Aircraft dimension Drawings in inches

$$F_{LW} > F_{LT}$$

4.3

Equation 3.3 suggests that the lifting force due to wing's control surface deflection is more than three times the lifting force due to horizontal tail's control surface deflection, which directly affect the heave rate overshoot and steady state output. Settling time and the remaining dynamics are assumed to be unaffected by the tail's elevator input.

The second step is to find the pitching moment transfer function due to deflections of the horizontal tail elevator. In order to do so, the locations of the center of gravity and aerodynamic centers at wing and tail, respectively, need to be identified in order to construct the shear force and torque moment diagram.

Location of the aircraft's center of gravity has a crucial role in determining the resultant motion resulted from the applied aerodynamic forces and moments on the aircraft, due to the deflection of the control surfaces. However, shifting the payloads, of the fuel continuously affects weight reduction, sloshing of fluid inside the fuel tank and dumping of bombs from jet fighters all contribute in changing the distribution of mass and the location of the center of gravity (Roskam, 2001).

Fortunately, from the concept of small perturbation about the equilibrium and within relatively small period of time, these effects can be eliminated without affecting the accuracy of the analysis. Several textbooks, such as (Cook, 2007), suggested that the location of the center of gravity varies between 10% and 40% of the mean aerodynamic chord. The Mean aerodynamic chord is the line connecting the leading edge, of the wing or tail, to the trailing edge, as shown in figure 4.4.

Finally, the wing and tailplane aerodynamic centers are defined by (Stevens and Lewis, 2003) as points at which the aerodynamic moments do not vary with the changing aircraft angle of attack. The assumption of (Roskam, 2001) that the aerodynamic centers are roughly located at the quarter chord is followed.

Constructing moment diagram around center of gravity and aerodynamic centers is accordance with the dimensional drawing shown in figure 4.3 and 4.4 respectively, will identify the effect of step inputs on the horizontal tail control surface, see figure 4.5. Henceforth, the suggested transfer function with two inputs two outputs model in this contribution is:

$$G(s) = \frac{\begin{bmatrix} 63.997(s+74.506) & 2(s+74.506) \\ -6.8847(s+0.6933) & -100(s+0.6933) \end{bmatrix}}{\nabla} \quad 4.4$$

The resulting heave rate and pitch rate due to step inputs from the control surfaces on the tail are shown in figure 4.6

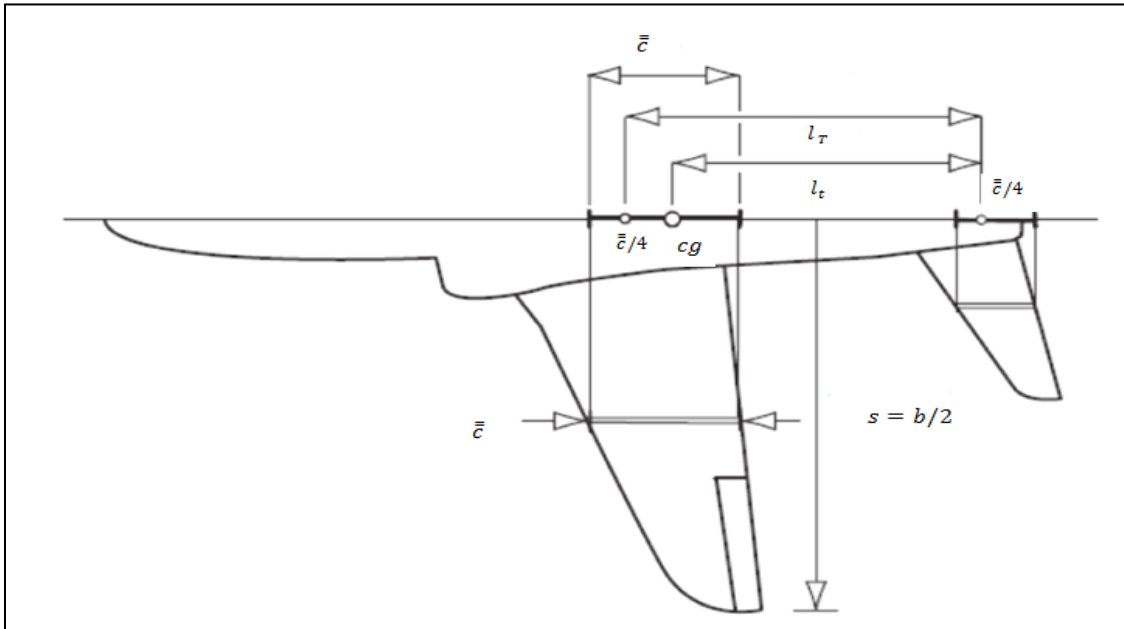


**Figure 4.4** Longitudinal reference geometry

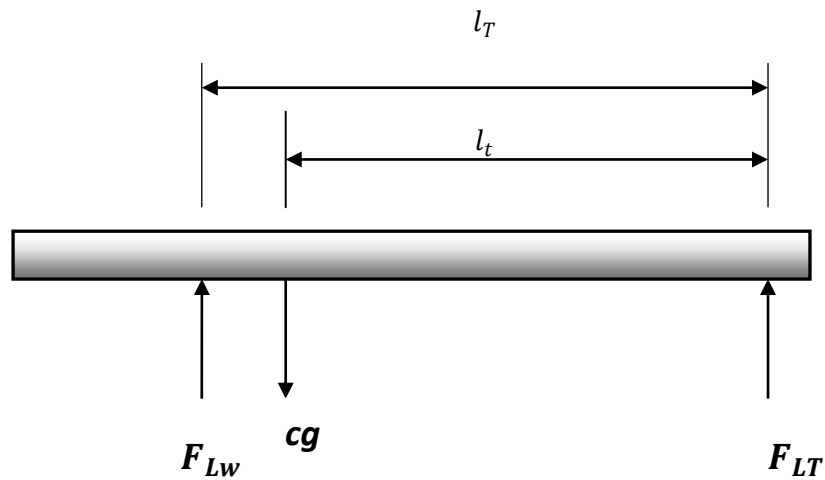
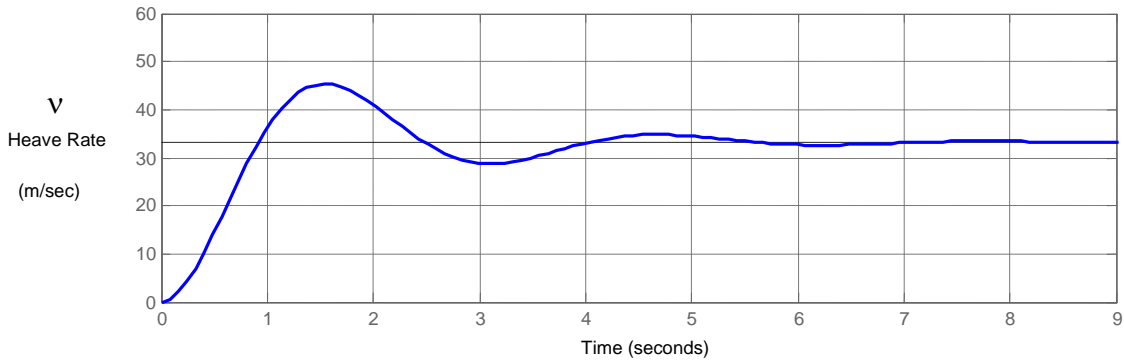
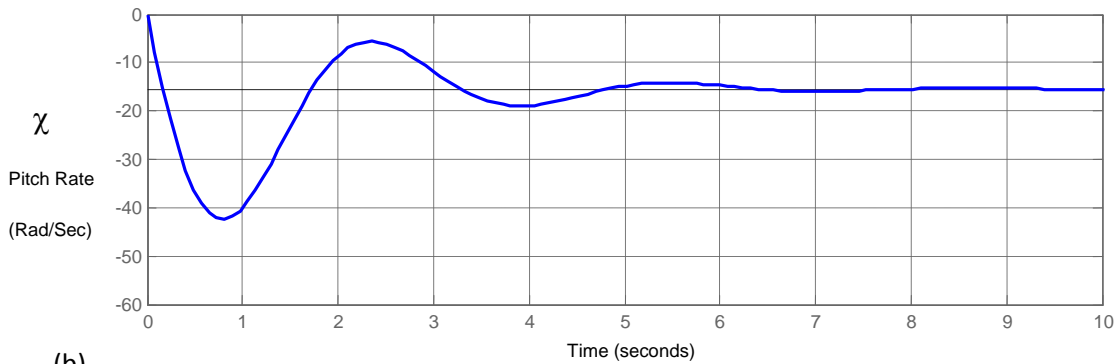


**Figure 4.5** Schematic for aerodynamic forces exerted on the aircraft



(a)



(b)

**Figure 4.6** Open-loop heave and pitch rate following a unit change in input  
(at horizontal tail)

## 4.2 Least Effort Control Method

The Least effort controller design method consists of two parts including: an inner loop and an outer loop analysis. The Inner loop aims to achieve acceptable dynamic characteristics and ensure suitable disturbance recovery. The steady state is achieved by the selection of a pre compensator in the second part of least effort method, outer loop analysis (Whalley and Ebrahimi, 1999).

The following mathematical derivation is based on Whalley and Ebrahimi (2006).

The equation representing the system with disturbance is:

$$y(s) = G(s)u(s) + \delta(s) \quad 4.5$$

While the control law for the system is :

$$u(s) = k(s)[\bar{r}(s) - h(s)y(s)] + P[r(s) - Fy(s)] \quad 4.6$$

The first part of equation 4.6 represents the inner loop controller, or alternatively, the dynamics of the control system. The second part of equation 3.7 represents the outer loop, or steady state of the control system.

For n inputs, and m outputs:

$$F = \text{Diag}(f_1, f_2, \dots, f_m), \quad 0 < f_i < 1, \quad 1 < i < m$$

Assume  $\bar{r}(s) = 0$ , then the closed loop equation becomes:

$$y(s) = \{I + G(s)[k(s) \succ h(s) + PF]\}^{-1}[G(s)Pr(s) + \delta(s)] \quad 4.7$$

The term  $\|G(s)k(s) \succ h(s) + PF\|_\infty$  in equation 4.7 is finite for all values of  $s$  in  $D$  contour.

The steady state matrix is then selected such that:

$$y(s) = S_s r(0)$$

From equation 3.7 with zero disturbances:

$$P = [G(0)^{-1} + k(0) \succ h(0)]S_s[I - FS_s]^{-1} \quad 4.8$$

From equations 4.7 and 4.8, then:

$$y(s) = \{I + G(s)[k(s) \gg h(s) + [G(0)^{-1} + k(s) \gg h(s)][I - F]^{-1} F]\}^{-1} [G(s) Pr(s) + \delta(s)] \quad 4.9$$

To fulfill the requirement of steady state decoupling, the steady state matrix  $S_s = I$ . Alternatively, to minimize steady state interaction, off diagonal elements should be selected such as  $|s_{i,j}| \ll 1$ ,  $1 \leq i, j \leq m$ , and  $i \neq j$ , With unity diagonal elements.

Substituting the value  $I_m$  and equation 4.9 in equation 4.8 results:

$$y(s) = \{I_m + G(s)[k(s) \gg h(s) + (G(0)^{-1} + k(s) \gg h(s))(I_m - F)^{-1} F]\}^{-1} X \{G(s) Pr(s) + \delta(s)\} \quad 4.10$$

At low frequencies:

$$G(s) \cong G(0) \text{ and } G(s)G(0)^{-1} = I$$

Equation 4.10 becomes as steady state is approached

$$y(s) = I_m r(s) + S(s) \delta(s) \quad 4.11$$

Hence, equation 4.10 becomes:

$$y(s) \cong \{I + G(s)k(s) \gg h(s)\}^{-1} [G(s) Pr(s) + \delta(s)] \quad 4.12$$

The sensitivity matrix at low frequency is:

$$S(s) = (1 - f)(I_m + G(s)k(s) \gg h(s))^{-1}, \quad 0 < f < 1$$

Equation 4.11 implies that with reference input change, non interacting, steady state can be achieved. With increasing  $f$  from 0 toward 1, disturbance rejection at steady state is also increased with maintained stability.

From the closed loop equation 4.7, with inclusion of forward path  $K(s)$  and feedback compensator for multivariable regulator, the closed loop equation is:

$$y(s) = (I_m + G(s)K(s)H(s))^{-1}[GK(s)r(s) + \delta(s)] \quad 4.13$$

Equation 4.13 and 4.7 implies that:

$$K(s) = P \quad 4.14$$

And

$$K(s)H(s) = k(s) \gg h(s) + PF \quad 4.15$$

Then

$$H(s) = P^{-1}k(s) \gg h(s) + F \quad 4.16$$

From the last two equations, the forward path compensator  $K(s)$  is constant, and the feedback compensator is a stable, full rank, proper, and minimum phase matrix. This will imply that  $H(s)$  can be selected from passive elements.

The inner loop vectors  $k(s)$  and  $h(s)$  will be designed to fulfill dynamic behavior requirement. Then, the compensator  $P$  will be configured in a way that minimizes the coupling of steady state output. Finally, the loop feedback gain  $f$  selection enables suppression characteristics of final dynamic and disturbance (Whalley and Ebrahimi ,2006).

#### 4.2.1 Inner-Loop Analysis

Assuming that the system model  $G(s)$  is proper, regular, and  $m \times m$  linear, then from equation 4.5 the transfer function can be factored as follows:

$$G(s) = L(s) \frac{A(s)}{d(s)} R(s) \Gamma(s) \quad 4.17$$

Where:

$$L(s), A(s), R(s), \text{ and } \Gamma(s) \in H_\infty$$

The terms in equation 3.16 satisfy the following conditions:

$$L(s) = \text{Diag} \left( \frac{\lambda_i(s)}{p_j(s)} \right), \quad R(s) = \text{Diag} \left( \frac{\rho_j(s)}{q_j(s)} \right), \quad \Gamma(s) = \text{Diag}(e^{-sT_j}) \quad 1 < j < m$$

$A(s)$  is a non-singular matrix of rational functions with a nonzero determinant,

$$a_{ij}(s) = a_{ij}s^m + b_{ij}s^{m-1} + \dots + \gamma_{ij} \quad 1 \leq i, j \leq m \quad 4.18$$

Referring to the inner loop control law in equation 4.6:

$$u(s) = k(s)[r(s) - h(s)y(s)] \quad 4.19$$

Then, equation 4.5 and equation 4.19 are combined and give:

$$y(s) = [I + G(s)k(s) >< h(s)]^{-1} [G(s)k(s)r(s) + \delta(s)] \quad 4.20$$

The finite time delay in  $\Gamma(s)$  may be ordered with  $T_i > T_j$ ,  $1 < j < m$ ,  $i \neq j$ , so that the

forward path gain vector can be arranged as:

$$k(s) = [k_1(s)e^{-s(T_i-T_1)}, k_2(s)e^{-s(T_i-T_2)}, \dots, k_i, \dots, k_m(s)e^{-s(T_i-T_m)}]^T \quad 4.21$$

Knowing that

$$h(s) = [h_1(s), h_2(s), \dots, h_m(s)] \quad 4.22$$

and assuming

$$k_j(s) = k_j \phi_j(s) \text{ and } h_j(s) = h_j \chi_j(s) \quad 1 \leq j \leq m$$

The functions  $\phi_j(s)$  and  $\chi_j(s)$  are proper, or strictly proper, realizable, stable, and minimum phase, hence, equation 4.19 becomes

$$y(s) = [I + e^{-s(T_i)} n(s) \frac{A(s)}{d(s)} k \gg h]^{-1} \left[ n(s) \frac{A(s)}{d(s)} k e^{-sT_i} r(s) + \delta(s) \right] \quad 4.23$$

Where

$$k = [k_1, k_2, \dots, k_m]^T \quad 4.24$$

And

$$h = [h_1, h_2, \dots, h_m] \quad 4.25$$

$$d(s) = s^{\kappa} + a_1 s^{\kappa-1} + \dots + a_0$$

The determinant of first term in equation 4.23, which represents the characteristic equation for the transfer function is:

$$\det[I + e^{-s(T_i)} n(s) \frac{A(s)}{d(s)} k \gg h]^{-1} = 1 + e^{-s(T_i)} n(s) \langle h(s) \frac{A(s)}{d(s)} k(s) \rangle \quad 4.26$$

The inner product in equation 4.26 can be expressed as:

$$\langle h(s) \frac{A(s)}{d(s)} k(s) \rangle = [1, s, \dots, s^{m-1}] \begin{bmatrix} \gamma_{11} & \gamma_{12} & \dots & \gamma_{mm} \\ \vdots & \vdots & \ddots & \vdots \\ b_{11} & b_{12} & \dots & b_{mm} \\ a_{11} & a_{12} & \dots & a_{mm} \end{bmatrix} \begin{bmatrix} k_1 h_1 \\ k_2 h_1 \\ \vdots \\ k_m h_m \end{bmatrix} \quad 4.27$$

$$\text{Let: } k_2 = k_1 n_1, \quad k_3 = n_2 k_1, \quad k_m = n_{m-1} k_1 \quad 4.28$$

$$\langle h(s) \frac{A(s)}{d(s)} k(s) \rangle = b(s) \quad 4.29$$

then

$$k_1[Q]h = (b_m, b_{m-1}, \dots, b_0)^T \quad 4.30$$

where

$$Q = \begin{bmatrix} \gamma_{11} + \gamma_{12}n_1 + \dots + \gamma_{1m}n_{m-1} & \vdots & \gamma_{21} + \gamma_{22}n_1 + \dots + \gamma_{2m}n_{m-1} & \vdots & \dots & \gamma_{m1} + \gamma_{m2}n_1 + \dots + \gamma_{mm}n_{m-1} \\ & \vdots & & \vdots & & \vdots \\ b_{11} + b_{12}n_1 + \dots + b_{1m}n_{m-1} & \vdots & b_{21} + b_{22}n_1 + \dots + b_{2m}n_{m-1} & \vdots & \dots & b_{m1} + b_{m2}n_1 + \dots + b_{mm}n_{m-1} \\ a_{11} + a_{12}n_1 + \dots + a_{1m}n_{m-1} & \vdots & a_{21} + a_{22}n_1 + \dots + a_{2m}n_{m-1} & \vdots & \dots & a_{m1} + a_{m2}n_1 + \dots + a_{mm}n_{m-1} \end{bmatrix}$$

The matrix above is invertible, so there is a unique solution to  $[h_1, h_2, \dots, h_m]k_1$  exists. A suitable choice for the function  $b(s)$  and the gain ratios  $n_1, n_2, \dots, n_{m-1}$  lead to full definition of closed loop dynamics raised by equation 4.23

### 4.2.2 Least Effort Optimization

The closed loop model has been established using the transfer function matrix and output measurements. To optimize this process a free choice of  $n_1, n_2, \dots$  is considered.

A benchmark for detecting the absolute least control effort is to meet the requirement of disturbance suppression under the existing controller model constraints. The controller polynomial directly influences the pattern of the closed loop pole migration in the presence of disturbances. Therefore, the inner loop system response can be analyzed simultaneously with control effort minimization (Whalley and Ebrahimi, 2006).

The control effort at any time  $t$  is:

$$(|k_1 h_1| + |k_2 h_1| + \dots |k_m h_1|)|y_1(t)| + (|k_1 h_2| + |k_2 h_2| + \dots |k_m h_2|)|y_2(t)| + \dots + (|k_1 h_m| + |k_2 h_m| + \dots |k_m h_m|)|y_m(t)| \quad 4.31$$

Hence, the control energy cost is proportional to:

$$E(t) = \int_0^T (\sum k_i^2 \sum h_j^2 y_j^2) . dt \quad 4.32$$

Output change due to arbitrary disturbance, minimizing:

$$J = \sum_{i=1}^m h_i^2 \sum_{j=1}^m k_j^2 \quad 4.33$$

Would minimize the control effort given by equation 4.32; then substituting the following relations:

$$k_2 = n_1 k_1, \quad k_3 = n_2 k_1, \quad k_m = n_{m-1} k_1$$

In equation 4.33 then:

$$J = (k_1)^2 (1 + n_1^2 + n_2^2 + \dots + n_{m-1}^2) (h_1^2 + h_2^2 + \dots + h_m^2) \quad 4.34$$

Referring to equations 4.29 and 4.30, then:

$$h = k_1^{-1} Q^{-1} b \quad 4.35$$

Then, by substituting equation 4.35 into equation 4.34:

$$J = (1 + n_1^2 + n_2^2 + \dots + n_{m-1}^2) b^T (Q^{-1})^T Q^{-1} b \quad 4.36$$

where  $J$  is minimized when:

$$\frac{\partial J}{\partial n_1} = 0 \text{ and } \frac{\partial J}{\partial n_2} = 0 \text{ etc.}$$

while second derivative of  $J$  should be positive for each value of  $n$ .

To this point, inner loop analysis is completed. Although the inner loop analysis improves dynamic behavior and disturbance recovery for transient response, this will not guarantee disturbance suppression for the steady state response.

The outer loop gain  $f$  which varies between zero and one is employed to fulfill steady state, disturbance recovery requirement. Values of  $f$  would affect the transient behavior of the system, such as overshoot and settling time, and the value of  $f$  should be tuned in a way that dynamics of the inner loop stay within acceptable limits.

### 4.2.3 Stability of Combined System

The input output stability condition is dependent on the dominator of equation 4.9. The outer loop feedback is simplified:

$$f_1, f_2, \dots, f_m = f$$

This will simplify the denominator of equation 4.9 to be:

$$\det \left\{ I_m + G(s) \left[ \frac{k(s) \gg h(s)}{(1-f)} + \frac{G(0)^{-1} f}{(1-f)} \right] \right\}$$

It is evident from the above equation that with  $f \rightarrow 1$  the determinant will become infinite which will lead to instability.

### 4.3 Inverse Nyquist Array Method

This method was developed by (Rosenbrock, 1969) to combine the advantages of classical control theory and modern control theory for systems with multiple-inputs, multiple outputs.

As shown in figure 4.1 the multivariable system block diagram shows similarity with single input single output system. Another way to depict the system is as shown in figure 4.7 where unity feedback assumed and the plant and compensator are split to two blocks.

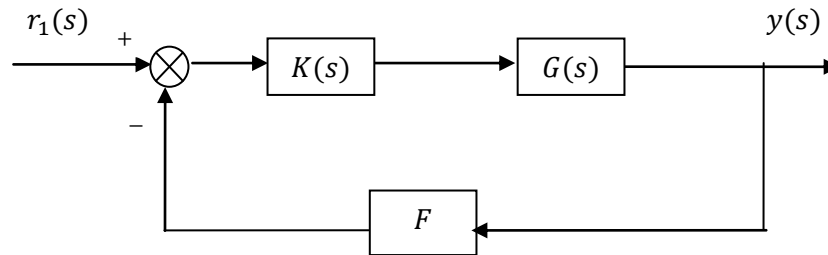


**Figure4.7** A general form for multivariable control system.

The representation for the system shown in figure 4.7 shows a transfer function and a compensator which are both in  $s$  domain and both must be invertible. As this method heavily leans on the concept of Nyquist stability methodology explained in section 3.8, an important condition should be fulfilled that the system is open loop stable. The third assumption in this method that the pre compensator matrix  $K(s)$ , if used to meet the requirement of diagonally dominance, need to have all its elements stable.

Fortunately, the first glance at the transfer function  $G(s)$  as shown in equation 4.4 clearly shows high degree of row diagonally dominance, which mathematically means:

$$|q_{ii}(s)| > r_i(s) \text{ for } 1 \leq i \leq n \text{ and for all values of } s.$$

$$r_i(s) = \sum_{j=1, j \neq i}^n |q_{ij}(s)| \text{ for row dominance}$$

In this case, the painstaking procedure for designing pre-compensator to achieve diagonally dominance can be avoided. This will be further emphasized in chapter VI when the Nyquist diagram for the transfer function  $G(s)$  is plotted with Gershgorin circles superimposed.

Graphically, none of Greshgorin circles should encircle the origin point to ensure the requirement of diagonally dominance is met.

From Figure 4.7 and figure 4.1, the open loop transfer function is:

$$Q(s) = G(s).K(s) \tag{4.37}$$

Taking the inverse

$$Q^{-1}(s) = [G(s)K(s)]^{-1} = K^{-1}(s)G^{-1}(s) \tag{4.38}$$

The above transfer function can be extended to include a non unity feedback matrix F:

$$y(s) = [I_m + Q(s)F]^{-1}Q(s)r(s) \tag{4.39}$$

Then the transfer function become:

$$H(s) = [I + Q(S)F]^{-1}Q(s) \tag{4.40}$$

By inverting the closed loop transfer function, the equation becomes

$$H^{-1}(s) = Q^{-1}(s)[I + Q(s)F] = Q^{-1}(s) + F \tag{4.41}$$

Finally, the radius of imposed Gershgorin circles are:

$$d_i = r_i^{-1}(s) = \sum_{j=1, j \neq i}^n |q_{ij}^{-1}(s)| \tag{4.42}$$

The closed loop block diagram showing the pre compensator , controller, and transfer function are shown in figure 4.8

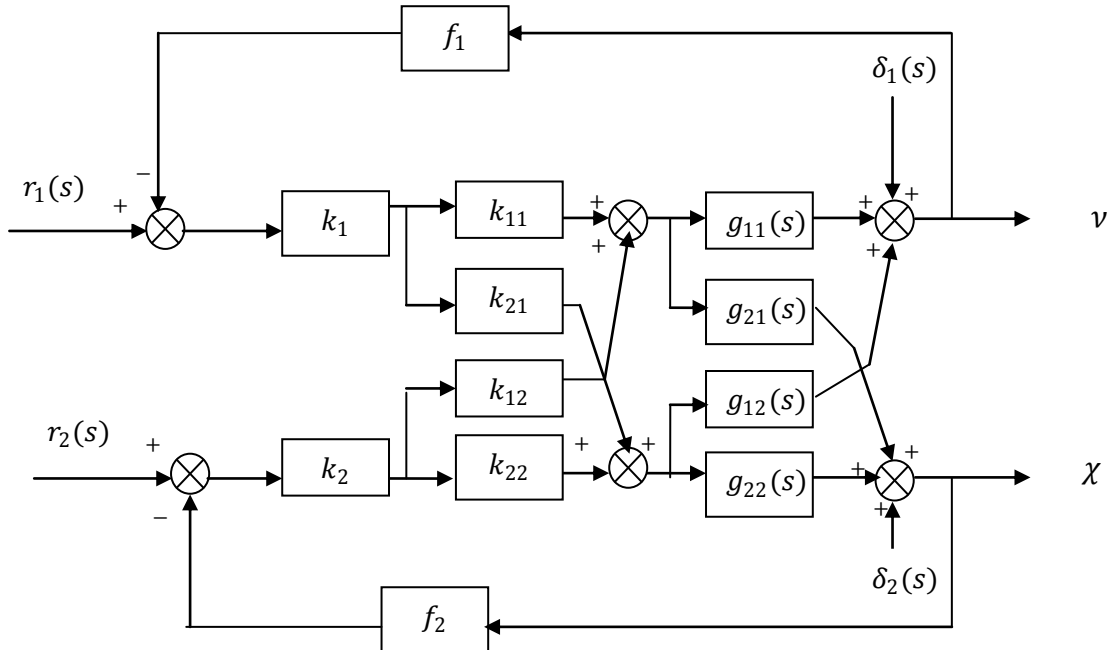


**Figure 4.8** Block Diagram for the system with pre compensator and controller

Eventually, after achieving the row diagonally dominance, the system stability can be investigated with ease using two single-input, single-output loops as elements on the diagonal of the transfer function matrix are also the main contributors in system response and stability.

#### 4.4 Aircraft Deck Landing

The landing of aircraft on carrier holds many challenges. The limited distance the aircraft has to stop after the wheel touching the deck surface necessitates the use of another mechanism to stop the aircraft besides the aircraft brakes.

One mechanism is shown in figure 4.9

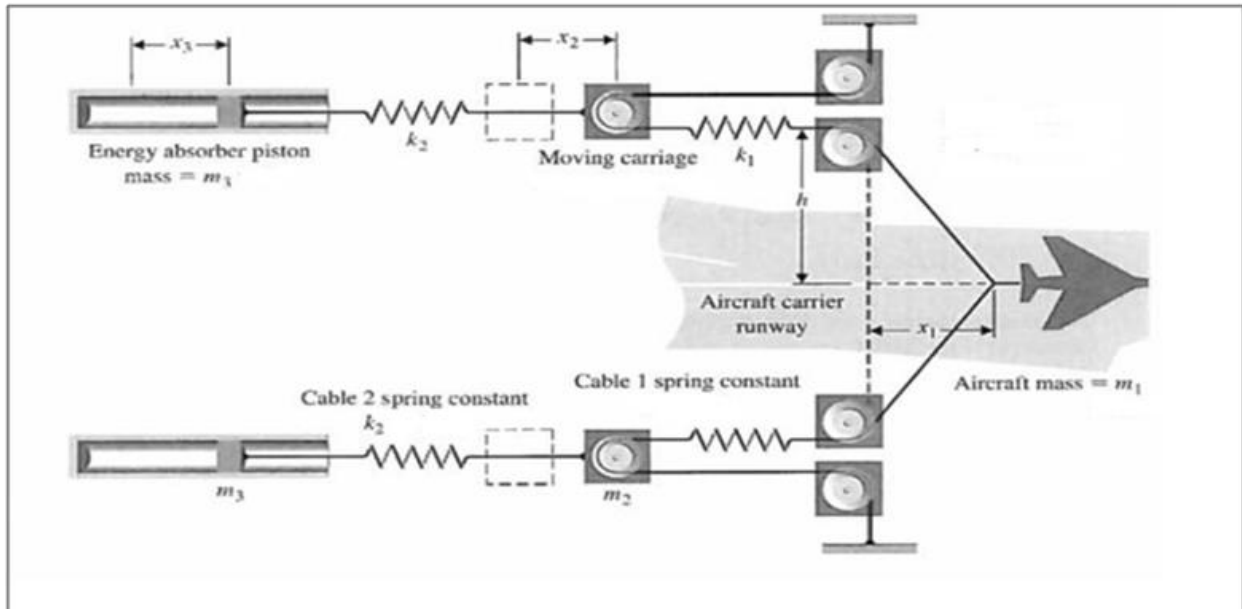


**Figure 4.9** Arresting gear configuration in an aircraft carrier

(Dorf and Bichop, 2011)

To simplify the arresting gear mechanism, the model in figure 4.10 will be used and analyzed to determine the distance aircraft will travel before reaching complete halt.

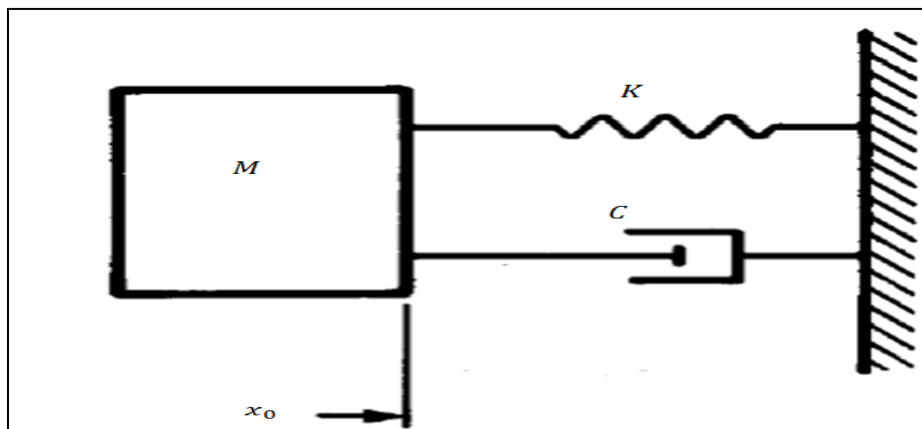


**Figure 4.10** simple spring-damper schematic

The governing equation for the spring mass configuration shown in figure 4.10 is:

$$M\ddot{x}_0 + C\dot{x}_0 + Kx_0 = 0 \quad 4.43$$

The Laplace transform for governing equation leads to:

$$M[s^2X_0(s) - sx_0(0) - x_0'(0)] + C[sX_0(s) - x_0(0)] + KX_0(s) = 0 \quad 4.44$$

Rearranging equation 4.44

$$[Ms^2 + Cs + K]X_0(s) = M[sx_0(0) + x_0'(0)] + Cx_0(0) \quad 4.45$$

Then

$$X_0(s) = \frac{M[sx_0(0) + x_0'(0)] + Cx_0(0)}{[Ms^2 + Cs + K]} \quad 4.46$$

# Chapter V

## Simulation Results and Discussion

### 5.1 Least Effort Controller

Implementing the methodology of chapter III will be presented here. The transfer function matrix in equation 4.4 for 2 input 2 output system model is:

$$G(s) = \frac{\begin{bmatrix} 63.997(s + 74.506) & 2(s + 74.506) \\ -6.8847(s + 0.6933) & -100(s + 0.6933) \end{bmatrix}}{s^2 + 1.2956s + 4.4867}$$

The transfer function  $G(s)$  can be written in the form of equation 4.17:

$$G(s) = L(s) \frac{A(s)}{d(s)} R(s) \Gamma(s)$$

Where

$$L(s) = R(s) = \Gamma(s) = I = \begin{bmatrix} 1 & 0 \\ 0 & 1 \end{bmatrix}$$

And

$$A(s) = \begin{bmatrix} 4769.1619 & 149.0241 & -4.7732 & -69.33 \\ 63.9979 & 2 & -6.8847 & -100 \end{bmatrix}$$

Then

$$d(s) = s^2 + 1.2956s + 4.4867$$

Referring to equation 4.27, the term:

$$[h \ A \ k] = [h_1 \ h_2] \begin{bmatrix} 4769.1619 & 149.0241 & -4.7732 & -69.33 \\ 63.9979 & 2 & -6.8847 & -100 \end{bmatrix} \begin{bmatrix} k_1 \\ k_2 \end{bmatrix}$$

which can be re-written in the following format:

$$[h \ A \ k] = [1 \ s] \begin{bmatrix} 4769.1619 & 149.0241 & -4.7732 & -69.33 \\ 63.9979 & 2 & -6.8847 & -100 \end{bmatrix} \begin{bmatrix} k_1 h_1 \\ k_2 h_1 \\ k_1 h_2 \\ k_2 h_2 \end{bmatrix}$$

From the fact that  $k_2 = nk_1$ , yields the matrix:

$$Q = \begin{bmatrix} 4769.1619 + 149.0241n & -4.7732 - 69.33n \\ 63.9979 + 2n & -6.8847 - 100n \end{bmatrix}$$

Now, root locus technique will be deployed to design the inner loop parameters according to mathematical analysis shown in section 4.2.1

$$\langle h \frac{A(s)}{d(s)} k \rangle = \frac{b(s)}{d(s)}$$

$$d(s) = s^2 + 1.2956s + 4.4867$$

The roots of  $d(s)$  or, alternatively, the system poles can now be found as:

$$-647.800010^{-3} \pm 2.0167i$$

In order to decrease the response time for the system while keeping acceptable dynamics, the parameters for the  $b$  matrix will be selected as:

$$b(s) = 50(s + 6)$$

Where the zero at  $-6$  will attract the poles of  $d(s)$  further to the left of imaginary axis which means faster response of the system. The value 50 will affect the overshoot of the dynamics, hence:

$$b = \begin{bmatrix} 1 \\ 6 \end{bmatrix} * 50$$

From the fact that  $k_1 = 1$  substituting in equation 4.35 results:

$$h = Q^{-1}b = [ 51.5537(10)^{-3} \quad -158.5409(10)^{-3} ]$$

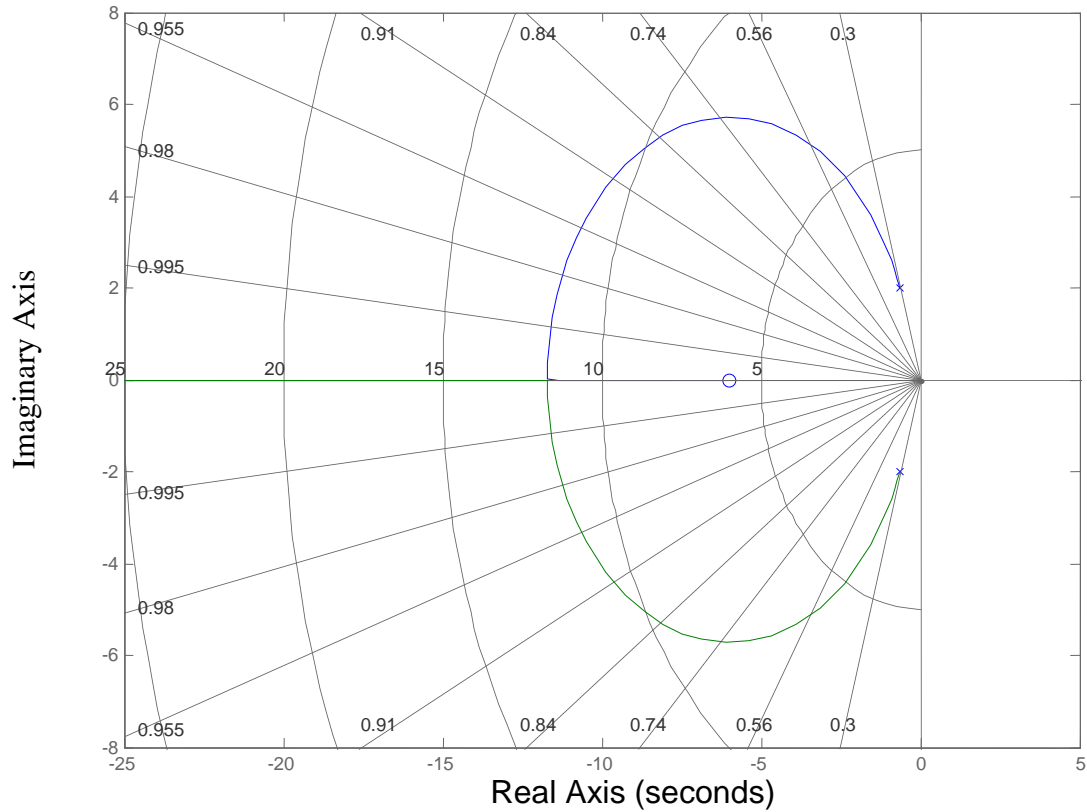


**Figure 5.1** Root Locus for  $b(s)/d(s)$

### 5.1.1 Least Effort Optimization

The performance index  $J$  at different  $n$  values is minimized, the minimum value of  $J$  can be found by taking the derivative of equation 4.36 with respect to  $n$  and equating the result to zero. From equation 4.36

$$J = (1 + n^2)b^T(Q^{-1})^T Q^{-1}b$$

By substitution

$$J = \frac{(1 + n^2)(2.2394n^2 + 127.3924n + 2037.9)}{0.218n^4 + 13.98n^3 + 225.158n^2 + 30.805n + 1.058}$$

Taking the derivative of  $J$  and finding the roots “extreme values”:

$$\frac{\partial J}{\partial n} = 0$$

The extreme  $J$ , either minimum or maximum, occurs at the following  $n$  values:

- At  $n_1 = -32$ , the value of  $J$  is  $J_1 = 5.175(10)^{30}$
- At  $n_2 = 2.858$ , the value of  $J$  is  $J_2 = 254.8456(10)^{-3}$
- $n_{3,4} = -98.866(10)^{-3} \pm 2.895$ , the value of  $J$  is  $J_{3,4} = (166.5038 \pm 13.180i)(10)^{-3}$
- At  $n_5 = -2.847$ , the value of  $J$  is  $J_2 = 288.658(10)^{-3}$
- At  $n_6 = -68.8470 (10)^{-3}$ , the value of  $J$  is  $J_2 = 1.9892(10)^{33}$

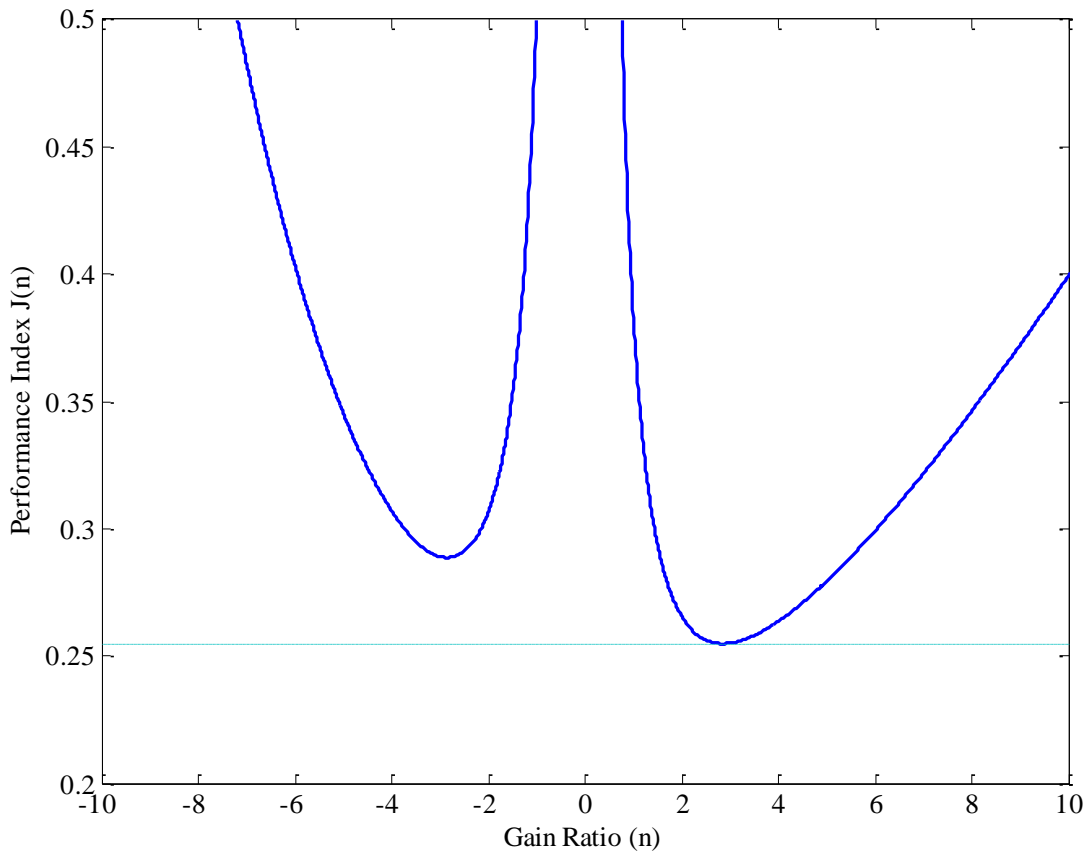


**Figure 5.2** Performance index with relation with gain ratio  $n$

Graphically, this can be depicted in figure 5.2 which show a plot of performance index  $J$  at different  $n$  values. The absolute minimum for the function  $J(n)$  is at  $n_2 = 2.858$ . Then

$$k_2 = n_2 k_1$$

By substitution

$$k_2 = 2.858(1) = 2.858$$

The forward gain for the internal loop becomes

$$k = \begin{bmatrix} 1 \\ 2.858 \end{bmatrix}$$

The internal loop heave rate and pitch rate responses for a step input are shown in figure 5.3 and 5.4 respectively.

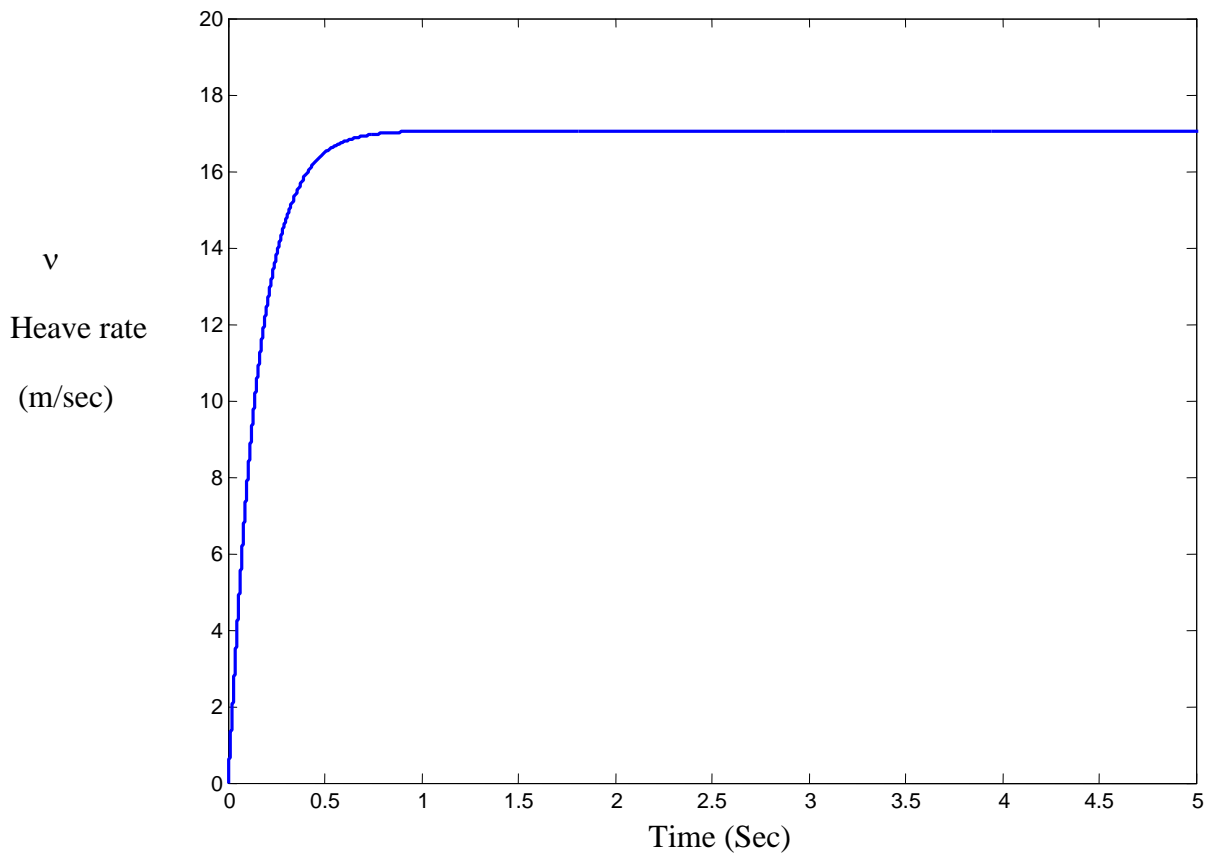


**Figure 5.3** Internal Loop Heave Rate response for a step input

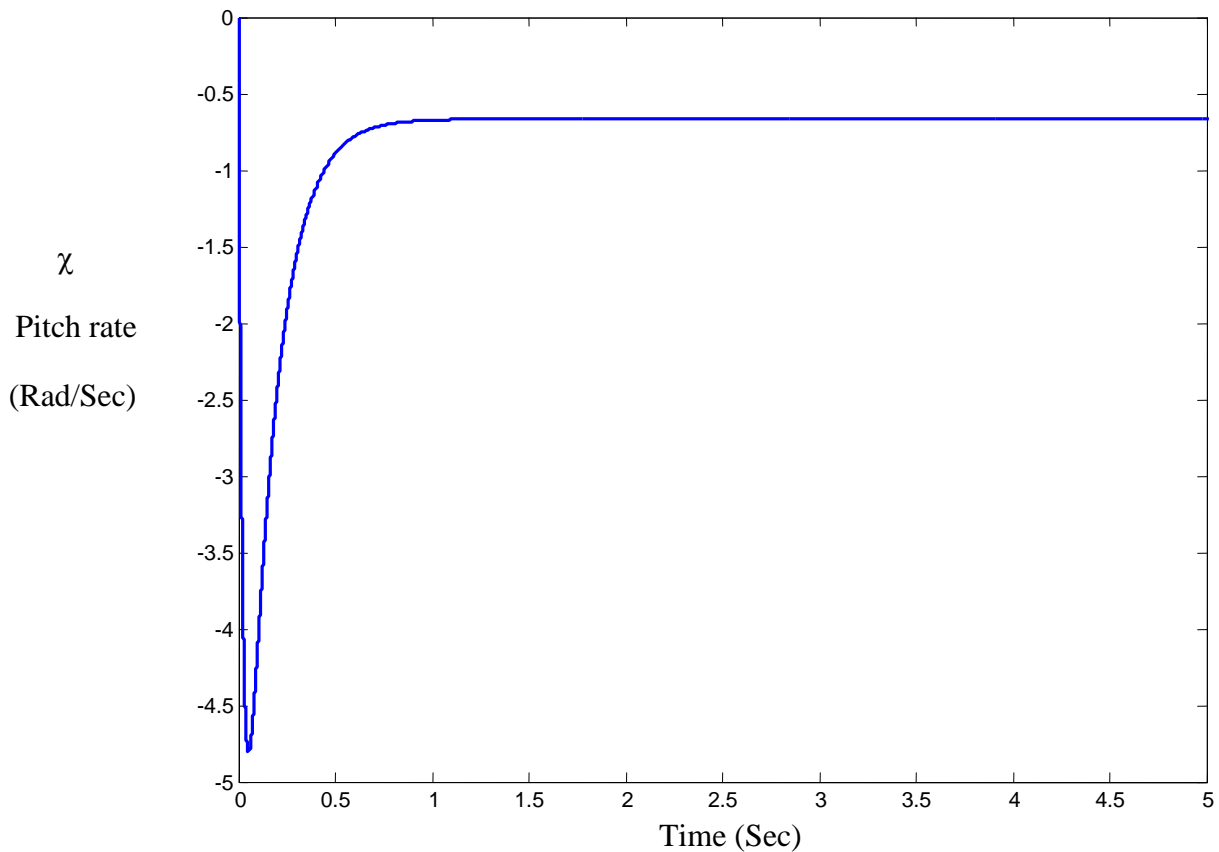


**Figure 5.4** Internal Loop Pitch Rate response for a step input

The internal loop plots exhibits acceptable dynamics in terms of settling time and overshoot. Hence, next step is to find the outer loop response.

### 5.1.2 Outer Loop design

The outer loop design involves finding the forward and feedback matrices gains. Reference to equation:

$$G(s) = \left\langle h \frac{A(s)}{d(s)} k \right\rangle$$

The transfer function matrix at steady state can be found from equation 4.4 by setting  $s = 0$ .

Then

$$G(0) = \begin{bmatrix} 1.0630(10)^3 & 33.2146 \\ -1.0638 & -15.4523 \end{bmatrix}$$

Hereafter, the maximum decoupling between system output can be achieved by considering the output matrix with summation of off diagonal elements less than 1.

Hence

$$S_s = \begin{bmatrix} 1 & 0.005 \\ -0.005 & 1 \end{bmatrix}$$

There is no special reason for choosing the minus sign at one of the off diagonal elements. However, it was chosen to demonstrate that off diagonal elements are small values regardless of the sign. The outer loop gains lays within the range  $0 < f < 1$  and has a direct impact on the dynamics of the output response and disturbance recovery. To investigate the effect of  $f$  on the closed loop response and disturbance rejection, heave rate and pitch rate response for closed loop system will be found at different  $f$  values.

- For  $f_1 = 0.1$  the feedback gain is:

$$F = \begin{bmatrix} 0.1 & 0 \\ 0 & 0.1 \end{bmatrix}$$

To find the forward gain, the values are substituted in equation 3.8

$$P = [G(0)^{-1} + k(0) \times h(0)] S_s [I - F S_s]^{-1}$$

Then

$$P = \begin{bmatrix} 59.2954 & -173.5803 \\ 166.8490 & -574.6438 \end{bmatrix}_{f_1=0.1} \times (10)^{-3}$$

Computation of feedback gain requires substitution values in equation 3.16

$$H(s) = P^{-1}k(s) \times h(s) + F$$

By substitution

$$H = \begin{bmatrix} 891.7905(10)^{-3} & -2.4350 \\ -26.5247(10)^{-3} & 181.5702(10)^{-3} \end{bmatrix}_{f_1=0.1}$$

Repeating the above steps for  $f_2 = 0.5$  and  $f_3 = 0.8$  the resulting forward and feedback gains are:

- For  $f_2 = 0.5$ , then  $F = \begin{bmatrix} 0.5 & 0 \\ 0 & 0.5 \end{bmatrix}$

The Feed forward gain is:

$$P = \begin{bmatrix} 108.1179 & -311.9632 \\ 304.9185 & -1.0330 \end{bmatrix}_{f_2=0.5} X (10)^{-3}$$

And the feedback gain is

$$H = \begin{bmatrix} 939.9502(10)^{-3} & -1.3530 \\ -12.7809(10)^{-3} & 539.3047(10)^{-3} \end{bmatrix}_{f_2=0.5}$$

- For  $f_3 = 0.8$ , then  $F = \begin{bmatrix} 0.8 & 0 \\ 0 & 0.8 \end{bmatrix}$

The feed forward gain is

$$P = \begin{bmatrix} 281.9076 & -775.6213 \\ 800.7897 & -2.5703 \end{bmatrix}_{f_3=0.8} X (10)^{-3}$$

And the feedback gain is

$$H = \begin{bmatrix} 976.0700 & -541.4609 \\ -2.4731(10)^{-3} & 807.6055(10)^{-3} \end{bmatrix}_{f_3=0.8} X (10)^{-3}$$

The closed loop heave rate output response for a step input on aircraft's wing's elevator is shown in figure 5.5 at different  $f$  values. The settling time is significantly improved compared to the open loop settling time as shown in figure 3.6. In addition the output exhibits

less oscillation in case of lower values of  $f$  (i.e = 0.1) . However, with increasing  $f$  values oscillation and overshoot could reach to higher values with lesser response time as shown in figure 5.5. The system shows almost zero steady state error with no deviation from the reference input  $r_1$  which represents the input at the wing's elevator.

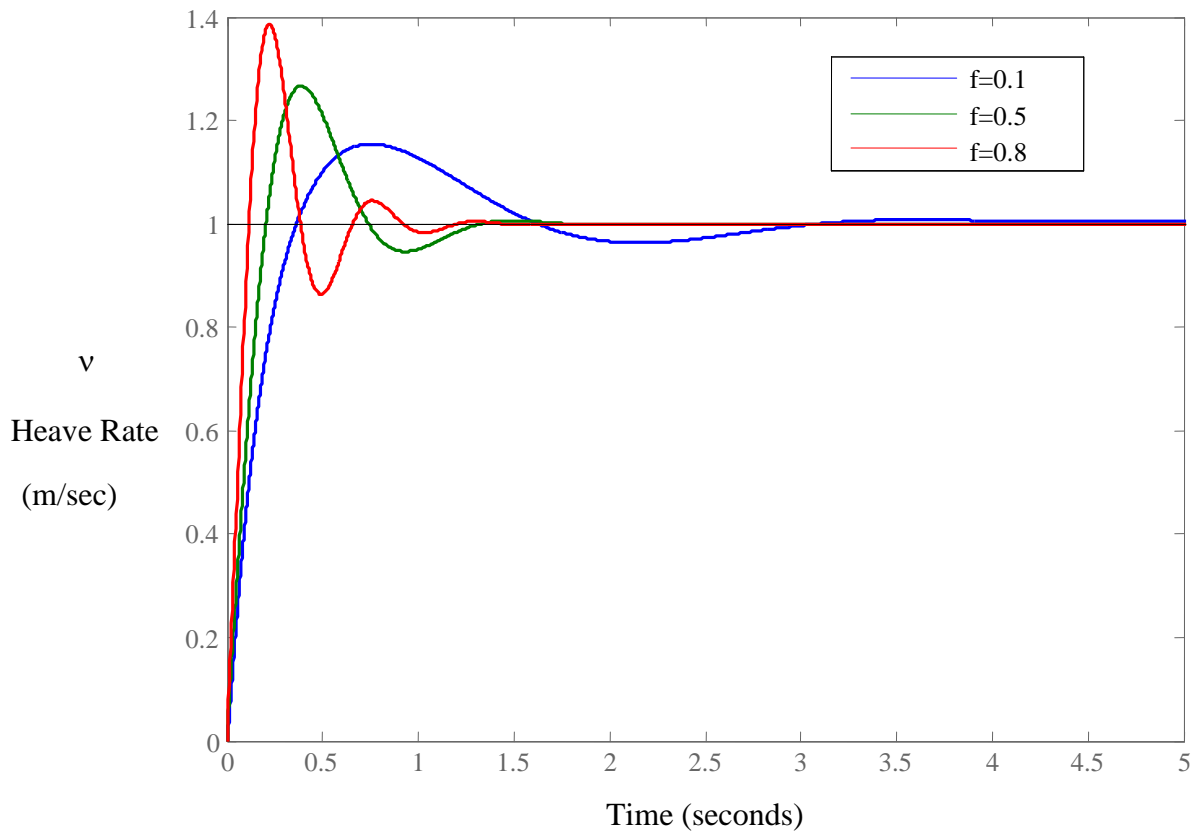


**Figure 5.5** Closed Loop Heave Rate Response to a step input  $r_1$  at different  $f$  values

Similarly, the dynamics of the closed loop pitch rate due to a step input  $r_1$  has a similar behaviour as heave rate's dynamics. The difference is in the steady state output response which follows the  $S_s$  matrix. The steady state pitch rate response will be  $-5X(10)^{-2}$  following a step

input at wing's elevator as suggested by the matrix  $S_s$ . The pitch rate response corresponding to a step input  $r_1$  is shown in figure 5.6 for different  $f$  values .

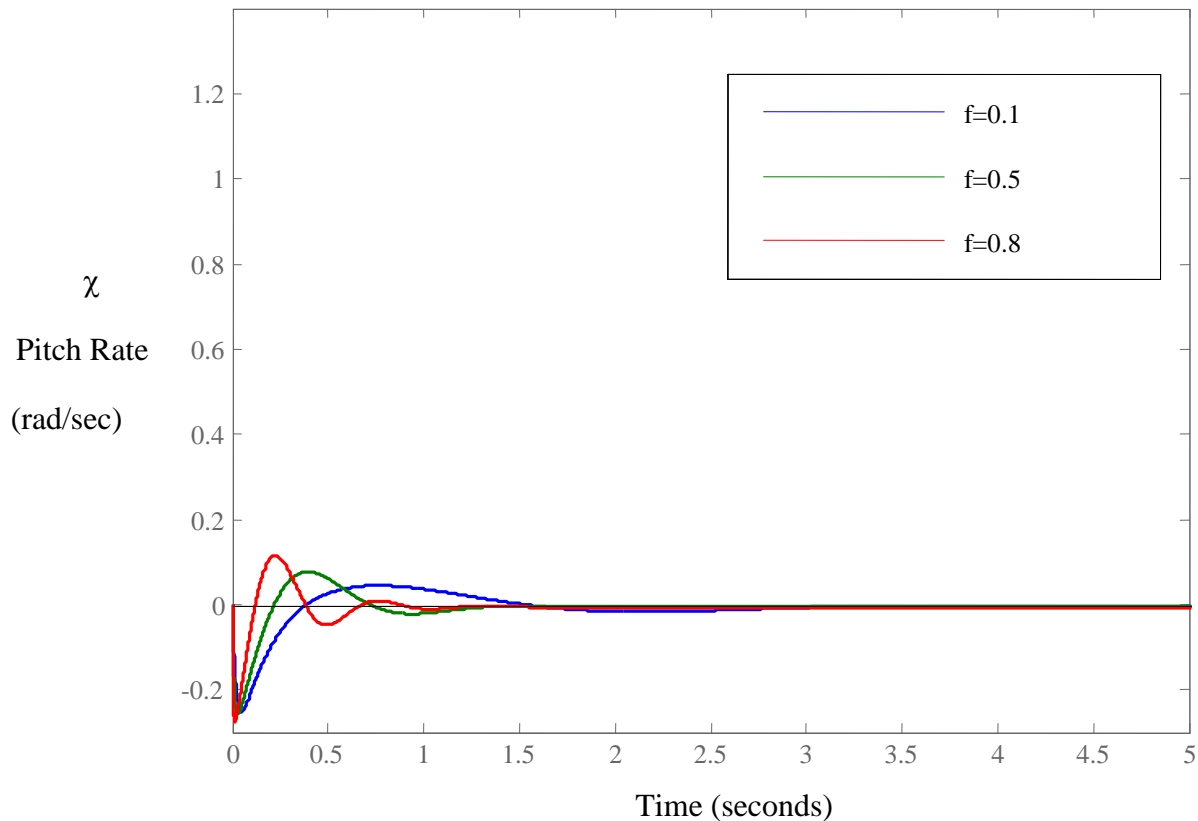


**Figure 5.6** Closed Loop Pitch Rate Response to a step input  $r_1$  at different  $f$  values

The closed loop response for a step input  $r_2$  at horizontal tail is shown in figures 5.7 and 5.8. The over shoot of pitch response at  $f = 0.1$  is unacceptably high. However, with increasing  $f$  value the over shoot decreases to about 25% at  $f = 0.8$

Settling time for closed loop pitch rate did not noticeably improved compared to open loop pitch rate response due to a step change on horizontal tail particularly at low feedback gain. But with increasing gain, settling time improves as well as the overshoot which is reduced

significantly from highly unacceptable to reasonably acceptable levels.

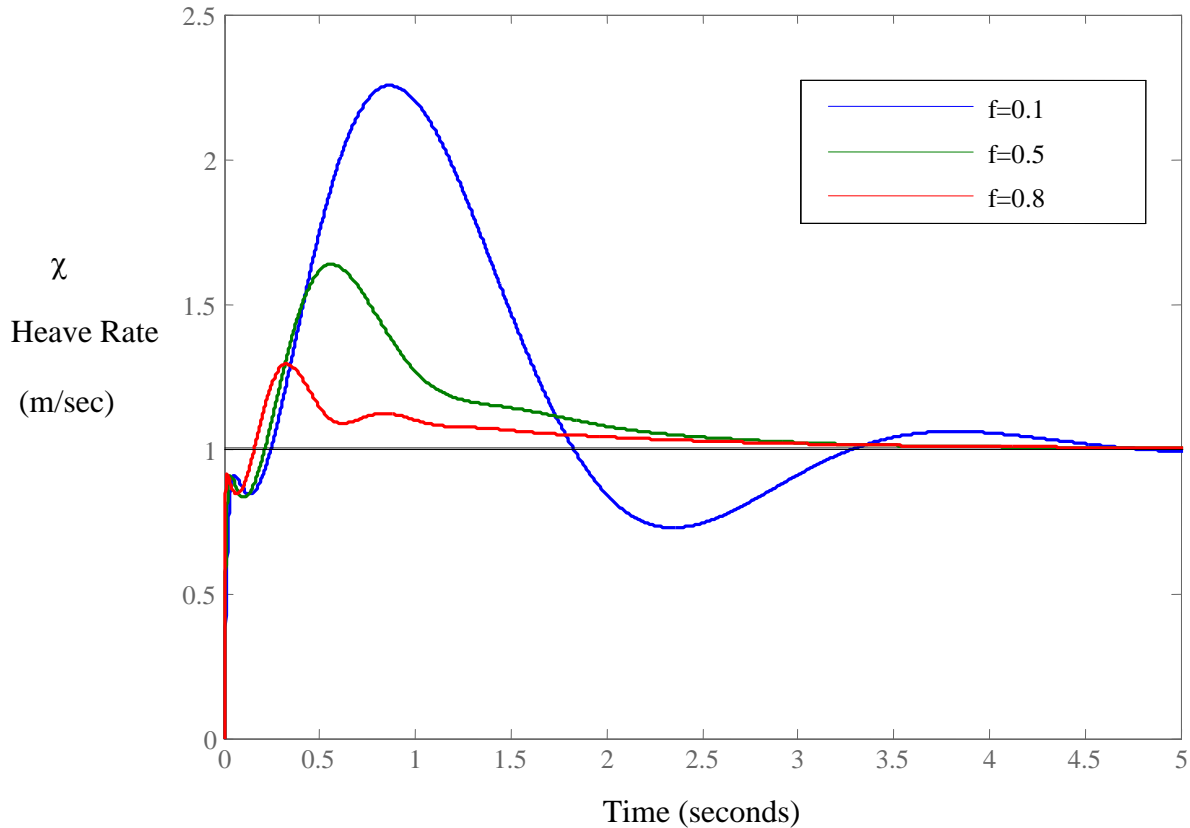


**Figure 5.7** Closed Loop Pitch Rate Response to a step input  $r_2$  at different  $f$  values

Although there are almost zero steady state errors in both plots in figures 5.6 and 5.7, they both share the characteristic of high overshoots at low feedback gains. While the output pitch rate settle at 1 following a step input  $r_2$  at tail, the output heave rate in figure 5.8 steady state response is at 0.005 as suggested by the  $S_s$  matrix. The plots show high level of decoupling between system outputs which is a desired performance characteristic.

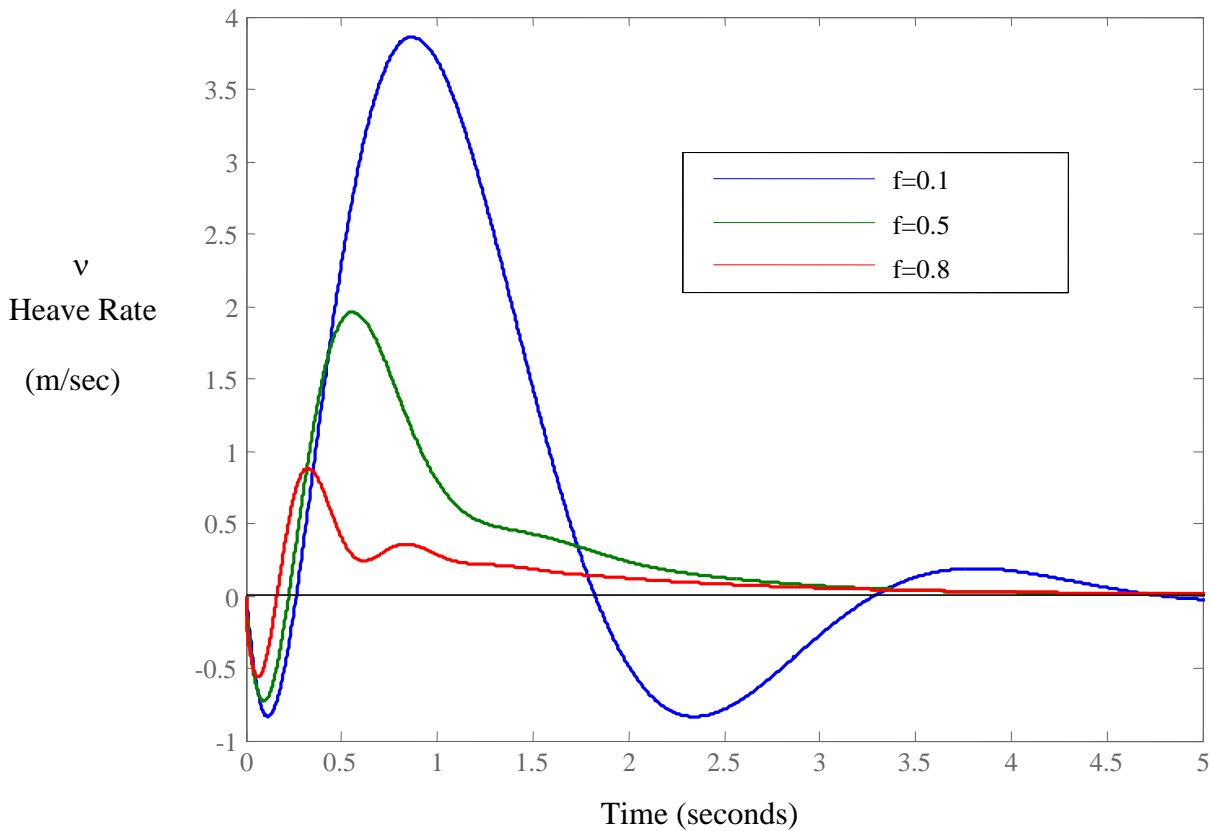


**Figure 5.8** Closed Loop Heave Rate Response to a step input  $r_2$  at different  $f$  values

## 5.2 Disturbance Rejection analysis for L.E.C

After studying the internal and closed loop response for step inputs  $r_1$  and  $r_2$  at different feedback gains  $f$  values, one aspect of the robustness of the system due to disturbance input  $\delta_1$  and  $\delta_2$  will be investigated.

To calculate the response for disturbance input, equation 4.12 is used:

$$y(s) \cong \{I + G(s)k(s) \gg h(s)\}^{-1}[G(s) Pr(s) + \delta(s)]$$

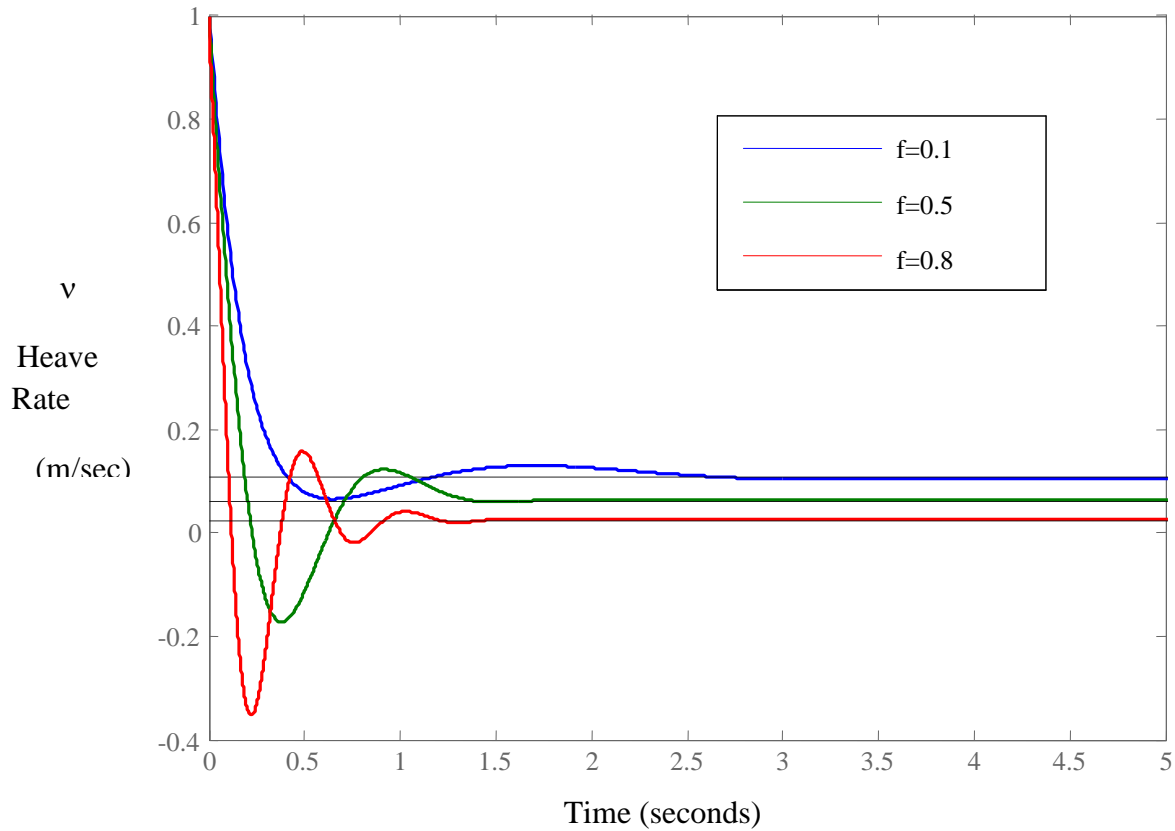


**Figure 5.9** Closed Loop Heave Rate Response following a step disturbance  $\delta_1$  at different  $f$  values

Then, the heave rate and pitch rate steady state response ( $s = 0$ ), due to a step input  $\delta_1$  is found by setting  $r_1 = r_2 = \delta_2 = 0$ , and setting  $\delta_1 = 1$ , then equation 3.13 becomes:

- At  $f_1 = 0.1$ :

$$\begin{bmatrix} v \\ \chi \end{bmatrix} = \left[ I + \begin{bmatrix} 1.0630(10)^3 & 33.2146 \\ -1.0638 & -15.4523 \end{bmatrix} \cdot \begin{bmatrix} 59.2954 & -173.5803 \\ 166.8490 & -574.6438 \end{bmatrix}_{f_1=0.1} \begin{bmatrix} 891.7905(10)^{-3} & -2.4350 \\ -26.5247(10)^{-3} & 181.5702(10)^{-3} \end{bmatrix}_{f_1=0.1} X (10)^{-3} \right]^{-1} \cdot \begin{bmatrix} 1 \\ 0 \end{bmatrix}$$

Hence

$$\begin{bmatrix} v \\ \chi \end{bmatrix} = \begin{bmatrix} 108.3421 \\ 30.9836 \end{bmatrix} \cdot (10)^{-3}$$

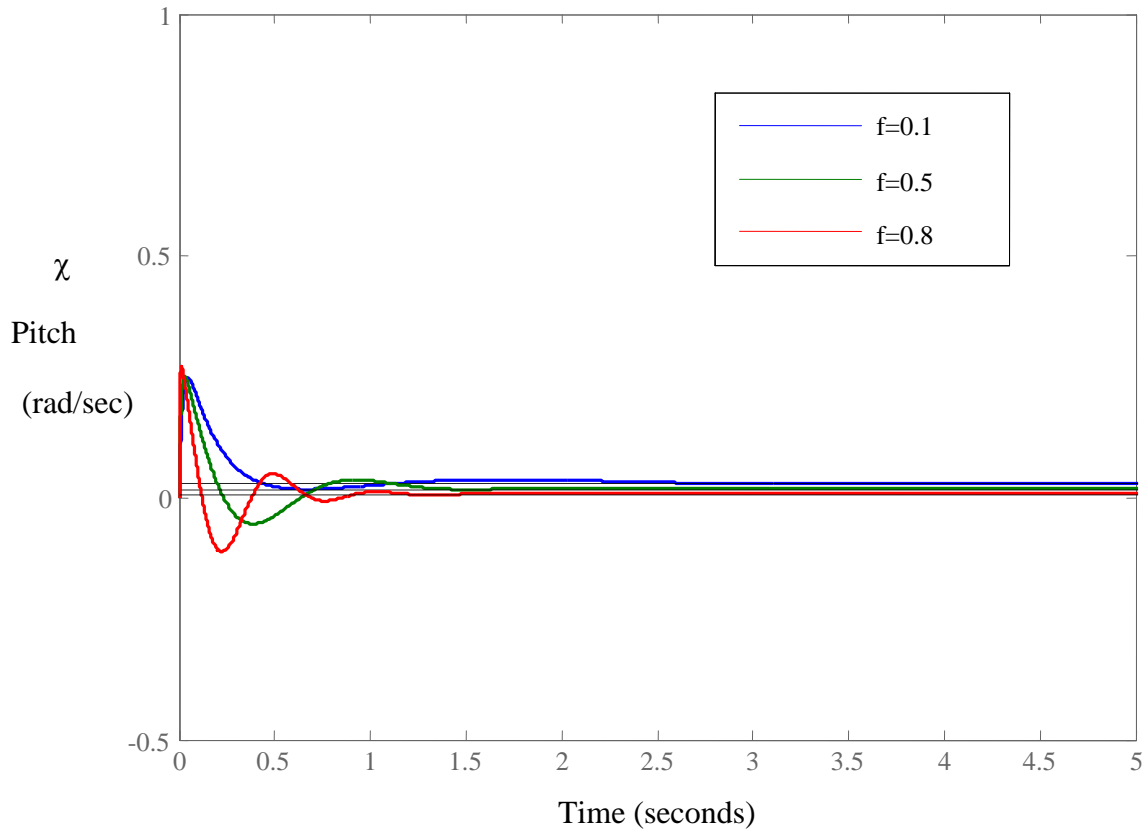


**Figure 5.10** Closed Loop Pitch Rate Response following a step disturbance  $\delta_1$  at different  $f$  values

- At  $f_2 = 0.5$ :

$$\left[ I + \begin{bmatrix} 1.0630(10)^3 & 33.2146 \\ -1.0638 & -15.4523 \end{bmatrix} \cdot \begin{bmatrix} 108.1179 & -311.9632 \\ 304.9185 & -1.0330 \end{bmatrix}_{f_2=0.5} \begin{bmatrix} 939.9502(10)^{-3} & -1.3530 \\ -12.7809(10)^{-3} & 539.3047(10)^{-3} \end{bmatrix}_{f_2=0.5} X (10)^{-3} \right]^{-1} \cdot \begin{bmatrix} 1 \\ 0 \end{bmatrix}$$

Hence

$$\begin{bmatrix} u \\ \chi \end{bmatrix} = \begin{bmatrix} 60.1137 \\ 17.4807 \end{bmatrix} \cdot (10)^{-3}$$

- At  $f_3 = 0.8$

$$\left[ I + \begin{bmatrix} 1.0630(10)^3 & 33.2146 \\ -1.0638 & -15.4523 \end{bmatrix} \cdot \begin{bmatrix} 281.9076 & -775.6213 \\ 800.7897 & -2.5703 \end{bmatrix}_{f_3=0.8} \begin{bmatrix} 976.0700 & -541.4609 \\ -2.4731(10)^{-3} & 807.6055(10)^{-3} \end{bmatrix}_{f_3=0.8} X (10)^{-3} \right]^{-1} \cdot \begin{bmatrix} 1 \\ 0 \end{bmatrix}$$

$$\begin{bmatrix} u \\ \chi \end{bmatrix} = \begin{bmatrix} 23.9424 \\ 7.3535 \end{bmatrix} \cdot (10)^{-3}$$

Figures 5.9 and 5.10 show the disturbance recovery for both heave rate and pitch rate, respectively, due to step input  $\delta_1$ . Figure 5.9 shows a significant output recovery for a step disturbance on wing's elevator. Similar to closed loop heave rate response due step input  $r_1$ , the overshoot increases with increasing value of  $f$ .

The pitch rate response due to step disturbance on wing's elevator is shown in figure 5.10. The response resemble the response of heave rate in terms of steady state response and the overshoot relation with  $f$ .

Now the step disturbance  $\delta_2 = 1$  will be applied and all other inputs and disturbance to be set to zero,  $r_1 = r_2 = \delta_1 = 0$ . Substituting in equation 4.36 yields

- At  $f_1 = 0.1$ :

$$\begin{bmatrix} v \\ \chi \end{bmatrix} = \left[ I + \begin{bmatrix} 1.0630(10)^3 & 33.2146 \\ -1.0638 & -15.4523 \end{bmatrix} \cdot \begin{bmatrix} 59.2954 & -173.5803 \\ 166.8490 & -574.6438 \end{bmatrix}_{f_1=0.1} \begin{bmatrix} 891.7905(10)^{-3} & -2.4350 \\ -26.5247(10)^{-3} & 181.5702(10)^{-3} \end{bmatrix}_{f_1=0.1} X (10)^{-3} \right]^{-1} \cdot \begin{bmatrix} 0 \\ 1 \end{bmatrix}$$

Hence

$$\begin{bmatrix} v \\ \chi \end{bmatrix} = \begin{bmatrix} 2.4341 \\ 806.2550 \cdot (10)^{-3} \end{bmatrix}$$

- At  $f_2 = 0.5$ :

$$\left[ I + \begin{bmatrix} 1.0630(10)^3 & 33.2146 \\ -1.0638 & -15.4523 \end{bmatrix} \cdot \begin{bmatrix} 108.1179 & -311.9632 \\ 304.9185 & -1.0330 \end{bmatrix}_{f_2=0.5} \begin{bmatrix} 939.9502(10)^{-3} & -1.3530 \\ -12.7809(10)^{-3} & 539.3047(10)^{-3} \end{bmatrix}_{f_2=0.5} X (10)^{-3} \right]^{-1} \cdot \begin{bmatrix} 0 \\ 1 \end{bmatrix}$$

Hence

$$\begin{bmatrix} v \\ \chi \end{bmatrix} = \begin{bmatrix} 1.3503 \\ 453.9305 \cdot (10)^{-3} \end{bmatrix}$$

- At  $f_3 = 0.8$

$$\left[ I + \begin{bmatrix} 1.0630(10)^3 & 33.2146 \\ -1.0638 & -15.4523 \end{bmatrix} \cdot \begin{bmatrix} 281.9076 & -775.6213 \\ 800.7897 & -2.5703 \end{bmatrix}_{f_3=0.8} \begin{bmatrix} 976.0700 & -541.4609 \\ -2.4731(10)^{-3} & 807.6055(10)^{-3} \end{bmatrix}_{f_3=0.8} X (10)^{-3} \right]^{-1} \cdot \begin{bmatrix} 0 \\ 1 \end{bmatrix}$$

$$\begin{bmatrix} v \\ \chi \end{bmatrix} = \begin{bmatrix} 537.4228 \\ 189.6872 \end{bmatrix} \cdot (10)^{-3}$$

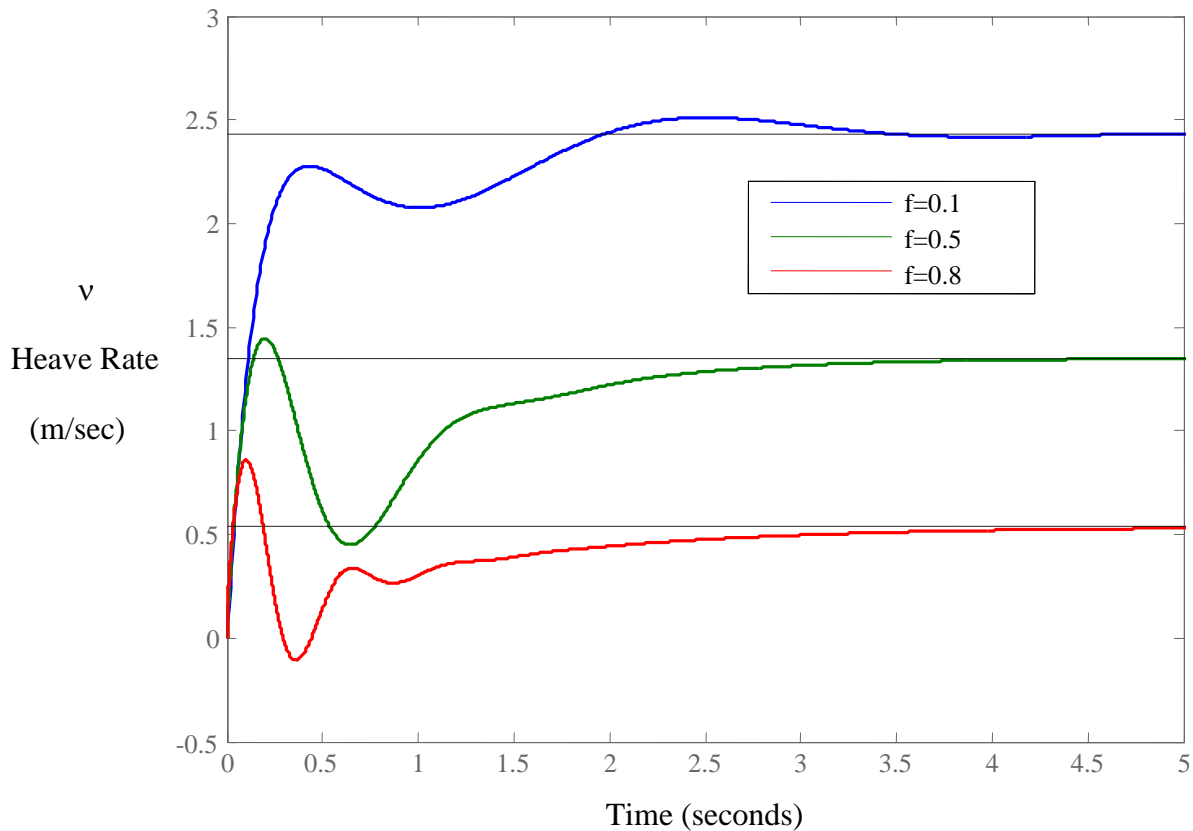


**Figure 5.11** Closed Loop Heave Rate Response following a step disturbance  $\delta_2$  at different  $f$  values

Figure 5.11 shows unacceptable level of disturbance recovery at  $f = 0.1$  and  $f = 0.5$ . However, with increasing  $f$  value to  $f = 0.8$ , about 47% disturbance rejection is achieved which meets the design requirement.

The pitch rate shows better performance than heave rate in terms of disturbance recovery due to applied disturbance  $\delta_2$  at horizontal tail. In the three trial  $f$  values, i.e,  $f = 0.1$ ,  $f = 0.5$ , and  $f = 0.8$  the disturbance rejection percentage are approximately 20%, 57%, and 81% , respectively, in which all meet the design requirement.

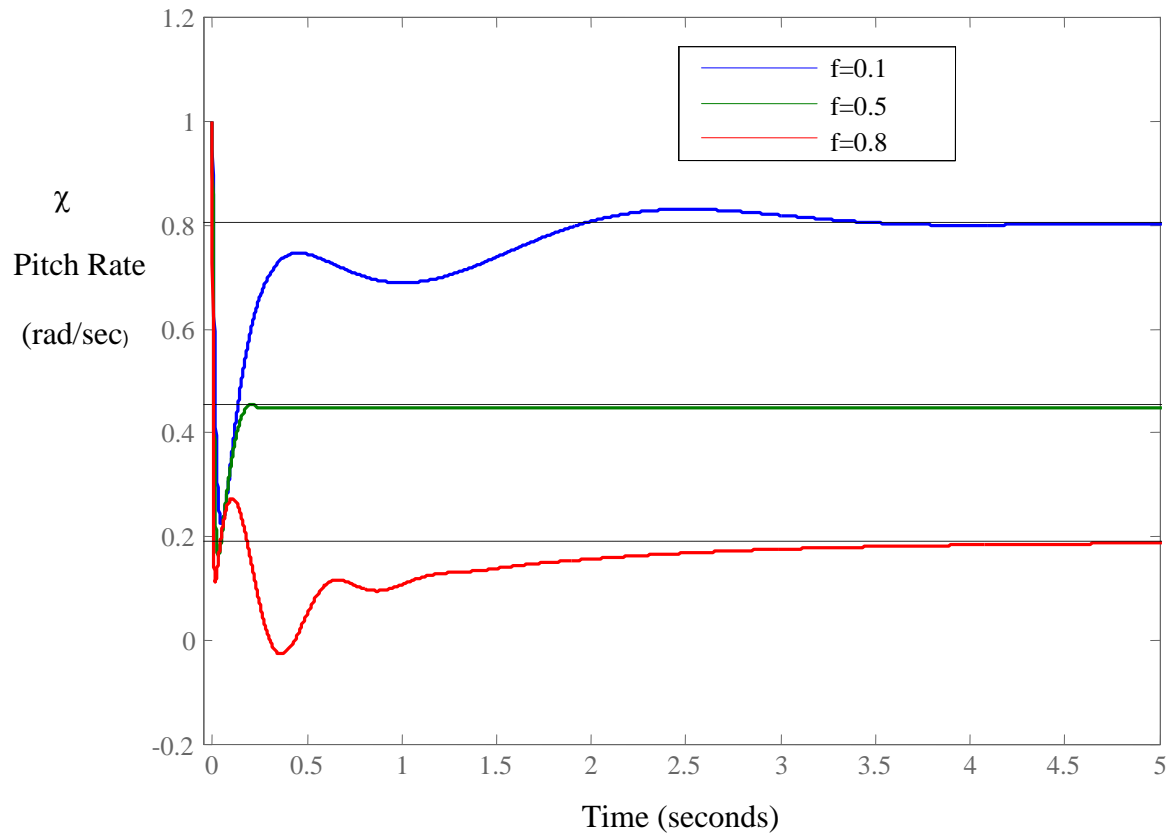


**Figure 5.12** Closed Loop Pitch Rate Response following a step disturbance  $\delta_2$  at different  $f$  values

### 5.3 Energy Dissipation at different gain ratios

The dissipated energy using least effort regulator should be the minimum energy used to recover the system from random disturbance. To verify this statement, simulation model is built in the appendix (figure A.1). Using this model, the consumed energy is depicted in figure 5.13 at two gain ratios  $n$  at which the two minimum values of performance index  $J$  are identified as shown in figure 5.2. As shown in figure 5.13 the minimum consumed energy occurs at  $n_{min}$  which satisfy the minimum value of performance index  $J$ .

At any other  $n$  value, the dissipated energy exceeds the one consumed at  $n_{min}$  which

cement the assumption of least effort, or minimum effort, regulator purpose.

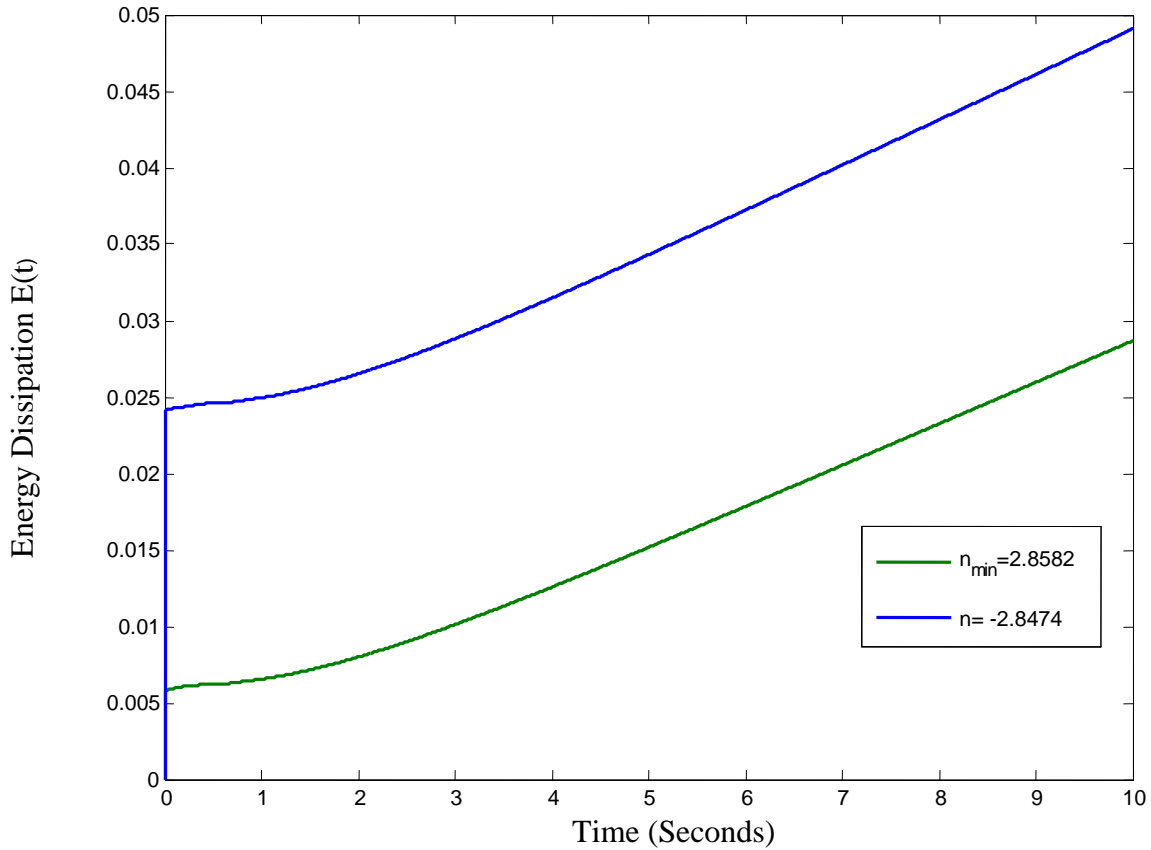


**Figure 5.13** The Dissipated Energy required recovering the aircraft from random disturbance input at different gain ratios

## 5.4 Inverse Nyquist Method

### 5.4.1 Diagonal Dominance

The condition of row diagonal dominance for the transfer function in equation 4.4 is fulfilled without the need for pre-compensator. Each diagonal element in the transfer function matrix is much larger than the element on the same row which implies the condition of row diagonal dominance.

Hence, the plot of the inverse Nyquist for the two elements at the diagonal with

Gershgorin bands superimposed are shown in figure 5.14 and figure 5.15 respectively.

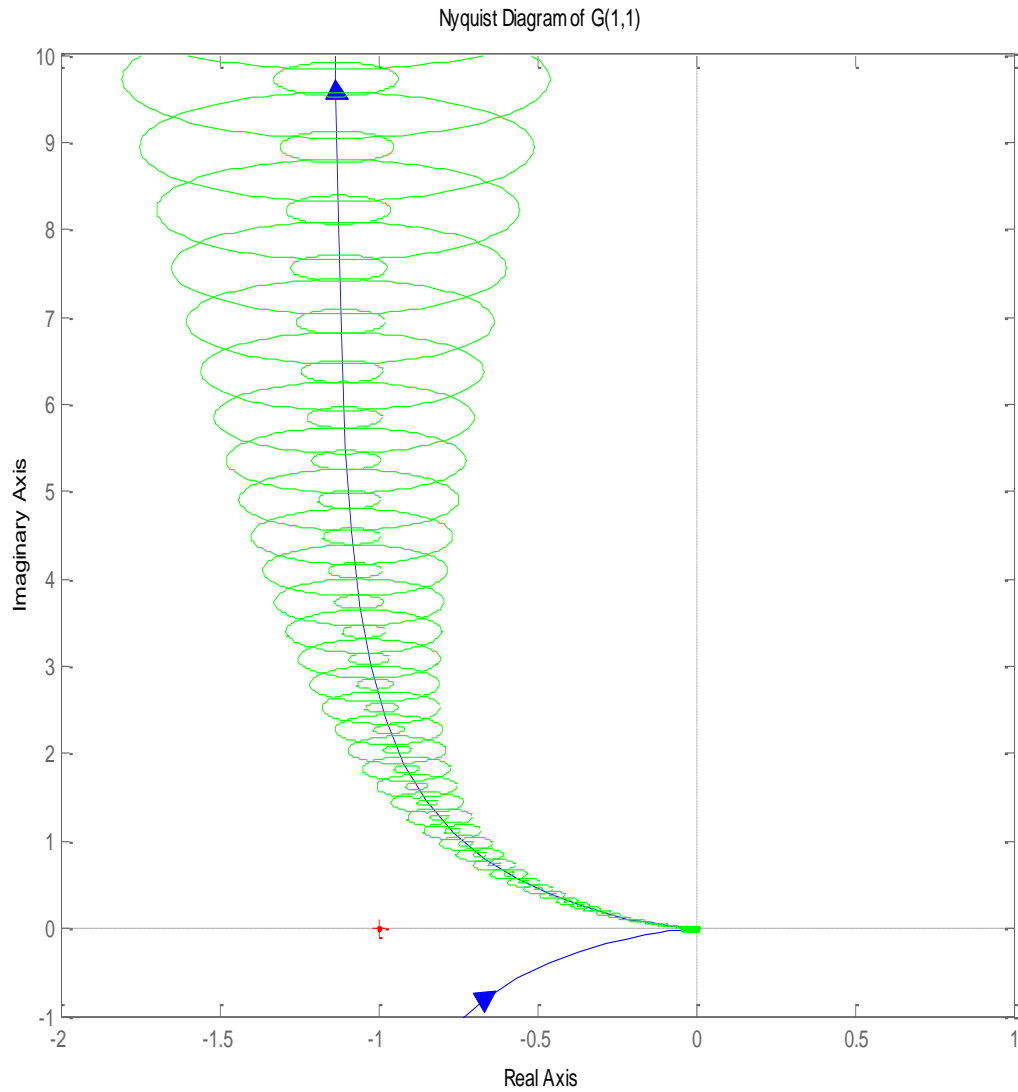


**Figure 5.14** Nyquist diagram of  $q_{11}^{-1}$  with Gershgorin circles

It is clearly shown in figures 5.14 and 5.15 that Gershgorin bands do not encircle the origin of the complex plane which satisfies the condition of row diagonal dominance. It is also worth noting that the Nyquist diagram in figure 5.14 never cross the negative axis which implies

that the feedback loop with infinite gains can be designed without adverse effect on system stability. However, the Nyquist diagram in figure 5.15 cross the negative axis and heads toward  $-\infty$ . This results into a need for careful design for the controller to attain acceptable system dynamics.

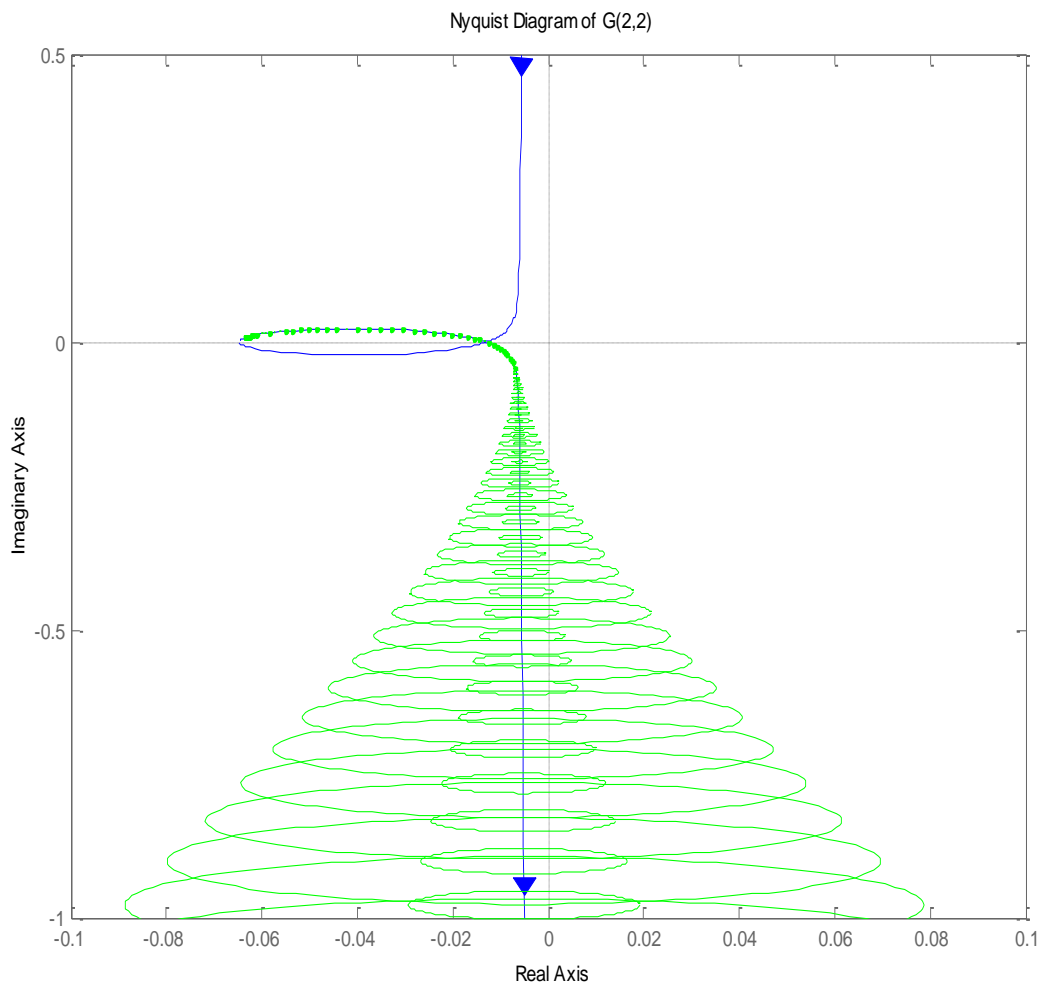


**Figure5.15** Nyquist diagram of  $q_{22}^{-1}$  with Gershgorin circles

### 5.4.2 Output Responses

The next step is to design a controller for each transfer function  $q_{11}^{-1}$  and  $q_{22}^{-1}$  independently with a unity feedback for each element. This was the purpose of investigating the row diagonal dominance. It is convenient to completely separate the study of each transfer function considering them as two different systems and simulate their response, then, a final check is performed by simulating the complete system with two inputs two outputs.

The block diagram in figure 4.8 shows the pre-compensator matrix and the controller matrix as follows:

$$K_1^{-1} = \begin{bmatrix} k_{11} & k_{12} \\ k_{21} & k_{22} \end{bmatrix}^{-1}$$

With no compensator required, the above matrix becomes

$$K^{-1} = I_m \text{ where } I_m = \begin{bmatrix} 1 & 0 \\ 0 & 1 \end{bmatrix}$$

This further eases the design for the controller matrix, while a simple gain is sufficient for the first transfer function  $q_{11}^{-1}$ , the second transfer function  $q_{22}^{-1}$  requires a PID controller as shown in the following matrix.

$$k = \begin{bmatrix} 0.4 & 0 \\ 0 & -1 \end{bmatrix}$$

The last matrix suggests a positive feedback on one of the loops because the transfer function  $g_{22}$  has a negative sign. With the above controller and unity feedback, the closed loop response due to step input at the wing and the horizontal tail are simulated in figures 5.16 to 5.19.

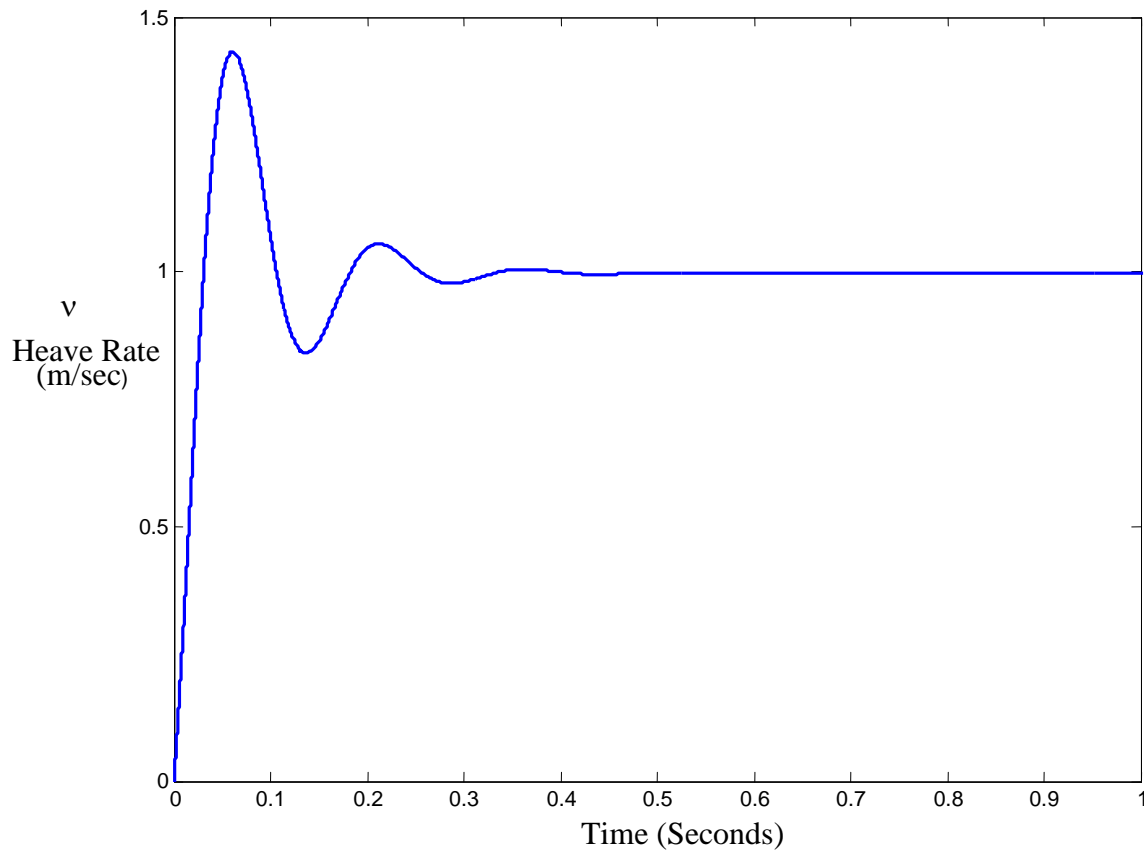


**Figure 5.16** Closed Loop Heave Rate Response to a step input  $r_1$  using INA method

The heave rate and pitch rate following a unit step input at wing's control surface exhibit a relatively quick settling time (less than a second) with almost zero steady state error. The heave rate shows an overshoot of 40% as shown in figure 5.16 while the pitch rate in figure 5.17 shows almost no response to a step input at wings surface which leads to a conclusion of high level of decoupling.

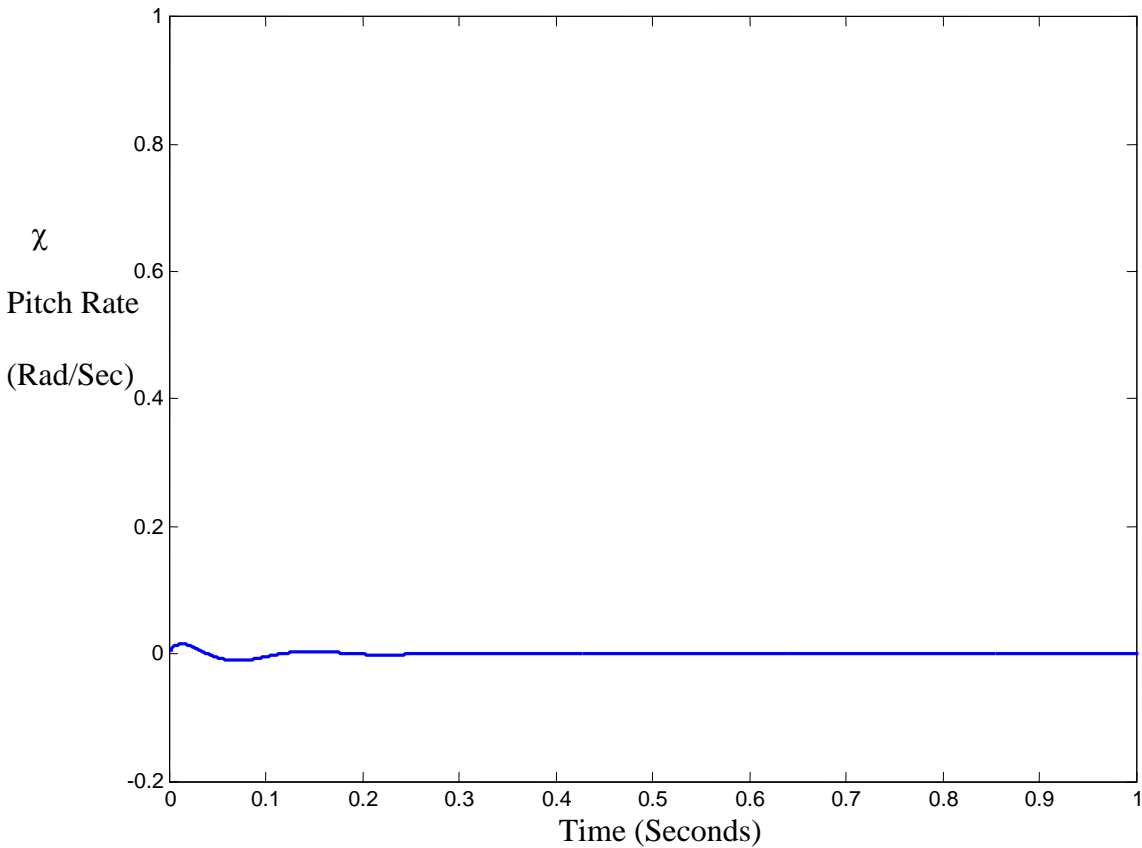


**Figure 5.17** Closed Loop Pitch Rate Response to a step input  $r_1$  using INA method

Similarly, with unit step input at horizontal tail, the output responses are simulated in figures 5.18 and figure 5.19. The pitch rate response in figure 5.18 is well behaved with zero overshoot, quick settling time, and slight steady state error (less than 5%).

The same decoupling effect can be shown in figure 5.19 with zero heave rate response due to a step input at horizontal tail. With slight negligible oscillation, a response time less than half a second, and a zero steady state response, it is reasonable to say that there is no response or change in heave rate due to a step input at horizontal tail, which is the perfectly desired outcome of this two input, two output system.

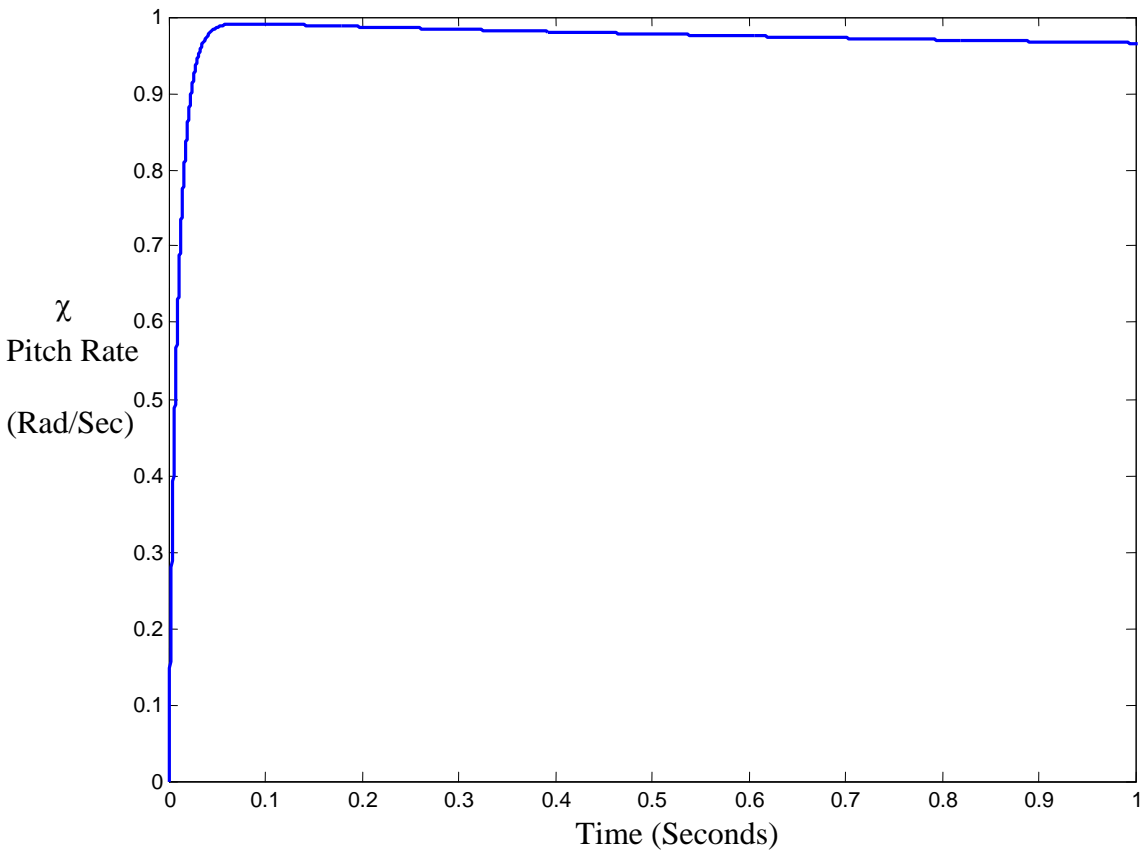


**Figure 5.18** Closed Loop Pitch Rate Response to a step input  $r_2$  using INA method

For sake of comparison between Inverse Nyquist method and least effort method, the response to disturbance at wing and tail should be also simulated using Inverse Nyquist method to investigate the system effectiveness in disturbance recovery using different design methodologies.

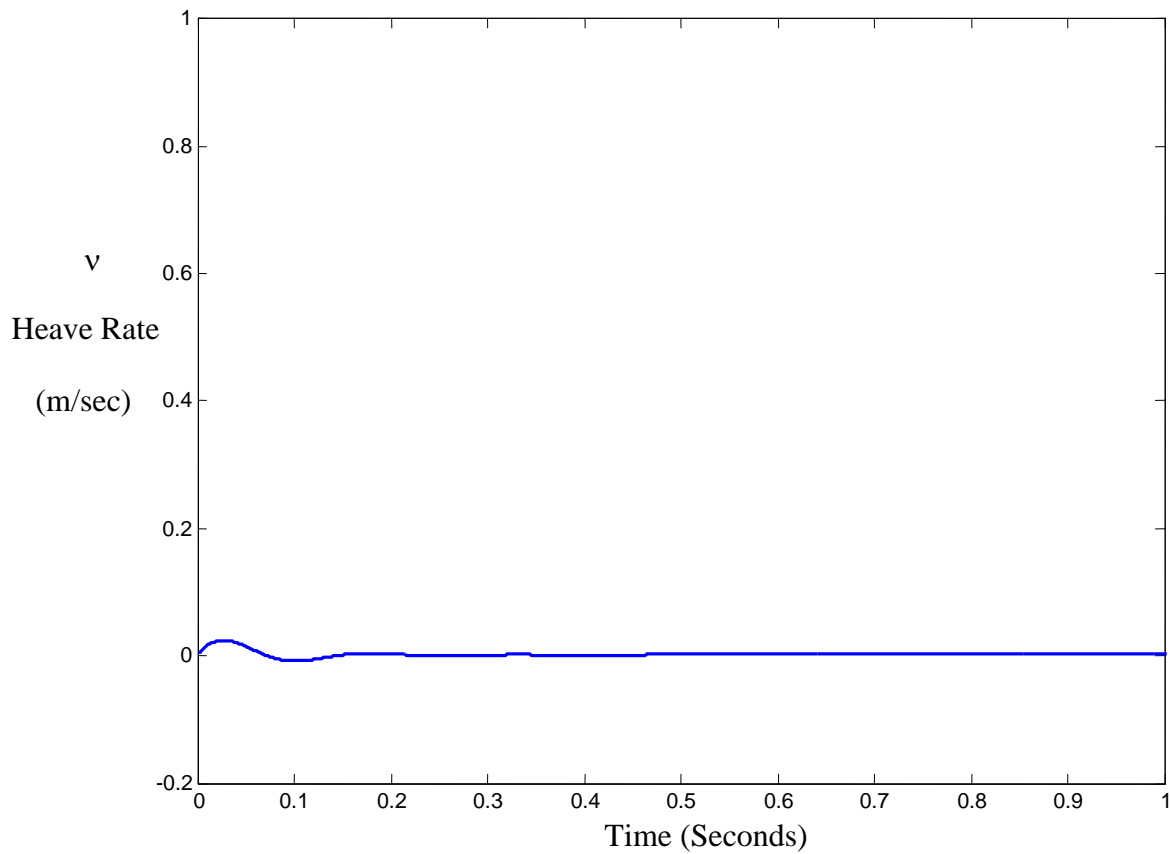


**Figure 5.19** Closed Loop Heave Rate Response to a step input  $r_2$  using INA method

### 5.4.3 Disturbance Rejection for INA method

The same simulation model used to investigate the output response for step inputs is used to simulate the output response by adding step disturbances at both the wing and horizontal tail and setting inputs to zero.

The first simulation is for the heave rate disturbance recovery due to a step disturbance at wing as shown in figure 5.20. With maximum overshoot of  $-0.4$  the settling time is less than  $0.5$  seconds with the response effectively comes down to zero.

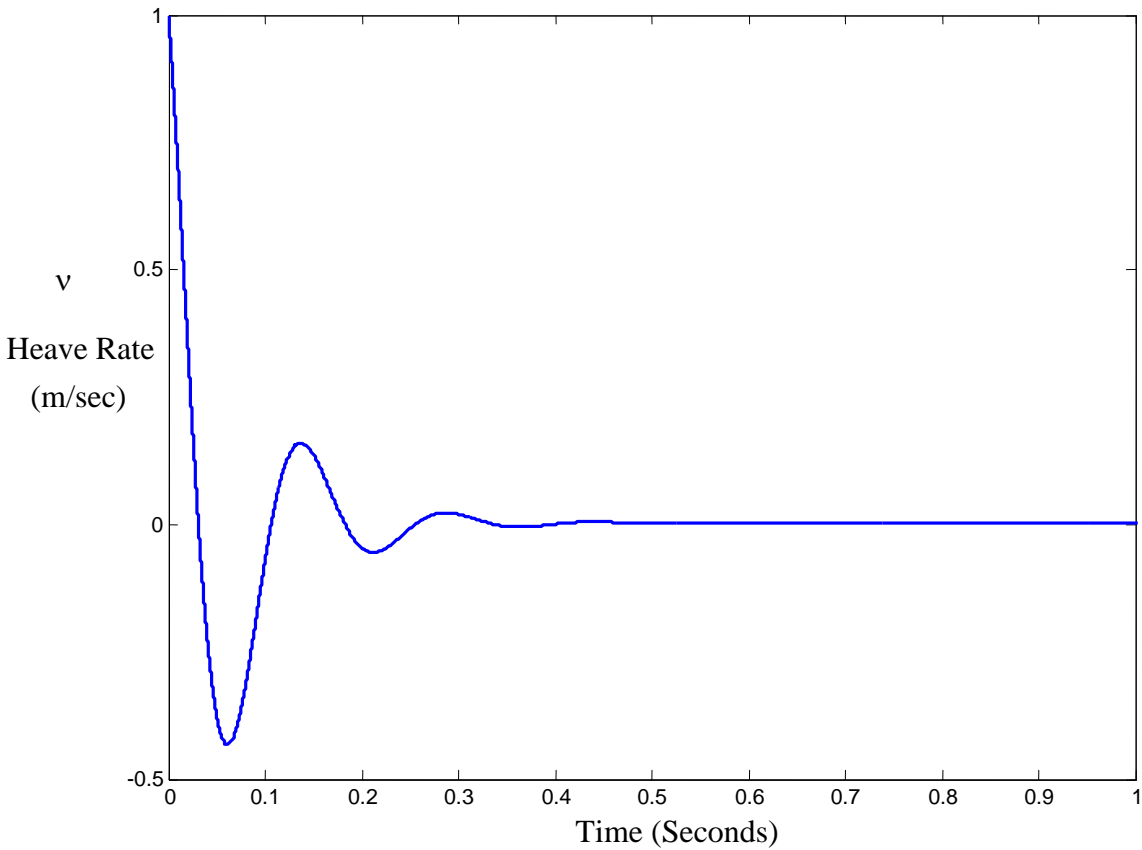


**Figure 5.20** Closed Loop Heave Rate Response to a step input  $\delta_1$  using INA method

The pitch rate response due to disturbance on wing is shown in figure 5.21. Again, the pitch rate shows high degree of disturbance recovery. A minimal oscillation leads a quick settling to zero response within 0.2 seconds.

In the same manner, the output responses due to a step disturbance at horizontal tail are shown in figures 5.22 and 5.23.

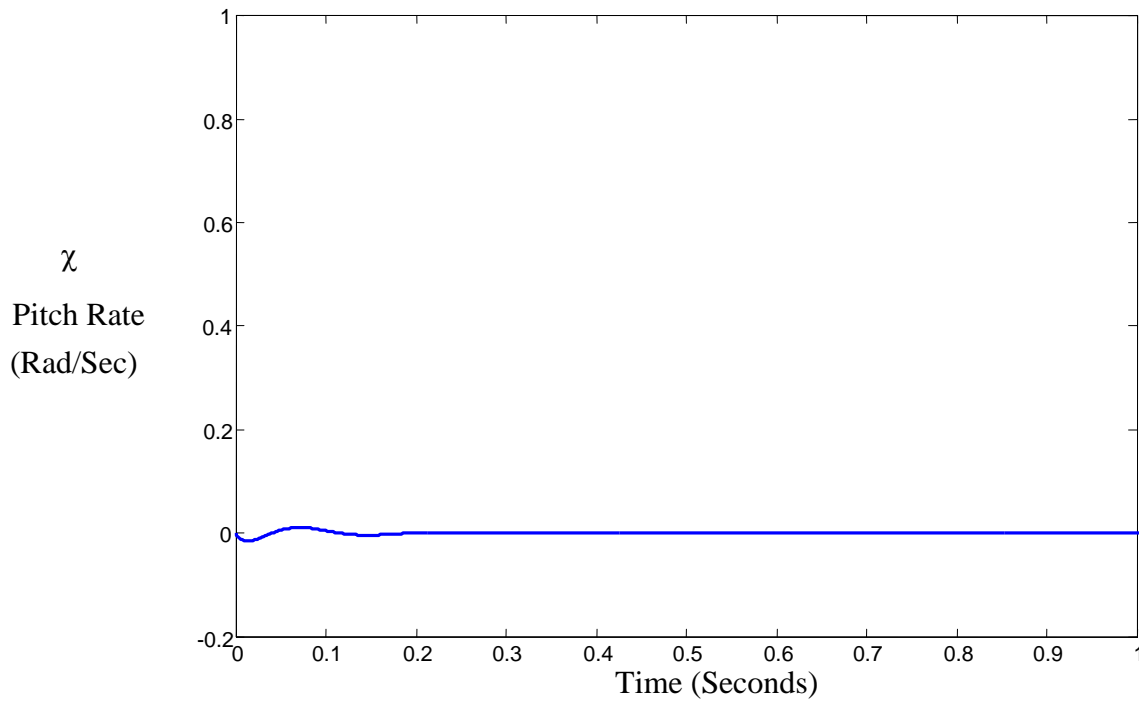


**Figure 5.21** Closed Loop Pitch Rate Response to a step input  $\delta_1$  using INA method

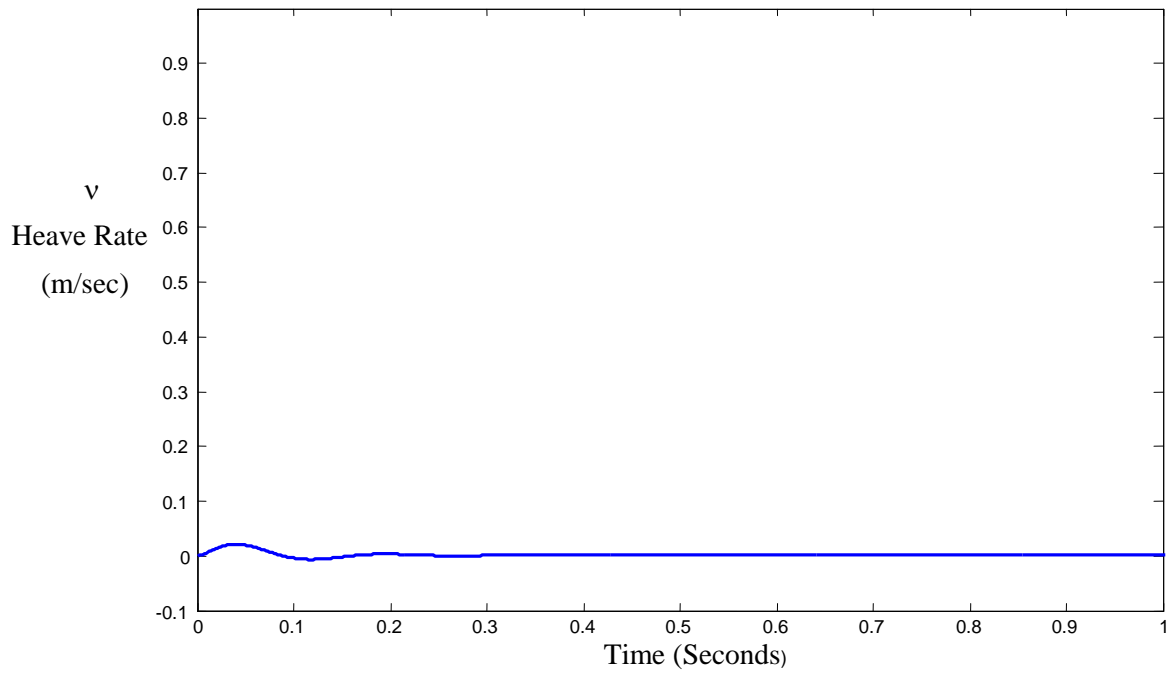


**Figure 5.22** Closed Loop Heave Rate Response to a step input  $\delta_2$  using INA method

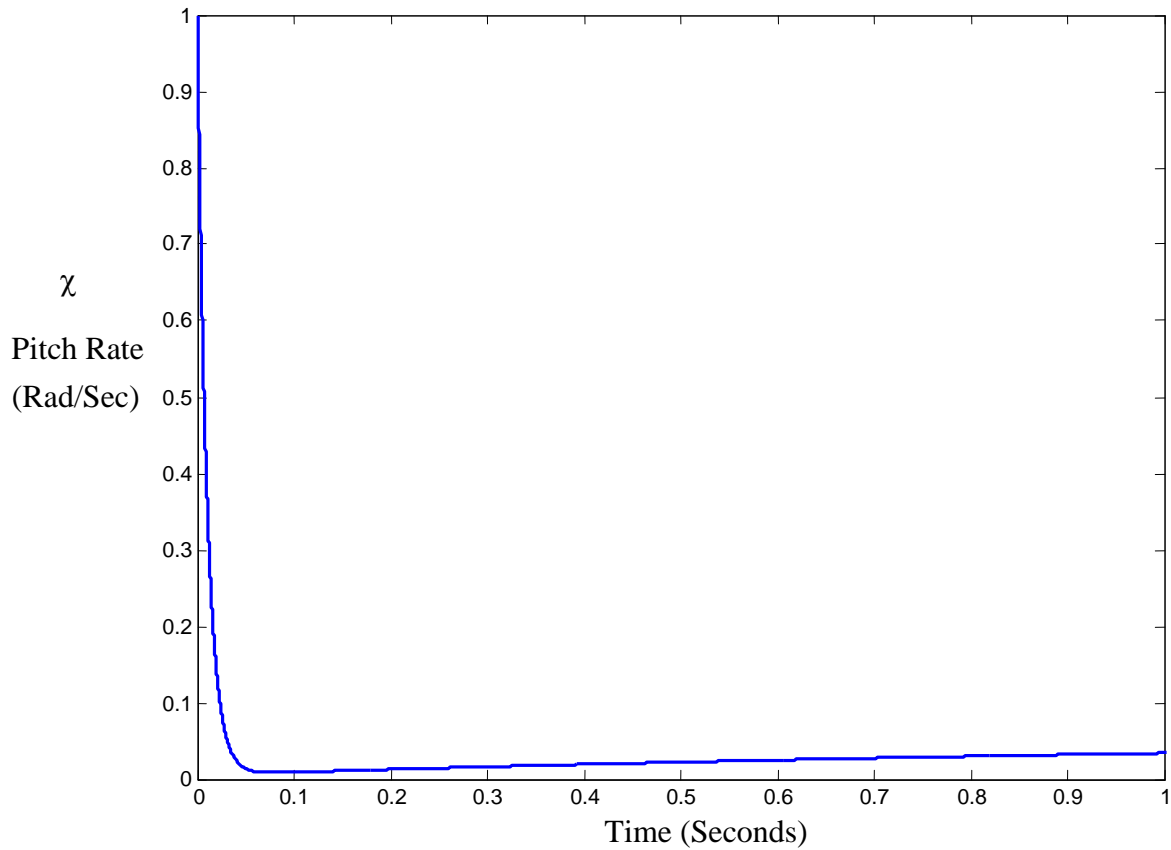


**Figure 5.23** Closed Loop Pitch Response to a step input  $\delta_2$  using INA method

Generally, it is clear that the system poses high level of disturbance recovery for step disturbance which is a highly desired characteristic. In addition, all responses reach zero with relatively very short time. Finally, with exception in the figure 5.20, overshoot is negligible for all responses due to disturbance.

## 5.5 Control Energy Cost Comparison

The system is subjected to variable disturbance during operation, these disturbance are mainly to wind gusts. Either using the least effort method or Inverse Nyquist method, the

aircraft motion showed acceptable level of disturbance recovery. However, the energy required to recover the system to its original state following random disturbances at both wing and horizontal tail is differ from one design method to another.

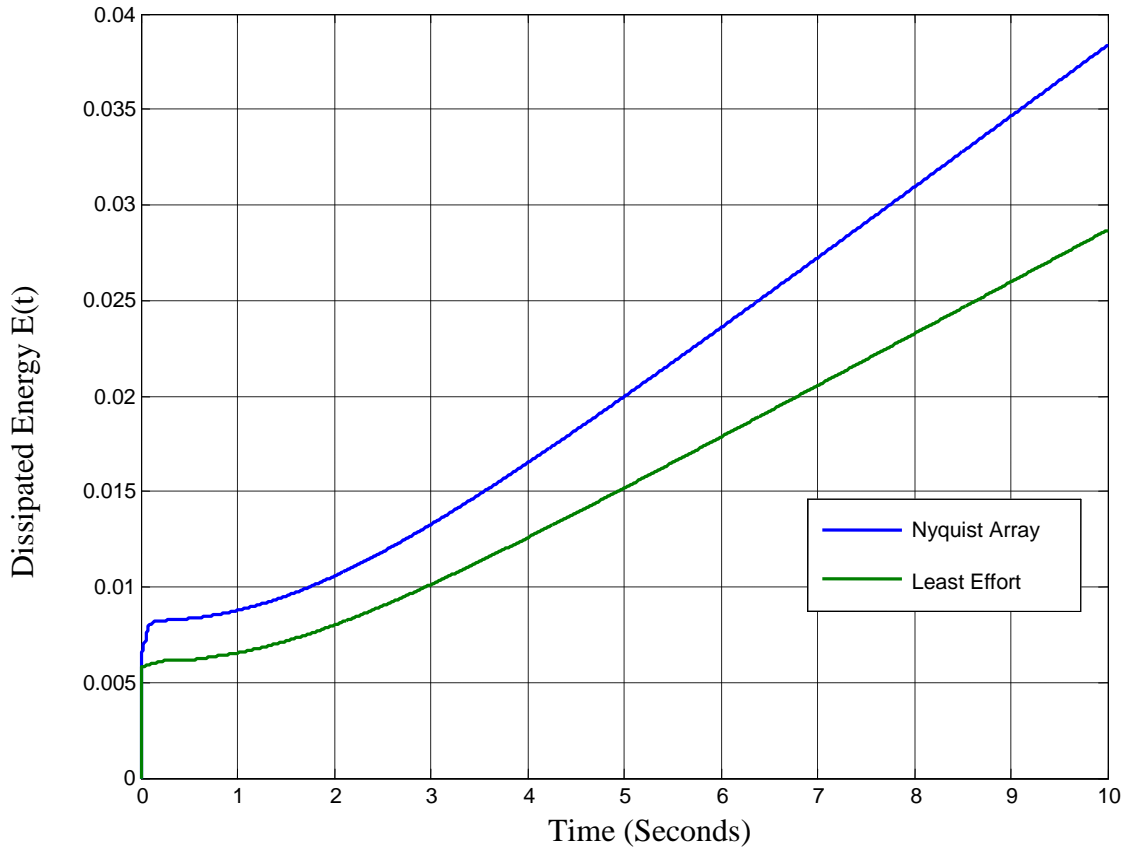


**Figure 5.24** Energy Dissipation following random disturbances  $\delta_1(t)$  and  $\delta_2(t)$

In order to compare the dissipated energy using least effort and inverse Nyquist methodologies, figure 5.24 is constructed. During the first 10 seconds, the used energy with least effort controller is 25% less than the dissipated energy when Inverse Nyquist compensator is used. The gap between the dissipated energy between the two methods is increasing with time. This implies that least effort has better characteristic in terms of energy dissipation to recover random disturbances.

## 5.6 Landing Distance to Complete Halt

The distance from the point where the wheels of the aircraft touch the carrier surface deck to the point where the aircraft reach complete stop is very important in designing the arresting gear, parameters, landing speed and weight of the aircraft at landing. However, it is necessary to assume a condition where there is zero slippage between the wheels of the aircraft and landing surface. This could be reasonable assumption as long as the deck surface is relatively dry.

It is also worth noting that the braking force applied by the pilot are considered zero in this calculation and will be an added safety factor at actual landing design. Figure 5.25 shows the distance travelled versus time in which the aircraft expected to stop after about 7 seconds.

The slope of the curve start with drastic negative values (about  $-90$ ) and increases slowly to reach zero at 3.5 seconds. This slope represents the speed of the aircraft which decelerate to a point where speed is zero.

Mathematically, the travelled distance can be found using equation 4.40:

$$X_0(s) = \frac{Msx'_0(0) + Cx_0(0)}{[Ms^2 + Cs + K]}$$

Using the following parameters:

$M=18000$  KG (the weight of aircraft at landing)

$C=70,000$  KG/Second.

$K=50,000$  N

$x_0(0) = 60$  m

$x'_0(0) = -25$ m/s

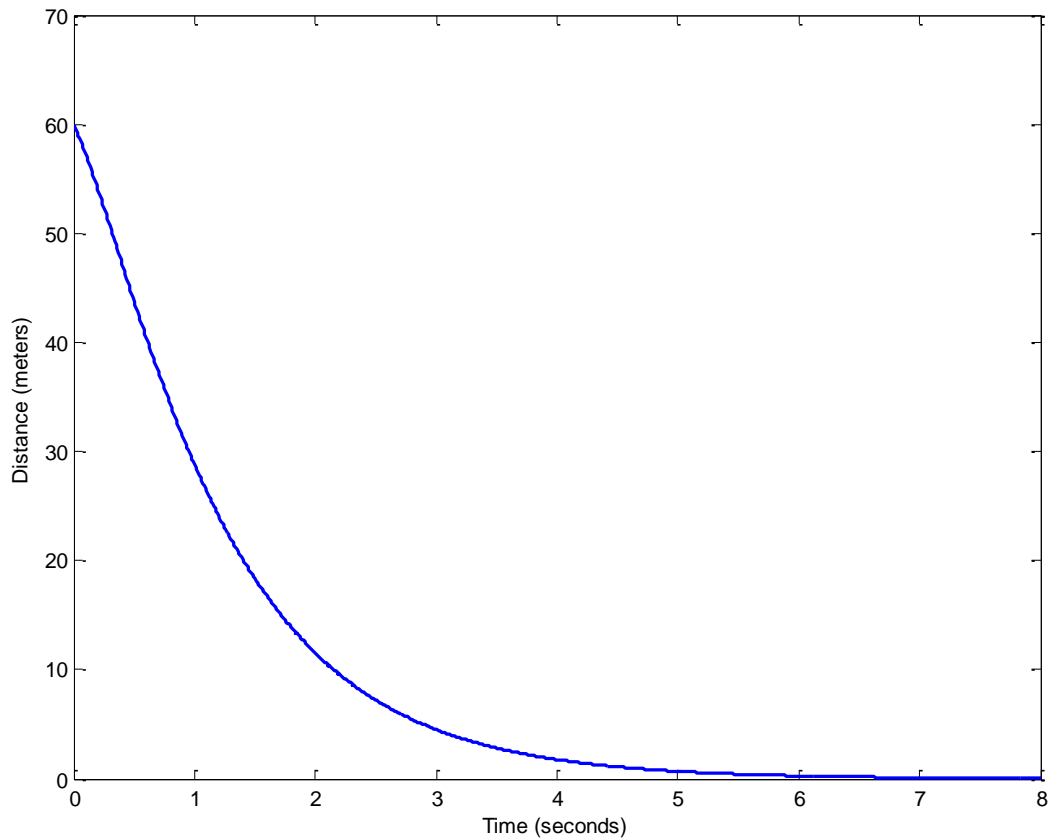


**Figure 5.25** The travelled distance on Carrier's Deck surface till complete stop

Then by Substitution:

$$X_0(s) = \frac{18,000[60s - 25] + 60C}{[18000s^2 + 70000s + 50000]}$$

Simplify

$$X_0(s) = \frac{60s + 208.33}{s^2 + 3.889s + 2.778}$$

Using expansion factor

$$\frac{60s + 208.33}{s^2 + 3.889s + 2.778} = \frac{A}{s + 2.94} + \frac{B}{s + 0.94}$$

Then

$$A + B = 60$$

$$0.94A + 2.94B = 208.33$$

From the above two equations

$$A = -15.9$$

$$B = 75.9$$

Substitute the values

$$X_0(s) = \frac{-15.9}{s + 2.94} + \frac{75.9}{s + 0.94}$$

Taking inverse Laplace

$$\mathcal{L}^{-1}[X_0(s)] = x_0(t) = Ae^{-2.94t} + Be^{-0.94t}$$

Then

$$x_0(t) = -15.9e^{-2.94t} + 75.9e^{-0.94t}$$

The total travelled distance is about 60 meters without applying the braking force, that means once the brake is applied the travelled distance becomes less.

# Chapter VI

## Comparison Study

### 6.1 Comparison between single input and dual inputs systems

This study was motivated by the paper introduced by (Whalley and Ebrahimi, 2000) for aircraft heave and pitch rates control. In that paper, a controller with single input dual output system was designed and has posed several advantages and improved performance characteristics. The pilot had a single control column with a direct influence on both heave rate and pitch rate simultaneously. However, the main limitation was the level of handling quality for the aircraft. The system showed high level of coupling between the system outputs and lack in pilot's ability to control the heave rate and pitch rate separately. Figure 6.1 shows the heave and pitch rates responses for a single step input.

In this contribution, two inputs two output system is introduced. The additional control surface suggested at aircraft's horizontal tail provides better ability for the pilot to control the system outputs efficiently. The system, in this paper, showed a high level of decoupling between the two outputs, in turn, handling quality is significantly improved.

Although in both contributions the pilot has access to a single control column, the configuration of the control system shown in figure 6.2 provides higher degree of safety at critical landing phase on aircraft carriers. Pitch rate can be controlled without significant change in heave rate which gives the pilot more freedom to focus on other tasks which need to be performed simultaneously during landing, such as controlling the speed, the lateral movement of the aircraft, and ensure the engagement of the hook with arresting gear at aircraft carrier's deck.

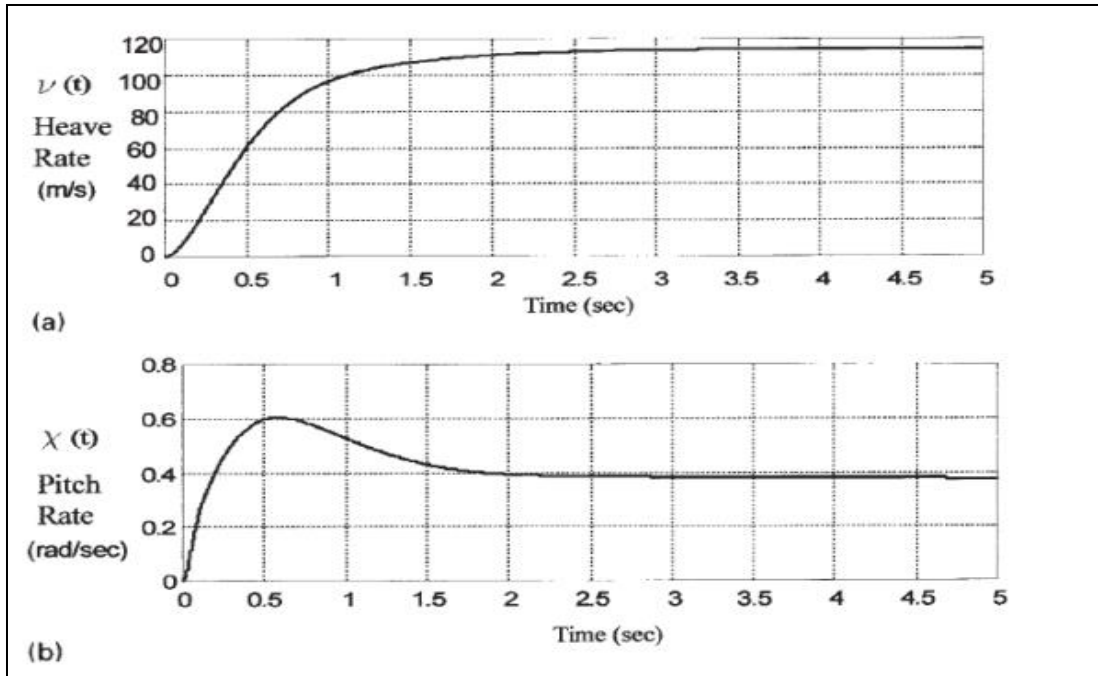


**Figure 6.1** Closed-loop heave and pitch rate response following a unit step change. (Whalley and Ebrahimi, 2000)

## 6.2 Least Effort versus Inverse Nyquist controllers

The Least effort and inverse Nyquist methodologies both have shown acceptable performance level. They both pose well behaved responses to system inputs and acceptable disturbance recovery characteristics. However, the techniques used for each method differ in many aspects especially the one that related to the level of involved difficulty.

Inverse Nyquist technique has the reputation of being difficult to apply for several applications. The difficulty mainly comes from the achievement of diagonal dominance and selecting suitable pre-compensators. The reason for this difficulty is the lack of standard technique which can be applied efficiently on all applications. Fortunately, the transfer function in equation 4.4 poses row diagonal dominance without the need for pre-compensator, which indeed not a common practice for many applications.



# Chapter VII

## Conclusion

The least effort regulator design in this contribution proves to be efficient. The system of two inputs and two outputs were studied. The objective of the controller is to increase the aircraft handling quality level with minimum energy dissipation was fulfilled. The pitch rate and heave rate of the aircraft at landing stage exhibit high degree of coupling, however, this hurdle was overcome by proper selection of output matrix  $S_s$ . The system transient responses were tuned using inner loop analysis aiming to construct well behaved dynamics of the system output. It was also utilized to improve response time compared to existing open loop system. The outer loop analysis aimed to reduce the interaction between the heave and pitch rates and to improve disturbance recovery inputs on both wing and horizontal tail.

The optimization of the performance index  $J$  was targeted to ensure the minimal energy consumption required to recover the system subjected to random disturbance. A comparison of energy consumption at different gain ratio were conducted to further prove that gain ratio at  $J_{min}$  will lead to the minimum amount of consumed energy.

The required feedback gain which fulfill disturbance recovery requirement was determined based on the simulation of outputs due to disturbances. Besides disturbance perturbation, the chosen feedback gain guaranteed improved response time compared to open loop responses. The simplicity of applying the least effort controller motivates applying this method rather other methods which may involve some complication during designing the controller, such as Inverse Nyquist.

With increasing number of system inputs and outputs, approximation and numerical minimization would be required in the least effort techniques.

Inverse Nyquist controller design was also proposed in this paper as an alternative solution to control the system outputs. Fortunately, there was no need to design a pre-compensator to achieve diagonal dominance, as it is often the case, because the transfer function had already inherent row diagonal dominance.

The results of inverse Nyquist were simulated and compared with the outputs results from the least effort methodology. With almost same performance in output response due to step inputs (slight steady state error using Inverse Nyquist method), Inverse Nyquist exhibit superior performance in disturbance rejection capability. However, the dissipated energy using the least effort controller showed better performance compared to Inverse Nyquist Array method. Least effort controller dissipated less amount of energy to recover the system after random disturbances were applied as shown in figure 5.24. Aircraft experienced this type of disturbance during deck landing.

With short landing distances on aircraft carrier's deck, the handling of aircraft efficiently is crucial to pilot and his hands should control one control column in the cockpit. In this case, it should be the pitch rate control column.

The contribution of the structure of the aircraft was also investigated to find an approximated transfer function that relates the pitch and heave rate due to control surfaces' deflection.

Eventually, the distance aircraft would travel on aircraft carrier was calculated based on the available arresting gear elasticity and damping coefficient. The arresting gear force was only considered to stop the aircraft within 60 meters and 7 seconds without applying the brakes on the

aircraft after landing in order to increase the level of safety.

All design objectives were fulfilled using the least effort method in this paper. Nevertheless, other design strategies are recommended for same system to contrast the advantages and the limitation of this method. Inverse Nyquist Array is a popular design strategy which proves its efficiency on many other applications.

Least effort methodology is also recommended to be extended to other axis of movement of the aircraft; roll and yaw are among the most important movements of the aircraft in the lateral direction, hence, the least effort regulator design could be of great advantage if applied on designing these movements.